12-1-1997

Mathematical Modeling of Convective Heat Transfer in Mammoth Cave

Jonathan Jernigan
Western Kentucky University

MATHEMATICAL MODELING OF CONVECTIVE HEAT TRANSFER IN MAMMOTH CAVE

A Thesis

Presented to

the Faculty of the Department of Mathematics

Western Kentucky University

Bowling Green, Kentucky

In Partial Fulfillment

of the Requirements for the Degree

Master of Science

by

Johnathan William Jernigan

December 1997

MATHEMATICAL MODELING OF CONVECTIVE HEAT TRANSFER IN

MAMMOTH CAVE

Date Recommended_____

Randall J. Swift

Director of Thesis

David K. Neal

Christopher M. Groves

Edmer Gray 12-11-97

Dean, Graduate Studies and Research Date

ACKNOWLEDGMENTS

The project to restore the natural entrance ecotone in Mammoth Cave is of great importance to the inhabitants and contents of the cave system. It is a project that is being undertaken largely by Science and Resource Management personnel at Mammoth Cave National Park. Without Science and Resource Management personnel's large collection of data sets, this thesis would not be possible. It has been a privilege and an honor to play a part in this project.

Everyone with the National Park Service has been eager and willing to help, and there are three individuals from Science and Resource Management who have been especially helpful in the various aspects of this thesis: John Fry, Rick Olson, and Joe Meiman. I would like to thank John Fry for allowing me to tag along on trips into the cave when he has been downloading CAM data, explaining many of the characteristics of the data to me, and helping me to locate scientific papers on cave meteorology. He has given data to me, reviewed portions of my thesis, and provided useful suggestions on how to make the thesis better. John has also answered a plethora of questions, some related to the project but many not. It was Rick Olson who provided an excellent introduction to the project to restore the natural entrance ecotone in Mammoth Cave. I would like to thank him for this introduction and for giving to me copies of many of the historical references cited in Chapter 1. Joe Meiman has also explained many aspects of the restoration project and supplied copies of CAM data. It is because of his technical expertise that the quality of the CAM data is so extraordinary (he designed the CAM stations). I would like to thank him for his help as well.

I have been extremely fortunate to work under a thesis advisor who has been both motivating and willing to provide help where needed. Dr. Randall Swift has provided many of the useful ideas developed in my thesis. He has read many draft versions of this thesis and made valuable evaluations of each draft. To individually list every way in which he has helped would be impossible. I would like to thank him for his time, ideas, and encouragement.

I am privileged to have on my thesis committee Dr. Christopher Groves and Dr. David Neal. I would like to thank them for their time and useful suggestions.

The average outdoor daily temperature data in Chapter 2 was provided by the Department of Geography and Geology at Western Kentucky University. I would like to thank them for access to the data.

Sigma Stat, a high powered statistical software package, was used throughout this thesis. The software was purchased in part with a grant from the National Speleological Society, in part with funds provided by the Department of Mathematics at Western Kentucky University, and the remainder with funds provided in a grant of Dr. Swift's; I would like to thank all parties for their support.

TABLE OF CONTENTS

MATHEMATICAL MODELING OF CONVECTIVE HEAT TRANSFER IN MAMMOTH CAVE

Johnathan W. Jernigan December 1997 109 Pages

Directed by: Randall J. Swift

Department of Mathematics Western Kentucky University

Around two centuries ago, changes were made to the entrances of Mammoth Cave and its passages. Today the Historic Entrance to Mammoth Cave is enlarged and the passage just beyond the entrance known as Houchins' Narrows has been cleared of rubble and filled with sediments. These enlargements have resulted in an increase in airflow throughout the Historic Section of the cave causing environmental conditions such as air temperature and airflow to fluctuate. These fluctuations have negatively impacted inhabitants and contents of the cave system.

To restore natural conditions within the cave, Science and Resource Management personnel at Mammoth Cave National Park have been collecting large data sets on atmospheric conditions inside the cave. The author has access to data from eight sites within the cave.

In this thesis, the author provides a brief introduction to the effects of the increase in airflow as well as a short discussion of the data gathered by Science and Resource Management. The author then proposes a natural cause for airflow (i.e., convection) in Mammoth Cave, constructs empirical models with this as the underlying driving force,

and uses atmospheric data to verify the validity of the claim of convection as the force driving airflow in Mammoth Cave. Data from the site in Houchins' Narrows is used to predict atmospheric data at other locations in the cave. The author concludes this thesis with time series analysis on data from Houchins' Narrows.

CHAPTER 1

AIRFLOW IN MAMMOTH CAVE: STUDIES OF THE PHENOMENON AND ITS EFFECTS

1.1 Introduction

Modifications begun nearly two centuries ago to the Historic Entrance of Mammoth Cave in Mammoth Cave National Park have created major changes in environmental conditions within the cave. These changes were caused by the increase in air movement within the Historic Section of the cave and have negatively affected inhabitants and contents of the system. In order to improve present conditions and return the cave to its proper state, Science and Resource Management personnel at Mammoth Cave National Park have been collecting atmospheric data within the cave system to determine the driving force behind the increase in airflow. Once this driving force is identified, mathematical models may be constructed and used to determine the proper course of action to return the cave to its proper state.

1.2 Modifications by Humans to Mammoth Cave and their Effects

Beginning 175 years ago, modifications have been made to the Historic Entrance of Mammoth Cave in an effort to make the cave more accessible to a steadily increasing number of visitors. These changes have included enlargement of the entrance and clearance of rubble from what is now known as Houchins' Narrows. A map of the Historic Section of Mammoth Cave is found in Appendix 4. Olson (1995) makes several

references to historical documentation describing the Historic Entrance and Houchins' Narrows during the 1800's as being much smaller than they are today. For example, William Blane, in his visit to the cave in 1822 (Blane 1824), described Houchins' Narrows as follows:

"*Immediately upon entering the cavern the passage is very narrow, and so low, that I was obliged to stoop to avoid knocking my head against the roof.*"

Olson (1995) states that the most major changes to Houchins' Narrows were made in the 1930's when the Civilian Conservation Corps removed rock and sediment to widen the tourist's trail. The removal of these sediments enlarged the passage to 20 feet wide and 7 feet tall.

Unfortunately, these alterations to the cave entrances have brought about undesirable changes in the atmospheric conditions in the Historic Section of Mammoth Cave by decreasing resistance to airflow. With air more readily entering and exiting Mammoth Cave, environmental parameters such as air and rock temperature, relative humidity, and air flux are more readily influenced by outdoor conditions. These changes in environmental conditions within the cave have produced three observed results (Olson 1995):

1. The absence of bats, especially Gray bats (*Myotis grisescens)* and Indiana bats (*Myotis sodalis)* which are endangered species.
2. Formation of condensation above War of 1812 era saltpeter leaching vats, which results in biodegradation of these wooden artifacts.

3. An increase in the number of rockfalls in the Historic Section of Mammoth Cave.

1.2.1 Past Presence of Bats in the Historic Section of Mammoth Cave

Several sources document the past presence of bats in Mammoth Cave (most of the following may be found in a National Park Service document ("Cave Animals. . .")). Professor B. Silliman Jr. in 1850 (Silliman 1850) stated in a letter to a friend:

> *"Bats are numerous in the avenues within a mile or two of the mouth of the cave. . . in the galleries where they most abound, we found countless groups of them on the ceilings chippering and scolding for a foothold among each other. On one little patch of not over four by five inches, we counted forty bats, and were satisfied that one hundred and twenty at least were able to stand on a surface a foot square; for miles they are found in patches of various sizes, and a cursory glance satisfies us that it is quite safe to estimate them by millions."*

Olson (1995) states this clustering noted by Dr. Silliman is a characteristic of Gray bats. In a letter from an unknown author on January 21, 1810 ("The Subterranean. . ."), large quantities of bats are said to hibernate at some point beyond the Rotunda:

> *"We progressed but a little way before we discovered innumerable quantities of bats which had taken refuge there from the severities of the season; they were suspended from all parts of the rocks by their claws, with their heads down, and crowded so close that they resembled a continued black cloud; they appeared much disturbed at our intrusion which they manifested by a disagreeable hissing*

or twittering noise, and so tenacious were they of the hold which instinct had caused them to take, they would suffer themselves to be burnt to death sooner than relinquish it."

William N. Blane in 1822 wrote of "myriads" of bats in Audubon Avenue (Blane 1822). Godfrey T. Vigne in 1831 (Vigne 1831) makes reference to "thousands" of bats found in "clusters." Other references to bats in Mammoth Cave are made by Bird (1838), and even as late as 1870, Ralph Seymour Thompson (Thompson 1870) estimated the number of bats in the Historic Section of Mammoth Cave to be in the millions. Ebenezer Meriam in 1844 (Meriam 1844) stated the following:

"Bats are numerous in some of its extensive apartments in winter, and so numerous, that it is a wonder where they all come from, or how they all find their way to this great headquarters. These bats hang in clusters like bees in swarming. . ."

One place where bats are believed to have populated is Little Bat Avenue, and this claim is supported by Bullitt (1844) who reported "tens of thousands" of bats in this location. In addition, an undocumented source in 1856 ("The Mammoth Cave") noted "thousands" of bats here.

Not only are there historical references to support the notion that bats once inhabited the Historic Section of Mammoth Cave but there is also scientific evidence which may be seen today. Toomey (1995) indicates evidence of the use of Lookout Mountain behind Rafinesque Hall by bats as a roosting location. This evidence includes large amounts of bat guano and numerous bat skeletons. The nature of the humeri of

several of these skeletons indicates that they are the skeletons of the endangered Indiana bat. Toomey also notes that there are mummified remains of bats throughout the cave, one of which he believes to be of the genus *Myotis*, the genus of which Gray and Indiana bats are members.

It is interesting to note that even today both Gray and Indiana bats are present in Dixon Cave (Olson 1996) which is very near the Historic Entrance to Mammoth Cave.

1.2.2 Destruction of Remnants of a Nitrate Mining Operation

Prior to and during the War of 1812, saltpeter (potassium nitrate) was extracted from the soils of Mammoth Cave for use in the making of gunpowder by the Dupont gunpowder works of Delaware (Lyons 1993). The process for removing the calcium nitrate from the soil demanded the construction of large wooden leaching vats within the cave itself. Cave sediments were placed in the vats where water was passed through so that the desired calcium nitrate would be dissolved in the water. This solution was then pumped through hollowed tree logs (often large tulip poplar trees) to the surface where it was mixed with wood ash to form saltpeter (Palmer 1981).

Today, these wooden saltpeter leaching vats and the wooden piping system are in danger of being destroyed. The large volume of cool air flowing in through the Historic Entrance during the winter flows down through Broadway and Main Cave into Booth's Amphitheater where it collides with warm air flowing out of Gothic Avenue. These relatively cool and warm air masses collide and cloud formation results. Moisture from this process condenses onto the ceiling and drips onto the wooden leaching vats in this area resulting in the biodegradation of these artifacts.

1.2.3 The Increased Rate of Rockfalls in Mammoth Cave

Occasional rockfalls within a cave system are a normal occurrence (particularly within the variable temperature zone), and the accelerated rate of rockfall currently witnessed in Mammoth Cave is directly related to the increase in the flow of air throughout the Historic Section of Mammoth Cave. During an unusually cold period in the winter of 1993 - 1994, a low outdoor temperature of -16 °F was reached on January 18 (Olson 1995). The extreme differential between the air temperature in the cave and the air temperature outside the cave resulted in a large influx of cold air down Houchins' Narrows and into the Rotunda Room. Either through thermal contraction of the cooled rock ceiling or through ice formation within the crevices between neighboring rocks in the ceiling, a 40 ton slab of rock became dislodged from the ceiling and crashed to the floor damaging saltpeter mining artifacts and a handrail. Other smaller and less significant rockfalls have also been observed.

1.3 The Project to Restore the Natural Entrance Ecotone to Mammoth Cave

An effort to restore the bat hibernaculum which historically existed in the Historic Section of Mammoth Cave began with the installation of a bat friendly gate in July 1990 (Olson 1995). The gate that existed prior to this installation consisted of sheet metal panels which acted as a retardant against airflow. When that gate was replaced by one through which bats were able to fly, air exchange between the outdoors and the interior of the cave increased significantly.

In order to understand the driving forces behind this increase in airflow, Science and Resource Management personnel at Mammoth Cave National Park have been

collecting atmospheric data from within the cave. Analysis of the data should provide clues of the force which drives airflow allowing Science and Resource Management personnel to take appropriate action to regulate airflow. With airflow moderated, natural conditions within the cave may be restored to what they were prior to the modifications made to the Historic Entrance and Houchins' Narrows.

In this thesis, the process for modeling and predicting atmospheric data will consist of three stages:

1. Identify the natural phenomenon driving airflow in the Historic Section of Mammoth Cave.
2. Use data from a site near the entrance of Mammoth Cave to predict atmospheric conditions deeper within the cave.
3. Predict atmospheric data in the entrance to the cave.

Each of the three above steps in the data analysis may be combined to provide a mathematical model for predicting atmospheric conditions within the Historic Section of Mammoth Cave.

The idea of studying atmospheric conditions in Mammoth Cave is not a new one. In his letter dated November 8, 1850, Professor B. Silliman Jr. suggested the study of daily temperature and barometric data measurements to support the claim of the immense size of Mammoth Cave. He suggested the study could also determine the presence of more than one entrance (Silliman 1850). In a newspaper article, John M. Nelson (a former cave guide) writes of observations made within the cave system (Nelson 1934). Measurements were taken daily at the old iron gate (wind velocity), the Corkscrew, and

River Hall, with these last two being air temperature measurements. Nelson reported velocity measurements as high as 45 miles per hour into the cave. However, the temperatures at both Corkscrew and River Hall were reported to have varied by no more than one degree Fahrenheit.

The first of the current monitoring stations was installed in 1994 at Lookout Mountain behind Rafinesque Hall (Olson 1995). This site was the first of many Cave Atmospheric Monitoring (CAM) sites, with the current total being sixteen. Measurements are recorded in fifteen minute intervals, and typical data measurements taken at each site include air and rock temperature (°C), wind speed (m/sec), wind direction (degrees), and relative humidity (percent). The author has access to data from eight CAM sites, all located within or near the Historic Section of Mammoth Cave, as listed in Table 1.3.1. The locations of these sites are shown on the map found in Appendix 4.

CAM Site	Data Gathered
Houchins' Narrows	Air Temperature; Rock Temperature; Wind Speed; Wind Direction
Corkscrew	Air Temperature; Relative Humidity
Booth's Amphitheater	Air Temperatures at Floor, Ledge, Ceiling
Wright's Rotunda	Air Temperature; Relative Humidity
River Hall	Air Temperature; Relative Humidity
Little Bat Avenue	Air Temperature; Relative Humidity
Rafinesque Hall	Air Temperatures at Floor, Ceiling;Relative Humidity
Mushroom Vats	Air Temperature; Relative Humidity

Table 1.3.1 - Listing of CAM Sites Along the Historic Section of Mammoth Cave and the Data Gathered at Each

According to an illustration in the book by Palmer (1981), the Historic Section of Mammoth Cave is lower in elevation than the remaining cave system. Therefore, even though Houchins' Narrows is higher in elevation than the other CAM sites in the Historic

Section of Mammoth Cave, it will have airflow patterns consistent with lower entrances in caves. This fact will be important in Chapter 2.

Air flux, which is the directional change in the volume of air per unit time, in Houchins' Narrows is of particular interest. This data is not gathered directly in Houchins' Narrows but must be calculated using wind speed and direction measurements. The change in volume of air per unit time is obtained by multiplying the speed of the air (in meters per second) by the cross-sectional area of the passage at the CAM site (according to Science and Resource Management, at the Houchins' Narrows CAM station the cross-sectional area is 19.2 m^2). The directional element is introduced by defining air flux as positive when airflow is into the cave and negative when airflow is out of the cave. Therefore, air flux in Houchins' Narrows, denoted $\mathbf{F}_H$ (m^3/sec), is given by

$$\mathbf{F}_H = \begin{cases} 19.2\ m^2 \times \text{Wind Speed} & \text{If Incast,} \\ -19.2\ m^2 \times \text{Wind Speed} & \text{If Outcast} \end{cases} . \qquad (1.3.1)$$

There are several assumptions about the nature of the airflow required in the formulation given by (1.3.1). They are:

1. Airflow in Mammoth Cave behaves as an incompressible flow.
2. Airflow through Houchins' Narrows and past the CAM site is uniform across each cross-section.

Air is not an incompressible fluid, but velocities and pressures in Mammoth Cave are relatively insignificant; thus the flow of air in Mammoth Cave may be considered an incompressible fluid flow. Furthermore, Houchins' Narrows is a passage large enough so

that energy lost to friction between the sides of the passage and the air mass will be small when compared to the total energy flowing through the passage. Airflow in Houchins' Narrows may be assumed uniform over any cross-section.

There are three data measurements taken in Houchins' Narrows: temperature of the air, temperature of the rock, and flux of air. Plotting each of these measurements along the same time axis gives a useful look at the nature of the data. Figure 1.3.1 shows a typical set of line plots for Houchins' Narrows data gathered during the winter.

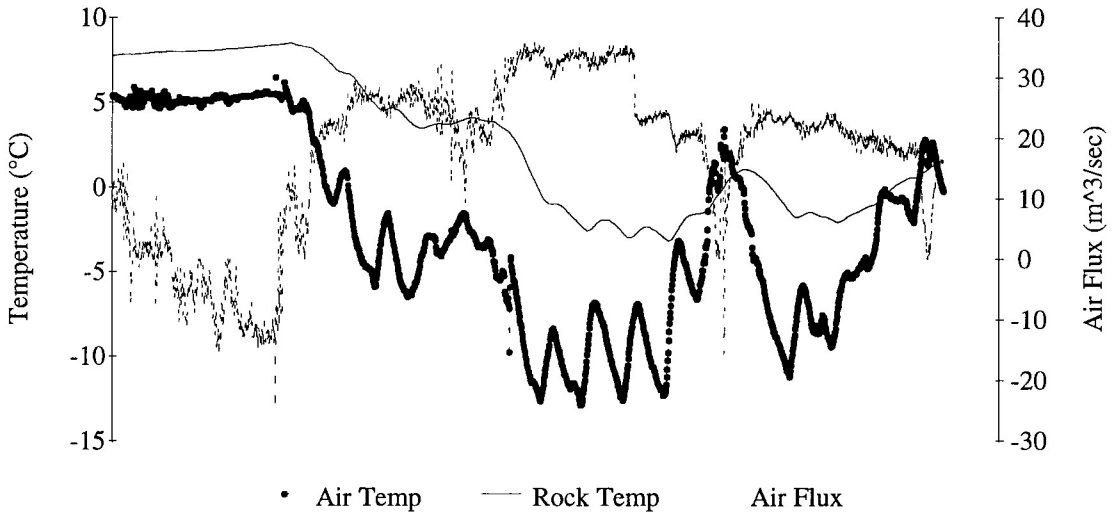

Figure 1.3.1 - Line Plots of Houchins' Narrows Data, Julian Days 1 - 20 of 1997

Figure 1.3.1 gives a good indication of how Houchins' Narrows data behaves. For example, air temperature is coolest when air is flowing into the cave and warmest when air is flowing out of the cave. Also, rock temperature tends to be a rough approximation of air temperature.

1.4 Plexiglas Panels on the Bat Gate in the Historic Entrance

In an effort to impede air movement through Houchins' Narrows and the Historic Section of Mammoth Cave, Science and Resource Management personnel placed Plexiglas panels over the bat friendly gate in the Historic Entrance. The reduction in airflow was almost instantaneous. The retrofit was done on March 1, 1996 (Julian day 61), and Science and Resource Management reported a 30% reduction in the volume of air flowing through Houchins' Narrows under equivalent air temperatures. This effect may be seen in Figure 1.4.1.

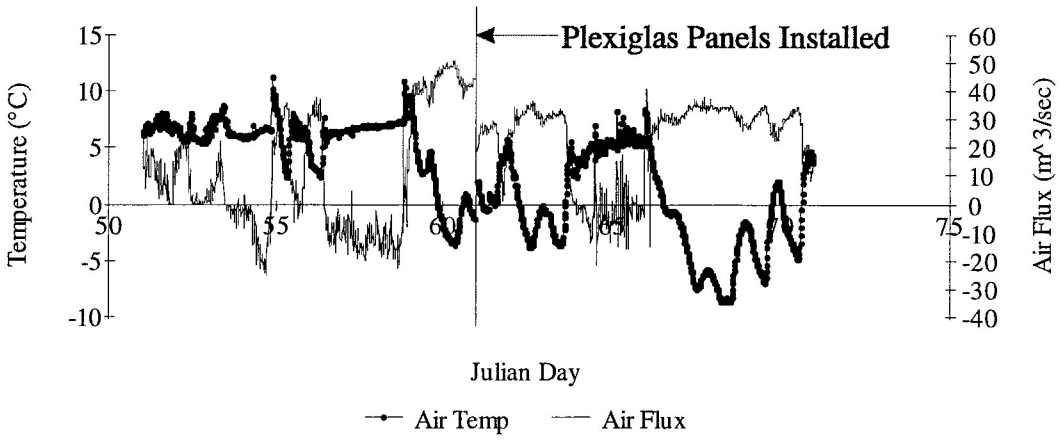

Figure 1.4.1 - Figure Showing Decrease in Airflow Due to Installation of Plexiglas Panels on Bat Gate in Historic Entrance on March 1, 1996

Another air panel configuration was completed around March 1997. This time the Plexiglas panels were placed on spring loaded hinges secured on the bat gate with the panels opening towards the outdoors. Ideally, when air is flowing into the cave at velocities that are too large, the panels will be pushed closed thereby blocking air currents and reducing airflow velocities.

1.5 Thesis Direction

This thesis consists of four chapters. This first chapter has been an introduction to the history of airflow and contents of the cave affected by airflow in the Historic Section of Mammoth Cave. In the first chapter, the author has also introduced the data gathered by Science and Resource Management personnel. In the second chapter, the author will use the data to show airflow is driven by a physical phenomenon known as the *chimney effect*. The author, in Chapter 3, will then construct a regression model which allows the prediction of temperature at a given CAM site based on atmospheric data from Houchins' Narrows. In Chapter 4, the author will describe how to use time series analysis as a tool for predicting air flux in Houchins' Narrows. In the final chapter, Chapter 5, the author provides a short summary of the thesis and reemphasizes the goals of Science and Resource Management personnel.

CHAPTER 2

EVALUATING THE CHIMNEY EFFECT HYPOTHESIS WITH DATA ANALYSIS

2.1 Introduction

Airflow in Mammoth Cave is believed to be driven primarily by temperature differentials, or, equivalently, density differentials, between air outside the cave system and air inside the cave system. To determine whether or not this belief is accurate, data gathered by Science and Resource Management personnel will be analyzed. If the data behaves in the manner predicted by the chimney effect hypothesis, then it may be concluded that the chimney effect is the driving force behind airflow in Mammoth Cave.

In this chapter, the analysis will include the construction of frequency distributions of air flux in Houchins' Narrows at different times throughout the year, scatter plots for air flux in Houchins' Narrows as a function of temperature differentials between the air in Houchins' Narrows and Booth's Amphitheater, and temperature stratification as seen in the Booth's Amphitheater temperature data.

2.2 The Chimney Effect Hypothesis

The *chimney effect* is a method of heat transfer, also known as *convection*, whereby cooler, more dense air will fall in elevation around warmer, less dense air. It is often called the chimney effect since it is the cause of airflow exiting the chimney of a

house in the winter. During the winter, when the outdoor air temperatures are cooler

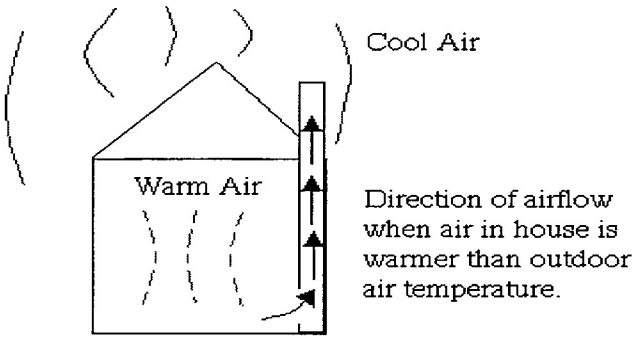

Figure 2.2.1 - Chimney Effect in a House

than those indoors, the warmer indoor air becomes buoyant since it is less dense than the cooler outdoor air. With the momentum of this buoyancy, the warmer indoor air rises out the chimney to be replaced by cooler air from openings in the lower portions of the house. This behavior is illustrated in Figure 2.2.1.

Airflow driven by temperature differentials in complex cave systems such as Mammoth Cave behaves analogously to airflow driven by temperature differentials in a house. For example, lower entrances to the cave will have air flowing into them when outdoor temperatures are cooler than indoor air temperatures (the air in the cave is less dense than the air outside the cave so that it rises out of upper entrances and is replaced through influx of air in lower entrances). When the outdoor temperature is warmer than the temperature of air within the cave, lower entrances to the cave will have air flowing out of them (air in the cave is more dense than air outside the cave and falls out of lower entrances to be replaced by air flowing in through upper entrances). This idea is illustrated in Figure 2.2.2. In his study of atmospheric conditions in Harrison's Cave in Barbados, West Indies, Fred L. Wefer discusses this same phenomenon (Wefer 1994).

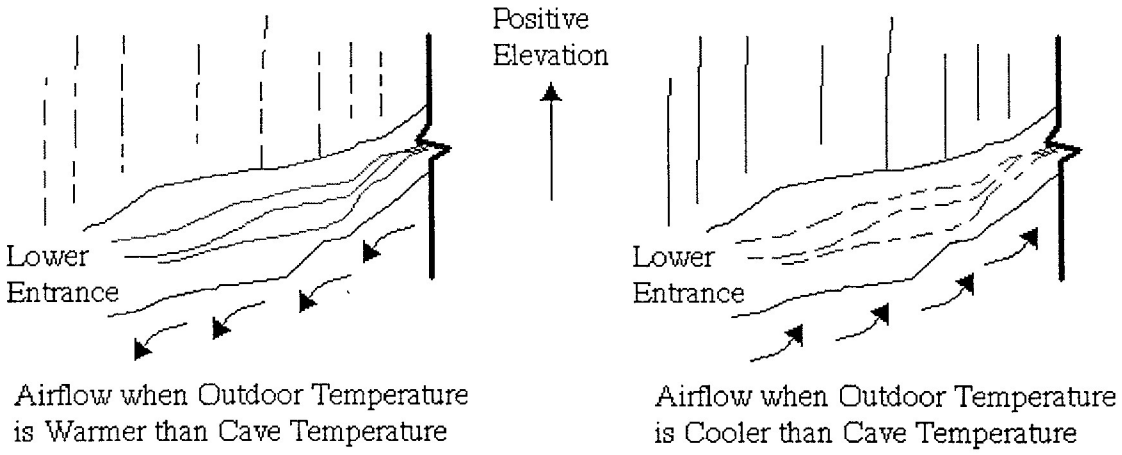

Figure 2.2.2 - Chimney Effect in the Lower Entrance to a Cave

2.3 Frequency Distributions and Sample Statistics of Air Flux in Houchins' Narrows

One way to evaluate the accuracy of the chimney effect hypothesis in Mammoth Cave is to consider the frequency distributions of air flux values in Houchins' Narrows. If these frequency distributions behave as the chimney effect hypothesis predicts, they will then serve as evidence in support of the hypothesis.

According to Palmer (1995), the average temperature beyond the variable temperature zone is about 55° - 57°F (13° - 14°C). In the summer, outdoor air temperatures are consistently above air temperatures within the cave system so that the cave air is cooler than the outdoor air and flows out of lower entrances. Similarly, outdoor air in the winter varies from being cooler to being warmer than air in the cave, and there is consequent alternation between inward and outward flow of air in a lower

Day	January	February	March	April	May	June	July	August	September
1	43	20	29	45	55	68	81	68	71
2	43	11	38	44	64	64	80	72	71
3	29	2	28	61	68	70	75	76	70
4	27	3	42	57	74	65	67	77	73
5	29	13	56	44	75	64	69	78	74
6	25	27	52	39	69	73	71	79	76
7	18	30	44	38	65	73	78	80	76
8	15	39	17	44	73	68	76	80	74
9	25	40	16	37	73	65	71	74	74
10	32	47	27	43	74	65	66	70	75
11	34	48	36	54	68	71	69	70	71
12	30	32	37	68	54	72	74	71	70
13	36	34	53	66	54	74	76	70	58
14	44	47	64	51	51	76	77	73	59
15	40	38	59	56	67	82	73	74	59
16	45	36	47	48	75	77	70	77	69
17	60	25	51	53	74	78	77	78	64
18	62	32	46	64	77	80	81	79	60
19	31	36	44	69	78	78	83	77	61
20	20	48	34	64	77	80	80	80	63
21	33	55	30	64	76	81	80	79	67
22	37	56	29	70	67	76	80	78	64
23	44	65	34	58	69	83	71	79	68
24	37	53	52	49	80	81	71	79	70
25	27	55	51	67	76	78	75	75	61
26	41	65	33	61	74	69	70	72	68
27	37	66	40	49	71	70	70	73	70
28	26	45	47	63	72	74	73	73	59
29	39	25	42	71	68	77	73	74	55
30	34		54	50	64	82	71	75	60
31	23		56		63		73	72	

Table 2.3.1 Mean Daily Outdoor Temperatures (°F) at Mammoth Cave National Park in 1996 (Data Courtesy of the Department of Geography and Geology at Western Kentucky University)

entrance. These characteristics of outdoor air temperatures in Mammoth Cave National Park may be seen in the daily mean outdoor air temperature data in Table 2.3.1. This data was provided by the Department of Geography and Geology at Western Kentucky University.

Houchins' Narrows is a lower entrance; so during the summer consistent outward air flux is expected, and in the winter air flux is expected to alternate between being into the cave and being out of the cave. This oscillation suggests a high degree of randomness in the air flux observations. Figures 2.3.1 and 2.3.2, respectively, show frequency distributions for air flux in Houchins' Narrows in the summer and in the winter. Summer data is tightly clustered around some mean value indicating a relatively small value for the sample standard deviation; the mean is -15.22 m^3/sec, which is out of the cave, and the sample standard deviation is 5.59 m^3/sec. This data is random

Julian Days and Year	Air Flux Sample Mean	Air Flux Standard Deviation
91 110, 1996	10.4764	17.0579
111 130, 1996	-6.3859	13.5356
131 150, 1996	-12.3937	15.2005
151 170, 1996	-12.9098	8.9594
195 - 210, 1996	-15.6752	5.1802
221 - 240, 1996	-14.6188	5.2937
245 - 265, 1996	-8.0686	10.5012
270 - 290, 1996	4.0606	14.7323
321 - 346, 1996	14.8697	9.3893
348 - 366, 1996	14.9118	11.0193
1 - 20, 1997	17.3895	130585
21 - 40, 1997	11.4814	7.3856
41 - 60, 1997	9.6473	11.3118
61 - 77, 1997	8.2528	8.3869

Table 2.3.2 - Sample Means and Standard Deviations for the Indicated Sets of Air Flux Data (All Values in m^3/sec)

but well behaved. In contrast, the winter data has a wide range of values and is highly random; the mean is 18.37 m^3/sec, which is into the cave, and the sample standard

deviation is 14.10 m^3/sec. This data is random but not well behaved (a list of several sets of air flux data along with their means and standard deviations are shown in Table 2.3.2). Hence, these frequency distributions for airflow data in Houchins' Narrows support the

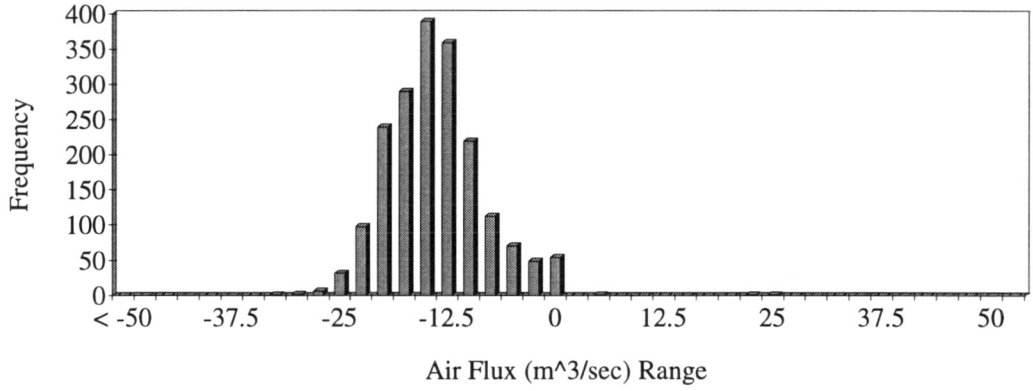

Figure 2.3.1 - Frequency Distribution for Summer Air Flux Data

chimney effect hypothesis. Frequency distributions of air flux in Houchins' Narrows throughout the year behave as the chimney effect hypothesis indicates they would; these frequency distributions are found in Appendix 1.

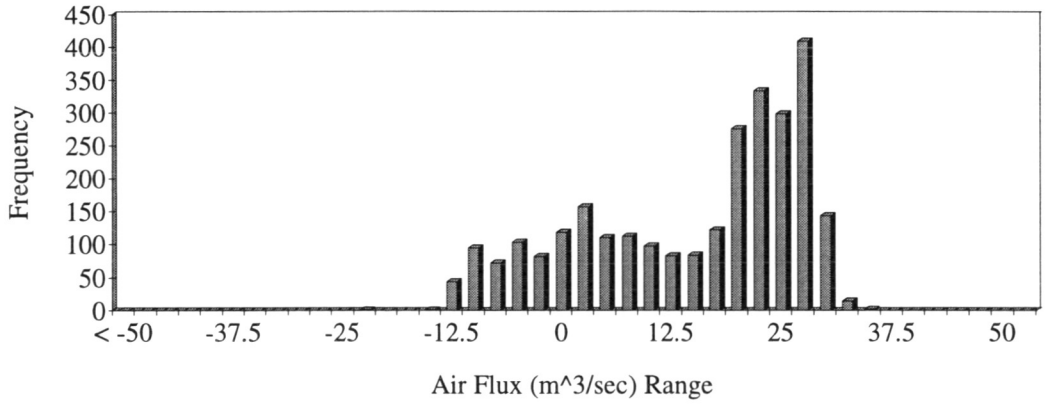

Figure 2.3.2 - Frequency Distribution for Winter Air Flux Data

The following section uses the average daily outdoor temperature in Table 2.3.1 to show further that air flux data in Houchins' Narrows supports the chimney effect hypothesis.

2.4 Air Flux in Houchins' Narrows as it Compares to Average Daily Outdoor Temperatures and Barometric Pressure

Section 2.3 showed the frequency distributions for air flux in Houchins' Narrows as they vary throughout the year. These frequency distributions show that, on average, air flux is highly dependent on the season of the year, and since air temperature varies greatly with season, it may be postulated that air flux in Houchins' Narrows is highly dependent upon outdoor air temperatures.

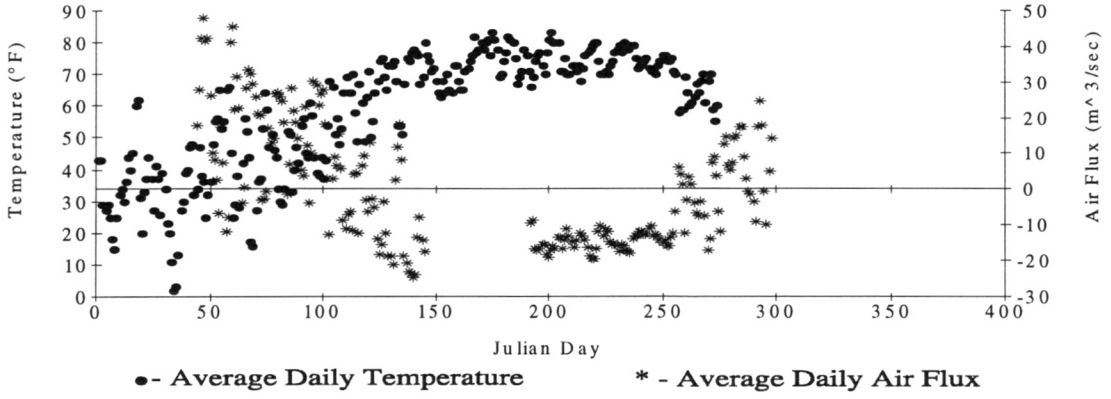

Figure 2.4.1 - Average Daily Air Flux in Houchins' Narrows and Average Daily Outdoor Temperature at Mammoth Cave National Park in 1996

To see further that airflow is driven by seasonal temperature variations, consider the data in Figure 2.4.1 which shows average daily air flux in Houchins' Narrows along the same time axis as average daily outdoor temperature. These values for average daily flux were calculated using the Sigma Stat transform in Figure 2.4.2. When temperatures

outside are relatively cold, as in winter, air flux has values greater than zero, indicating airflow is into the cave. When air temperatures outside are relatively warm, as in summer, air flux has values less than zero, indicating airflow is out of the cave. This is the behavior predicted by the chimney effect hypothesis.

```
'********************  Averaging Algorithm ******************************
'This transform goes through flux data in the Houchins' Narrows data sets
'averaging flux each day.
'It also takes the resulting averages and places them into the neighboring
'column so that viewing the averages for each time period is much easier.
'NOTES:  Air Flux data must be in column 3
'        Julian Day must be in column 4
'        Time must be in column 5
'        Columns after column 5 must be empty (except cell(15,1))
'        The last day of data will not be included if the day is not complete

cell(15,1)=1;                    Used to denote row to put averages into
cell(16,1)=1;                    Used to count measurements between days
cell(17,1)=cell(4,1);            Used to denote the day of current measurements

for i=2 to size(col(3)) do
 if cell(4,i) = cell(17,1) then
  cell(16,1)=cell(16,1) + 1
 else
  x=col(3,i-cell(16,1),i-1)
  cell(9,cell(15,1))=cell(4,i-1)
  cell(10,cell(15,1))=mean(x)
  cell(15,1)=cell(15,1)+1;       Increments row to move average info to
  cell(16,1)=1;                  Resets counting cell
  cell(17,1)=cell(4,i);          Resets current day
 end if
end for
```

Figure 2.4.2 - Sigma Stat Transform Used to Average Air Flux Data

It has been shown that the average daily air flux values in Houchins' Narrows are highly dependent upon average outdoor daily temperatures. But is average daily airflow

dependent upon any other outdoor parameters, such as average daily barometric pressure? To answer this question, consider the scatter plots of average daily air flux in Houchins' Narrows as a function of average daily

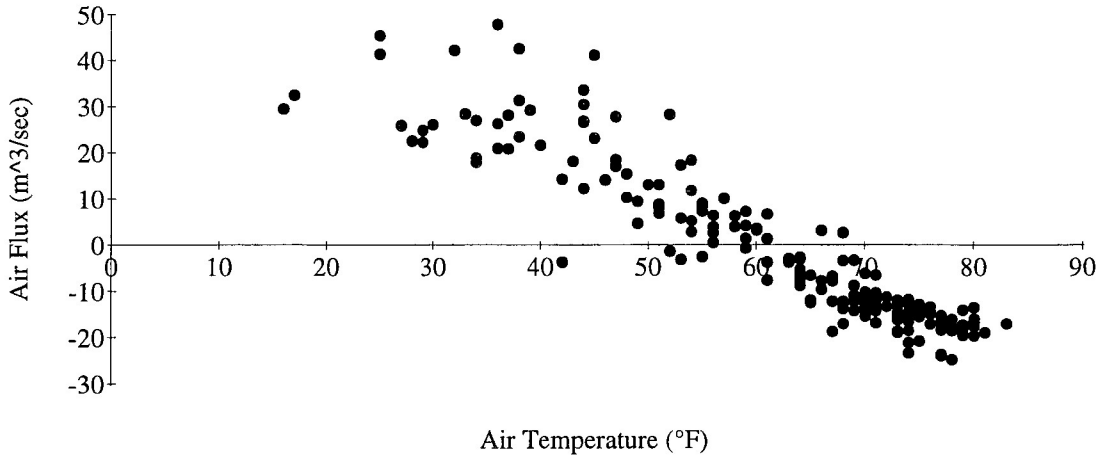

Figure 2.4.3 - Observed Dependence of Average Daily Air Flux in Houchins' Narrows on Average Daily Outdoor Air Temperature on Julian days 44 - 274 of 1996

barometric pressure shown in Figure 2.4.3 and Figure 2.4.4, respectively (average daily barometric pressure data for 1996 is found in Table 2.4.1 on the following page).

Notice the data in Figure 2.4.3 shows a clear dependence of average daily air flux in Houchins' Narrows on average daily outdoor temperature. In fact, using regression analysis (see section 3.1 for a detailed discussion of regression techniques) to fit a line to this data gives a value of R-squared equaling .865, so that 86.5% of the variations in air flux values may be accounted for by the behavior of the outdoor air temperature. So, at least on a daily basis, air flux in Houchins' Narrows is highly dependent upon outdoor air temperatures.

Day	January	February	March	April	May	June	July	August	September
1	1005	1021	1016	1018	1015	1021	1015	1016	1015
2	999	1025	1011	1020	1015	1020	1010	1016	1014
3	1012	1031	1027	1015	1015	1017	1011	1017	1014
4	1018	1039	1026	1014	1015	1016	1013	1018	1013
5	1023	1036	1013	1023	1017	1019	1015	1019	1012
6	1020	1032	1007	1018	1020	1016	1014	1020	1012
7	1019	1022	1018	1016	1021	1013	1011	1020	1012
8	1025	1013	1031	1015	1020	1010	1009	1019	1012
9	1018	1016	1036	1019	1021	1009	1013	1019	1012
10	1022	1012	1038	1021	1019	1013	1019	1017	1015
11	1011	1017	1033	1018	1017	1012	1019	1014	1015
12	1014	1024	1022	1012	1021	1013	1016	1013	1013
13	1015	1017	1017	1009	1012	1015	1013	1017	1013
14	1015	1005	1015	1013	1022	1016	1012	1019	1014
15	1022	1011	1009	1009	1017	1016	1016	1019	1013
16	1019	1018	1007	1017	1017	1016	1020	1020	1005
17	1014	1014	1009	1018	1016	1014	1021	1019	1016
18	1005	1014	1006	1014	1017	1010	1020	1020	1020
19	1021	1007	1001	1011	1014	1010	1016	1022	1018
20	1026	1011	1011	1011	1010	1012	1015	1023	1015
21	1028	1014	1014	1018	1000	1013	1014	1023	1011
22	1025	1011	1017	1016	1012	1013	1013	1021	1014
23	1012	1006	1021	1018	1012	1014	1015	1021	1017
24	1015	1020	1016	1021	1015	1014	1016	1020	1017
25	1025	1018	1016	1007	1015	1016	1016	1017	1017
26	1015	1013	1030	1007	1012	1019	1020	1015	1014
27	1026	1010	1025	1018	1010	1019	1022	1015	1012
28	1028	1020	1015	1013	1009	1019	1021	1018	1018
29	1020	1025	1016	1009	1012	1019	1021	1018	1022
30	1018		1013	1013	1017	1017	1018	1017	1024
31	1021		1008		1020		1017	1016	

Table 2.4.1 Mean Daily Barometric Pressures (mb) at Nashville WSG Airport in 1996 (Data Courtesy of the Department of Geography and Geology at Western Kentucky University)

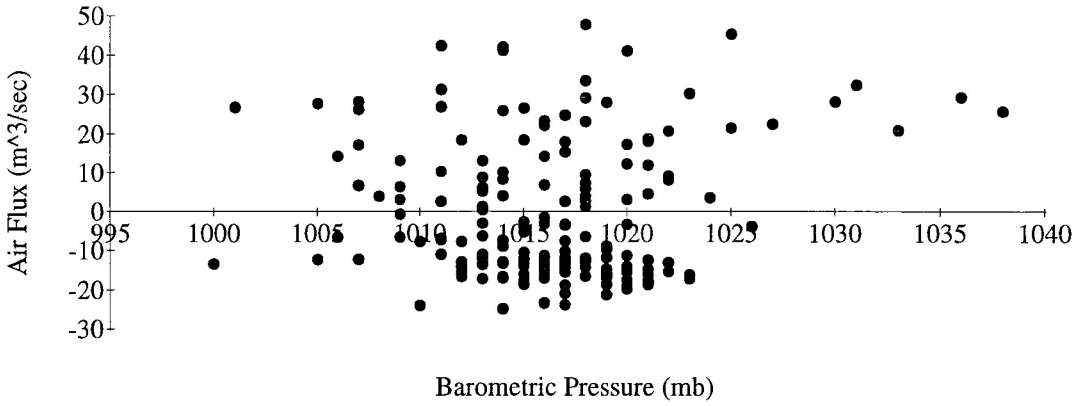

Figure 2.4.4 - Observed Dependence of Average Daily Air Flux in Houchins' Narrows on Average Daily Barometric Pressure at Nashville WSG Airport on Julian days 44 - 274 of 1996

In contrast, the data in Figure 2.4.4 does not show any relationship between air flux in Houchins' Narrows and the barometric pressure outside the cave system (the barometric pressure data was taken from a weather station in Nashville, Tennessee, but it will be assumed that barometric pressure at Mammoth Cave National Park is approximately the same as that in Nashville). Using regression analysis to fit a line to this data gives a value of R-squared equaling .01, so there is essentially no linear dependence of average daily air flux in Houchins' Narrows on average daily barometric pressure. It may be true that fitting a nonlinear set of basis functions to the data in Figure 2.4.4 will produce a higher value for R-squared, but the random nature of the scatter plot would imply that no such set of basis functions will exist.

Since the value of R-squared is high for the linear regression performed on average daily air flux as a function of average daily outdoor temperature and since the value of R-squared is low for average daily air flux as a function of average daily barometric pressure, it may be conjectured that, at least on a daily basis, airflow in the

Historic Section of Mammoth Cave is driven by temperature differentials and is not driven by changes in barometric pressure.

2.5 Diurnal Cycles in Houchins' Narrows Summer Air Flux Data

Outdoor air temperature in Mammoth Cave National Park during the summer is consistently above the average cave air temperature of 55° - 57°F. However, the temperature differential in the day is larger than the temperature differential at night. Thus, air exchange during the day is expected to be larger than air exchange during the night.

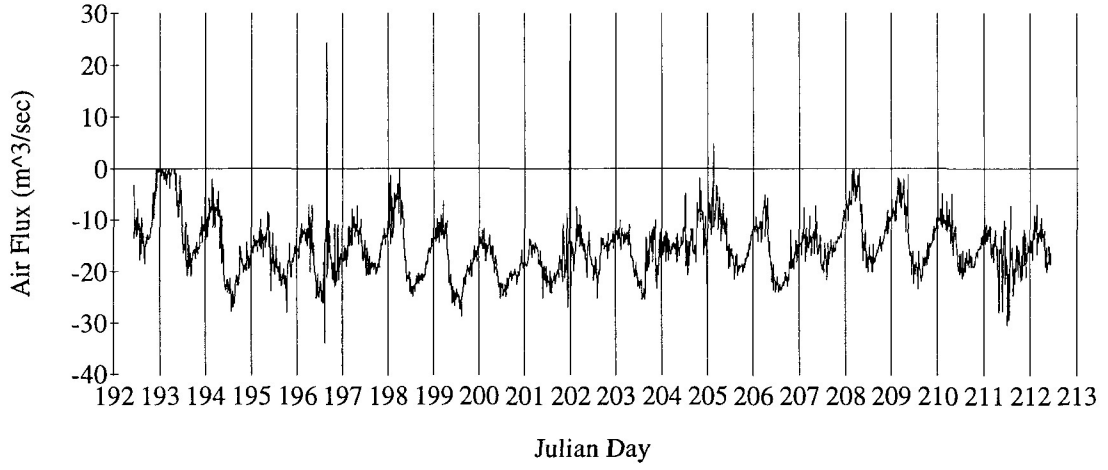

Figure 2.5.1 - Air Flux in Houchins' Narrows on Julian Days 192 - 212 of 1996

Figure 2.5.1 shows air flux in Houchins' Narrows for Julian days 192 - 212 of 1996. The vertical gridlines occur at midnight of the beginning of the day indicated. At this time or shortly thereafter, air flux values obtain the maximum for the day. Conversely, minimum values for air flux occur a little after noon each day. Since positive flux is into the cave and negative flux is outcast, maximum values of air flux

correspond to the smallest amounts of outcast air; this phenomenon occurs during the night, just as expected. Similarly, minimum values of air flux correspond to the largest amounts of outcast air; this phenomenon occurs during the day, just as predicted by the chimney effect hypothesis.

2.6 Air Flux in Houchins' Narrows as a Function of Temperature Differential Between the Air in Houchins' Narrows and the Air in Booth's Amphitheater

The chimney effect hypothesis states that cooler air will fall in elevation when in the presence of warmer air, which will rise to take the place of the cooler air. When it is winter in Mammoth Cave National Park and outdoor air is cooler than the air inside the cave, air within the cave rises out of upper entrances and is replaced through influx of cooler air through lower entrances such as the Historic Entrance. This cooler outdoor air rushes in through the Historic Entrance, down through Houchins' Narrows, into the Rotunda, and down Broadway into Main Cave where it passes the Booth's Amphitheater CAM site (see Appendix 4 for a map). As this air is flowing along the passage, it is absorbing heat from the walls of the cave system and becoming warmer. Therefore, it is expected that sites deeper within the cave system than Houchins' Narrows will have warmer air temperatures than those in Houchins' Narrows.

Let T_H denote the air temperature (in °C) at the Houchins' Narrows CAM site and let T_α denote the air temperature at the CAM site in question. As before, let $\mathbf{F}_H$ denote the air flux in Houchins' Narrows. When airflow is into the cave, that is when $\mathbf{F}_H > 0$, it is expected that T_α will be greater than T_H for α a CAM site lower in elevation than Houchins' Narrows. Letting

$$\Delta T = T_\alpha - T_H, \tag{2.6.1}$$

the chimney effect hypothesis implies that $\Delta T > 0$ when $\mathbf{F}_H > 0$.

Figure 2.6.1 shows a scatter plot of Julian Days 1 - 20 of 1997 for air flux in Houchins' Narrows as a function of the temperature differential

$$\Delta T = T_B - T_H, \tag{2.6.2}$$

where T_B is the temperature of the air at the floor probe in Booth's Amphitheater. Since it is true that when ΔT is approximately greater than zero, air flux in Houchins' Narrows is also greater than zero, the data in Figure 2.4.1 behaves as the chimney effect hypothesis implies it should. These scatter plots behave similarly at other times during the year and are shown in Appendix 2.

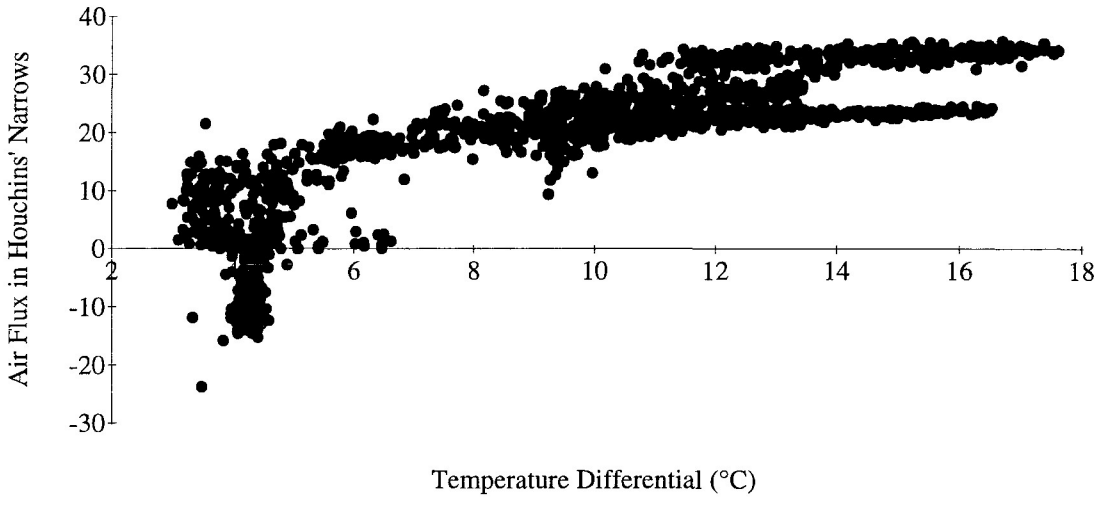

Figure 2.6.1 - Air Flux in Houchins' Narrows (m^3/sec) as a Function of the Temperature Differential $\Delta T = T_B \quad T_H$ for Julian Days 1 20, 1997

2.7 Temperature Stratification in Booth's Amphitheater Data as Local Evidence of the Chimney Effect

Figure 2.7.1 shows air temperature data at the floor, a ledge, and the ceiling in Booth's Amphitheater for Julian Days 57 - 80 of 1996. The temperature at the floor is consistently cooler than the air temperature at the ledge, which is consistently cooler than the air temperature at the ceiling. Therefore, this data set shows that locally warmer air

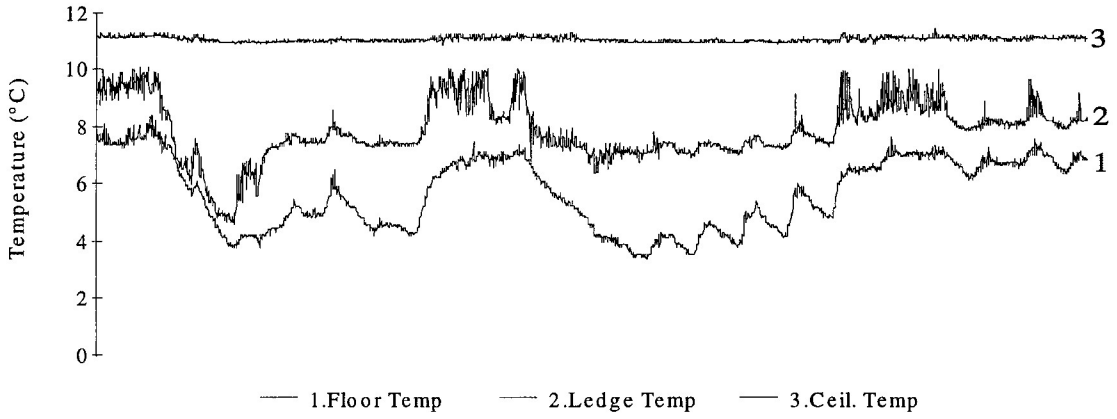

Figure 2.7.1 - Booth's Amphitheater Data for Julian Days 57 - 80, 1996

rises above locally cooler air. Extending this idea and applying it to the entire cave system gives further support of the chimney effect hypothesis. Other data sets for Booth's Amphitheater (found in Appendix 3) show a similar relationship between air temperatures at the three probes, although summer data sets show air temperature at the ledge to be cooler than that at the floor. Thus far, no explanation for this anomaly has been conceived.

2.8 Temperature Stratification Between CAM Sites

Similar to the temperature stratification in Booth's Amphitheater, levels in temperature may also be seen when air temperatures at the various CAM sites are plotted along the same axis. Figure 2.8.1 shows air temperatures at several CAM sites for Julian

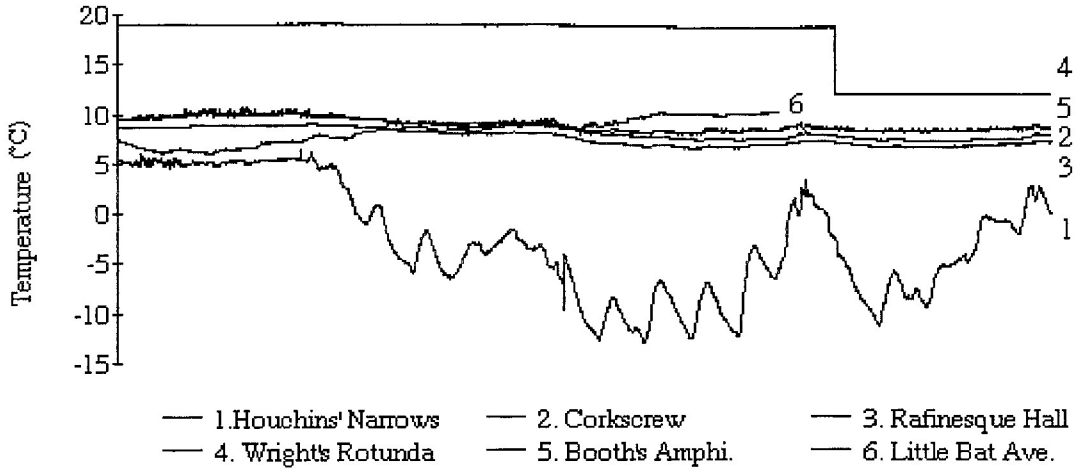

Figure 2.8.1 - Air Temperatures at Designated CAM Sites for Julian Days 1 - 20, 1997

days 1 - 20, 1997. The site labeled 1 is consistently cooler than 3 which is cooler than 2 and so forth. A complete listing of this order is found in Chart 2.8.1 below along with the elevations at each site (elevation data was estimated using an illustration in the book by Palmer (1981)).

Site Number	Site Name	Site Elevation (feet)
1	Houchins' Narrows	630
3	Rafinesque Hall	600
2	Corkscrew	625
5	Booth's Amphitheater	590
6	Little Bat Avenue	575
4	Wright's Rotunda	600

Chart 2.8.1 CAM Sites and their Elevations in Ascending Order of Air Temperature

Temperature increases as air moves from Houchins' Narrows to Rafinesque Hall. This course represents one of the possible paths that air may flow through the cave and shows air moves from higher elevations to lower elevations, getting warmed by its surroundings as it moves from one CAM site to the other (see map in Appendix 4). The same result is true for air flowing from Houchins' Narrows to Little Bat Avenue, as well as air flowing from Houchins' Narrows to the Corkscrew to Booth's Amphitheater. The exception is going from Booth's Amphitheater to Wright's Rotunda where the air at a higher elevation is warmer than that at a lower elevation. However, this temperature differential is driving airflow in the entire cave system and behaves exactly as the chimney effect hypothesis states it should.

2.9 Relation Between Air Temperatures at Distinct CAM Sites

In section 2.7, the stratification of air temperatures in Booth's Amphitheater was postulated to be caused by the chimney effect. Hence, another way to verify the chimney effect in the Historic Section of Mammoth Cave is to construct scatter plots of air temperatures at a higher elevation in the cave as a function of air temperatures at a lower elevation in the cave. If the form of this scatter plot is the same as that obtained when air temperature at the ledge of Booth's Amphitheater is plotted as a function of the air temperature at the floor of Booth's Amphitheater, then this data will provide further support of the chimney effect hypothesis.

Figure 2.9.1 shows air temperature at the ledge of Booth's Amphitheater as a function of air temperature at the floor of Booth's Amphitheater for Julian days 1 - 20, 1997. The relation looks as if it is approximately linear. The scatter plot for air temperature in Houchins' Narrows as a function of air temperature at the floor of Booth's

Amphitheater in Figure 2.9.2 is approximately linear as well; thus it supports the chimney effect hypothesis.

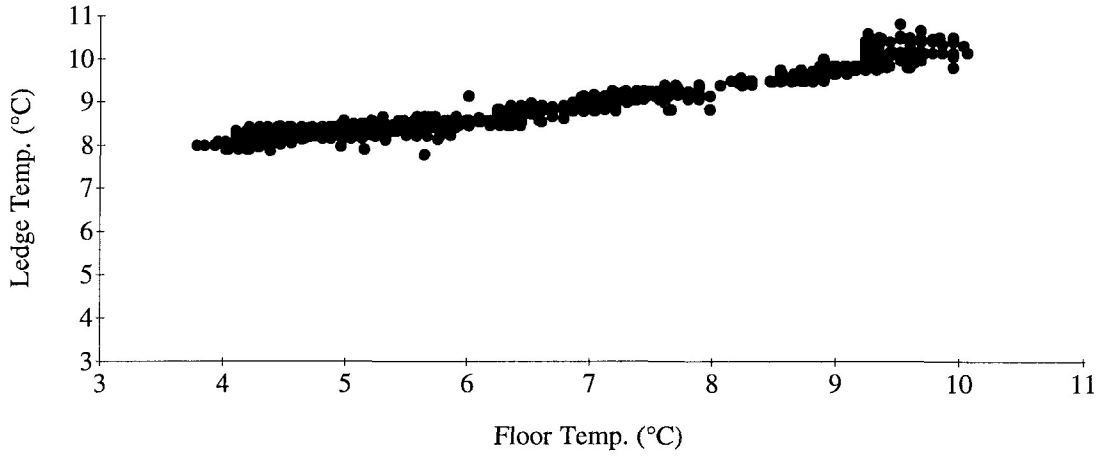

Figure 2.9.1 - Observed Dependence of Air Temperature at the Ledge of Booth's Amphitheater as a Function of Air Temperature at the Floor of Booth's Amphitheater, Julian Days 1 - 20, 1997

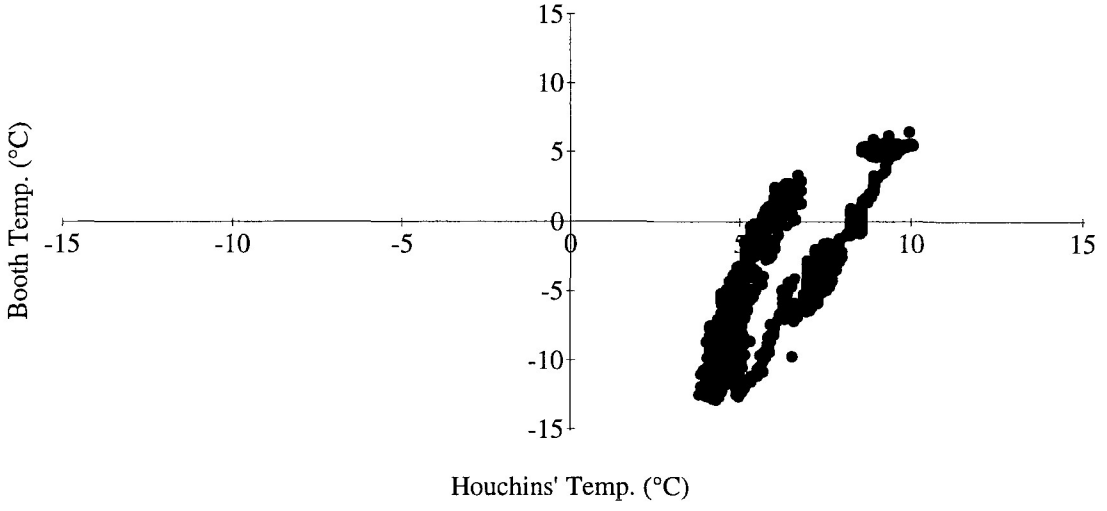

Figure 2.9.2 - Observed Dependence Between Air Temperature at Houchins' Narrows on Air Temperature at the Floor of Booth's Amphitheater, Julian Days 1 20, 1997

Figure 2.9.3 shows air temperature in the Corkscrew as a function of air temperature in River Hall; these two CAM sites are directly connected by a narrow, rubble filled passage. The relation is nearly linear, just as in Figure 2.9.1 and Figure 2.9.2. Therefore, these scatter plots reinforce the hypothesis that airflow in Mammoth Cave is driven by the chimney effect.

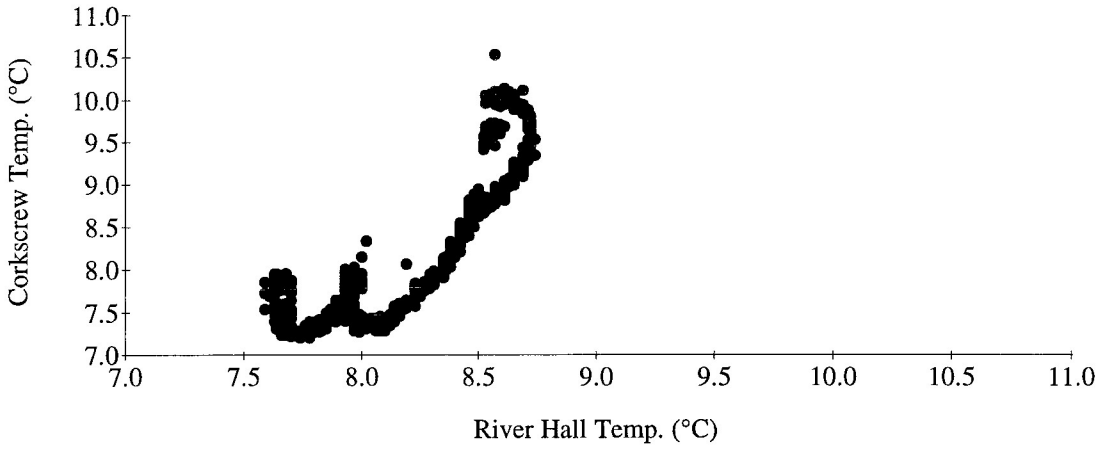

Figure 2.9.3 - Observed Dependence of Air Temperature in the Corkscrew on Air Temperature in River Hall, Julian Days 1 - 20, 1997

2.10 Conclusions

There is much evidence to indicate that the chimney effect is driving the flow of air in the Historic Section of Mammoth Cave. Frequency distributions and means of air flux values consistent with those expected under natural convective processes, a high level of correspondence between mean daily air flux and outdoor air temperature values, and diurnal patterns in the air flux values obtained during the summer are a few of the ways data from the CAM stations support the chimney effect hypothesis.

Now that it has been established that temperature differentials are the driving force behind airflow in Mammoth Cave, it will be possible to construct models which relate airflow and air temperature. An accurate model will allow the prediction of air temperature at one CAM site based on atmospheric data from another CAM station. The construction of such a mathematical model is the subject of Chapter 3.

CHAPTER 3

PREDICTING AIR TEMPERATURE IN THE HISTORIC SECTION OF MAMMOTH CAVE

3.1 Introduction

In Chapter 1 the goal was set forth to determine the temperature at various CAM sites within the Historic Section of Mammoth Cave based upon atmospheric conditions in Houchins' Narrows. In this chapter, the author will accomplish that task through regression analysis of data gathered by Science and Resource Management personnel at Mammoth Cave National Park.

Mooney and Swift (in press) describe the regression process of fitting data to a linear combination of *basis functions*. For example, the set of paired values (t , T_H), where t is Julian time and T_H is air temperature (in ^oC) in Houchins' Narrows, plotted in Figure 3.1.1 shows a linear relationship between Julian time and air temperature. Hence, the trend in the data may be approximated by the linear function $T_H = f(t) = \beta_o + \beta_1 t$, where β_o and β_1 are appropriate constants -- that is, the function f is a linear combination of the set of *basis functions* $\{1,t\}$. Regression may, in general, be performed with any set of independent basis functions.

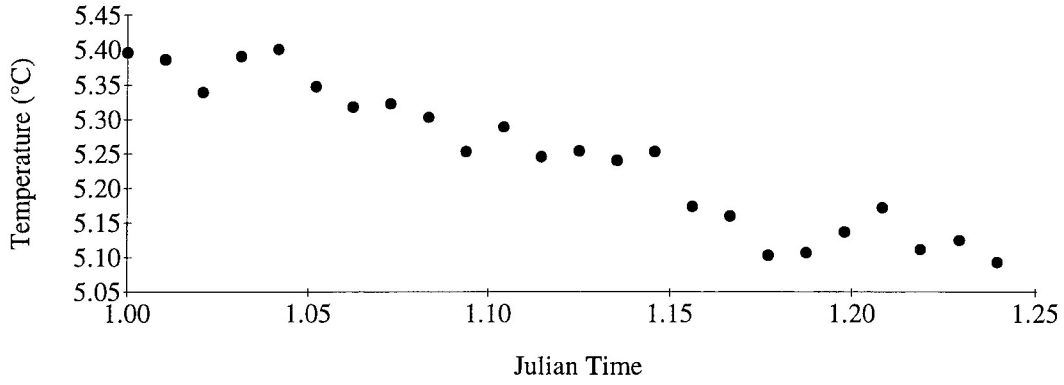

Figure 3.1.1 The First Six Hours of Air Temperature Data from Houchins' Narrows in 1997

Once the trend in the data is identified and a set of basis functions has been determined, the value of the coefficients must be determined. This computation is usually accomplished through the use of computer software (for the work in this thesis, Sigma Stat has been used). The data in Figure 3.1.1, for example, have best fit coefficients $\beta_0 = 6.762$ and $\beta_1 = -1.353$, so the line $f = 6.762 - 1.353t$ describes the trend in this data. Figure 3.1.2 shows the line f along with the original data.

There are measures which describe how well the regression equation fits the original data. The *residuals* are the vertical distances between each of the data points and the regression equation, so for a perfect fit each of the residuals is zero. In order to quantify the quality of a regression fit, a value known as *R-squared* is calculated. For paired data (x_i , y_i), the value of R-squared is given by

$$R^2 = \frac{\sum(\hat{y}_i - \overline{y})^2}{\sum(\hat{y}_i - \overline{y})^2 + \sum(y_i - \hat{y}_i)^2}, \qquad (3.1.1)$$

where $\bar{y}$ is the mean of the y_i's and $\hat{y}_i$ is the value for the y_i predicted by the regression equation. A value of R-squared close to one indicates a good fit and a value of R-squared close to zero indicates a poor fit. The regression fit in Figure 3.1.2 has a value of R-squared equaling .921 (92.1% of the deviation is accounted for by the model). For a detailed discussion of regression, see Mooney and Swift (in press).

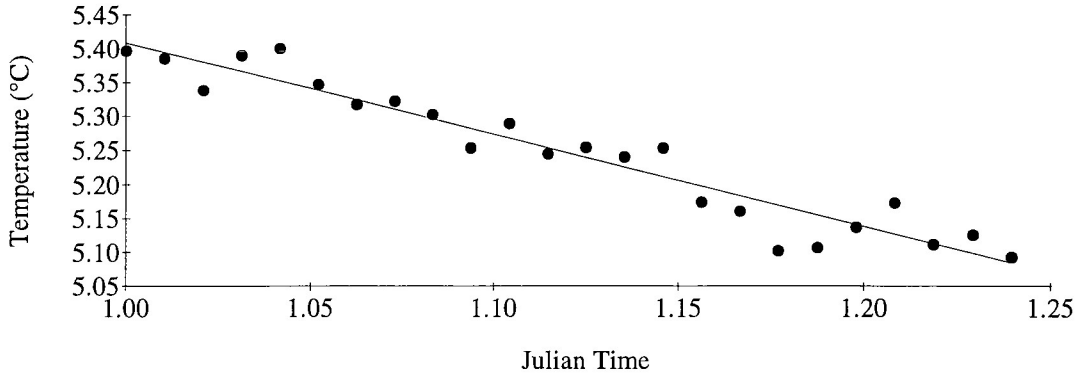

Figure 3.1.2 - Data in Figure 3.1.1 and Its Line of Best Fit

In order to determine the appropriate basis functions to be used in the linear regression performed in this chapter, it will be necessary to construct an approximate model of airflow throughout the Historic Section of Mammoth Cave. This model should relate air temperature, rock temperature, and air flux data from Houchins' Narrows to air temperature data at the CAM site in question. That is,

$$T_a = G(T_H, R_H, \mathbf{F}_H), \tag{3.1.2}$$

where G is the function defining the relation between the designated location and Houchins' Narrows, T_H is air temperature in Houchins' Narrows, R_H is rock temperature

(^oC) in Houchins' Narrows, $\mathbf{F}_H$ is air flux in Houchins' Narrows (m^3/sec), and the subscript α denotes the CAM site in question. For example, the subscript B will be used to denote air temperature data at the floor of Booth's Amphitheater. A complete list of the designations of α is given in Table 3.1.1.

CAM Site	α	CAM Site	α
Corkscrew	co	Booth's Amphitheater	ba or B
Wright's Rotunda	wr	Little Bat Avenue	lb
River Hall	ri	Rafinesque Hall	ra
Mushroom Vats	mu	Houchins' Narrows	hn or H

Table 3.1.1 - Notation Assigned to Each CAM Site

Constructing the appropriate model is a multiple step process. The first step will be to derive a model which is believed to account for the general trend in the data. From the derived theoretical model, nonlinear regression analysis will be applied to data gathered by Science and Resource Management personnel. Next, a refinement of the original model will be achieved by adding a new basis function which accounts for some physical phenomenon not previously considered. This process will be repeated until all effects are taken into account and the residuals are minimized so that the model is as accurate as possible. The final model will have the form

$$T_a = G_\beta (T_H , R_H , \mathbf{F}_H), \tag{3.1.3}$$

where β is the β^{th} step in the refinement process and α is an identification code for the CAM site in question.

3.2 The First Step - A Temperature Dependent Version of Bernoulli's Equation

Bernoulli's equation relates variables between two points in a fluid flowing within a tube, as illustrated in Figure 3.2.1. Mott (1979) states Bernoulli's equation as follows:

$$w\left(\frac{p_1}{\gamma}+z_1+\frac{v_1^2}{2g}\right)=w\left(\frac{p_2}{\gamma}+z_2+\frac{v_2^2}{2g}\right), \tag{3.2.1}$$

where w is the weight (metric tons) of some set volume of fluid at both points, γ is the specific weight (N/m^3) of the fluid, p_α is the pressure (N/m^2) at each point, z_α is the elevation (m) at each point, v_α is the velocity (m/sec) of the fluid at each point, and g is the acceleration due to gravity(m/sec^2).

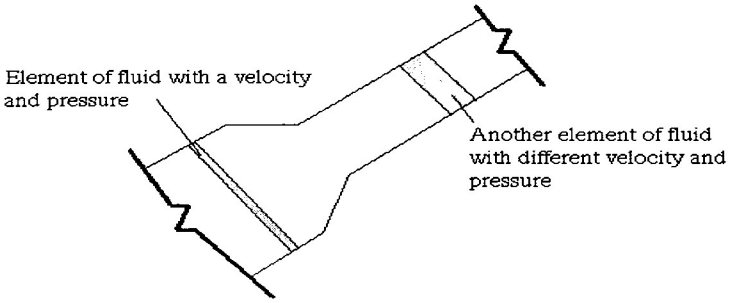

Figure 3.2.1 - Illustration Showing Conditions Under which Bernoulli's Equation may be Utilized

This relationship is valid only if temperature is assumed to be constant throughout the tube, so that weight and volume are constant and are therefore equivalent measures for the element of fluid. Bernoulli's equation requires either weight or volume of the fluid to remain constant. There are instances in the following derivation when it will be convenient to allow weight rather than volume to remain constant as well as situations where volume will be desired to remain constant rather than weight. Since the goal is to

get an idea of the nature of the temperature dependence of air flux and there is little change in the volume of air with temperature changes, interchanging which of volume and weight is considered constant will have little effect on determining the nature of such dependence.

Substances in an open system undergo volumetric expansion or contraction upon heating and, according to Joseph et al. (1978), do so according to the expression

$$V = V_0 \left(1 + \beta \Delta T\right), \tag{3.2.2}$$

where β ($^oC^{-1}$) is an expansion coefficient dependent upon the material, V and V_0 are volume (m^3), and ΔT is the change in temperature T T_0 (^oC). So if the temperature increases and $\beta > 0$, for example, then the value of $\beta\Delta t$ is positive, and the volume of the substance will increase from V_0 to V for the same mass of material. This idea is illustrated in Figure 3.2.2.

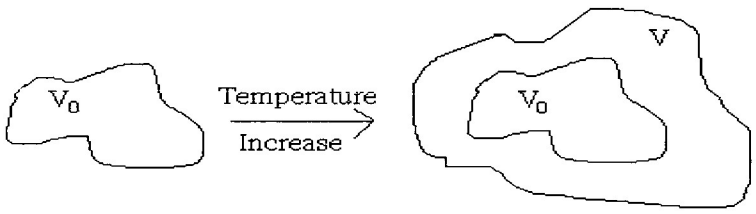

Figure 3.2.2 - When the Temperature of Most Substances Increases, so Does the Volume They Take Up

Density, denoted ρ (metric tons/m^3), is defined by

$$\rho = \frac{m}{V}, \tag{3.2.3}$$

where m is mass (metric tons) and V is volume. As volume increases and mass remains constant, the density must decrease. This idea is illustrated in Figure 3.2.3.

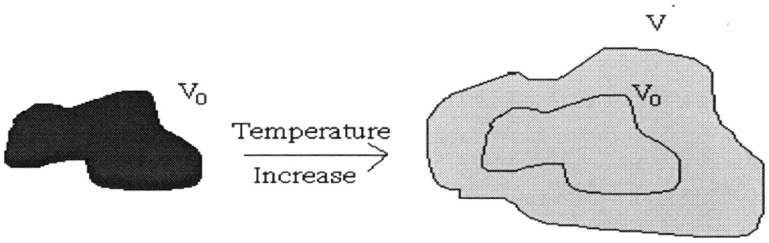

Figure 3.2.3 - If the Volume of a Set Mass of Material Increases, then the Density of the Mass throughout the Volume Decreases.

Mass is related to weight by the equation

$$w = mg, \tag{3.2.4}$$

where w denotes weight. Solving for m and substituting into (3.2.3) gives

$$\rho = \frac{w}{Vg}. \tag{3.2.5}$$

This equation implies if, for a fixed volume V_0, the density decreases, then so must the weight of the amount of material contained in that volume.

Combining these facts implies that the same volume of a material at different temperatures will have different weights (since its density has changed). Hence, the introduction of the variables w_1 and w_2 into Bernoulli's equation to account for the

temperature differential between site1 and site 2 is justified. Furthermore, the specific weight γ is also temperature dependent. So, Bernoulli's equation now becomes

$$w_1\left(\frac{p_1}{\gamma_1}+z_1+\frac{v_1^2}{2g}\right)=w_2\left(\frac{p_2}{\gamma_2}+z_2+\frac{v_2^2}{2g}\right). \tag{3.2.6}$$

Solving for w in (3.2.5), substituting into (3.2.6), and dividing by the constant Vg gives

$$\rho_1\left(\frac{p_1}{\gamma_1}+z_1+\frac{v_1^2}{2g}\right)=\rho_2\left(\frac{p_2}{\gamma_2}+z_2+\frac{v_2^2}{2g}\right). \tag{3.2.7}$$

A relation between the density of a material and its temperature is required. Letting the mass remain constant in (3.2.3) and considering two cases where the densities of the mass are different gives

$$\rho_1 V_1 = \rho_2 V_2. \tag{3.2.8}$$

Simple algebraic manipulation gives

$$\frac{\rho_1}{\rho_2} = \frac{V_2}{V_1}. \tag{3.2.9}$$

Recalling (3.2.2), letting $V = V_2$ and $V_0 = V_1$, dividing by V_1, and substituting into (3.2.9) yields

$$\frac{\rho_1}{\rho_2} = (1 + \beta \Delta T). \tag{3.2.10}$$

Solving for ρ_1, substituting into (3.2.7) and dividing out common terms, gives

$$(1 + \beta \Delta T)\left(\frac{p_1}{\gamma_1} + z_1 + \frac{v_1^2}{2g}\right) = \left(\frac{p_2}{\gamma_2} + z_2 + \frac{v_2^2}{2g}\right). \tag{3.2.11}$$

Equation (3.2.11) is a temperature dependent relation between conditions in two locations of a tube.

3.3 Applying Bernoulli's Equation to Houchins' Narrows and Booth's Amphitheater Data

Equation (3.2.11) gives a temperature dependent relation between airflow in two distinct locations within a tube. This equation will be used as a basis for the nonlinear regression in the following section -- that is, (3.2.11) will be used to determine the linear combination of functions of air flux and air temperature in Houchins' Narrows which best describes temperature in Booth's Amphitheater; and the coefficients for these functions will be determined using regression techniques. Since (3.2.11) will not be used explicitly to determine the relation between air temperature in Booth's Amphitheater and air temperature and flux in Houchins' Narrows, many of the conditions imposed on Bernoulli's equation may be disregarded.

The conditions for applying Bernoulli's equation are:

1. Fluid in question must be incompressible.
2. There must be no mechanical devices to add or to remove energy between the two sites in consideration.

3. There may be no heat exchange between the fluid and its surroundings.
4. There is no energy lost due to friction.

Air is a compressible fluid, but airflow through a cave system may be considered incompressible. Incompressible flows have the property that changes in parameter values at a given point instantaneously affect parameter values at another point. To support the claim that airflow in Mammoth Cave is behaving as an incompressible fluid, consider the data in Figure 3.3.1. Figure 3.3.1 shows airflow in Houchins' Narrows and air temperature at the floor of Booth's Amphitheater on the same set of axes for Julian days 1 - 20 of 1997. Observe that each event in Houchins' Narrows corresponds with each event in Booth's Amphitheater at the same point in time, indicating no time delay before the effects of conditions in one site are manifested in another. Hence, Figure 3.3.1 supports the claim that airflow is incompressible.

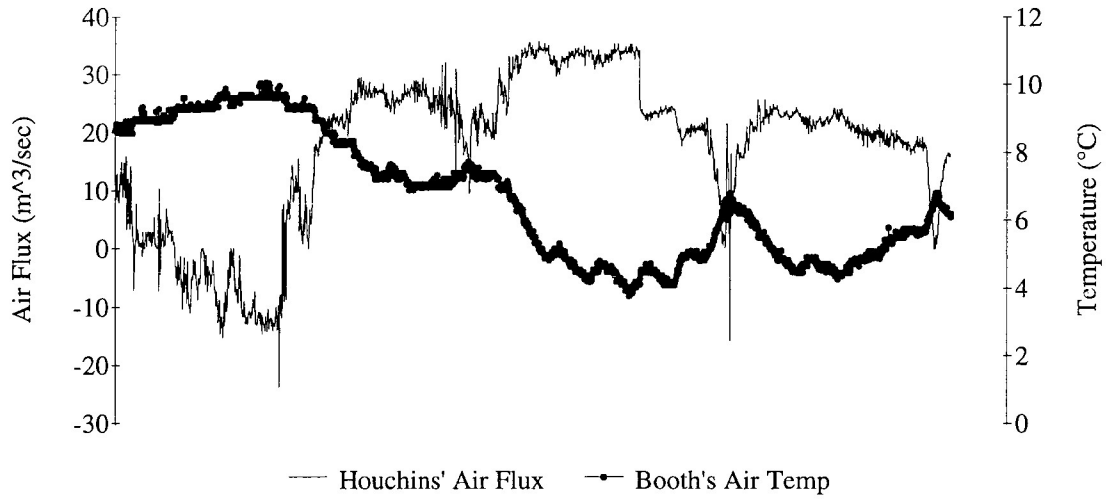

Figure 3.3.1 Airflow in Houchins' Narrows and Air Temperature at the Floor of Booth's Amphitheater along the Same Time Axis, Julian Days 1 - 20, 1997.

The second assumption of no mechanical devices adding or removing energy in going from site to site is invalid in going from Houchins' Narrows to Booth's Amphitheater (see the map of the CAM sites in Appendix 4 to visualize this airflow pattern). The passage branches in the Rotunda so that air may flow into Audubon Avenue or Broadway and Main Cave (where Booth's Amphitheater is located). Audubon Avenue could be either an energy source or an energy sink depending on the direction of airflow. This effect will be taken into account in the refinement process which follows in section 3.6.

Assumption 3 is invalid since there is constant heat exchange between the rock and the air throughout the cave. Figure 3.3.2 shows air temperature and rock temperature in Houchins' Narrows as each varies in time for Julian days 1 20 of 1997. Air temperature has a definite effect on rock temperature in Houchins' Narrows since rock temperature follows the same trend as does air temperature indicating heat exchange between air and rock in Houchins' Narrows. The same effect may be assumed throughout the Historic Section of Mammoth Cave and will be taken into account in section 3.7.

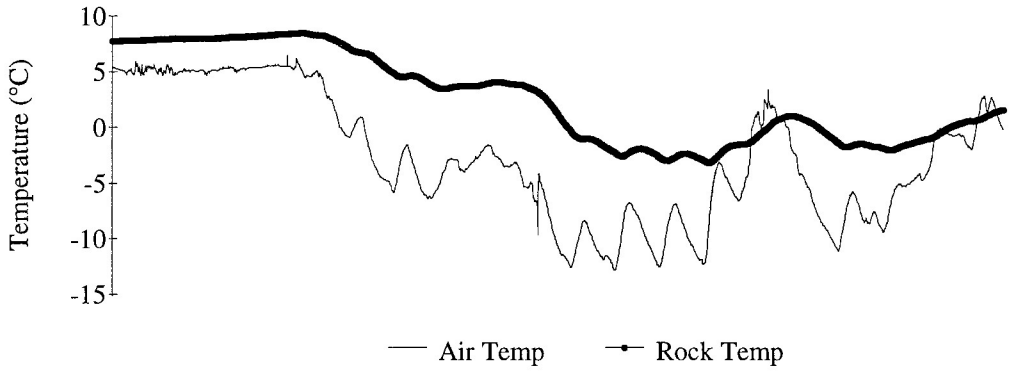

Figure 3.3.2 - Graph Showing Heat Exchange Between Air and Rock in Houchins' Narrows

The walls of the Mammoth Cave system are irregular and course, so friction losses are significant. However, as a simplifying assumption, friction losses will be assumed insignificant. This assumption is a reasonable one since air flux (and, therefore, flow of energy) is large throughout the cave.

3.4 Equations Defining Relationship Between Conditions in Houchins' Narrows and Booth's Amphitheater - Phase 1 Bernoulli Model

Allowing Booth's Amphitheater to be Site 1 and Houchins' Narrows to be Site 2, (3.2.11) may be applied to airflow from Houchins' Narrows to Booth's Amphitheater. There are no air velocity measurements available for Booth's Amphitheater since there is little flow through this section, so the wind speed (and therefore velocity) here may be assumed to be zero, and hence the flux is zero as well by (1.3.1). Therefore, (3.2.11) becomes

$$T_B = \frac{1}{\beta}\left(1 - \frac{\frac{p_H}{\gamma_H} + z_H + \frac{V_H^2}{2g}}{\frac{p_B}{\gamma_B} + z_B}\right) + T_H \,. \tag{3.4.1}$$

The quantities z_H and z_B are the elevations of the CAM sites and thus are constants. The values p_H and p_B are pressures at each CAM site, but pressure is assumed not to be a driving force behind airflow in Mammoth Cave. So, for the moment, p_H and p_B will be considered constants and equal. Recall that β and g are also constants.

The only remaining quantities on the right hand side of (3.4.1), other than V_H and T_H, are the specific weights of the air at each CAM site, γ_H and γ_B. The value of γ is temperature dependent and therefore varies over time since the temperature at each CAM

site varies over time. A table and graph showing the temperature dependence of γ are shown in Figure 3.4.1; the data is from Mott (1979).

In Houchins' Narrows, where air temperature varies most, the minimum and maximum air temperatures from April 1996 to March 1997 were -12.89° and 15.83°C, respectively (as shown in Table 3.4.1). Hence γ ranges from about 13 N/m^3 to 11.8 N/m^3 and has a range of 1.2 N/m^3. Equation (3.4.1) has a $1/\gamma$ term which will then vary from 1/13 m^3/N to 1/11.8 m^3/N and a range of (1/11.8 m^3/N - 1/13 m^3/N) or .00783 m^3/N. The variation in this term will be considered insignificant.

Temperature (°C)	Specific Weight (N/m^3)	Temperature (°C)	Specific Weight (N/m^3)	Temperature (°C)	Specific Weight (N/m^3)
-40	14.85	20	11.81	80	9.802
-30	14.24	30	11.42	90	9.532
-20	13.67	40	11.05	100	9.277
-10	13.15	50	10.71	110	9.034
0	12.67	60	10.39	120	8.805
10	12.23	70	10.09		

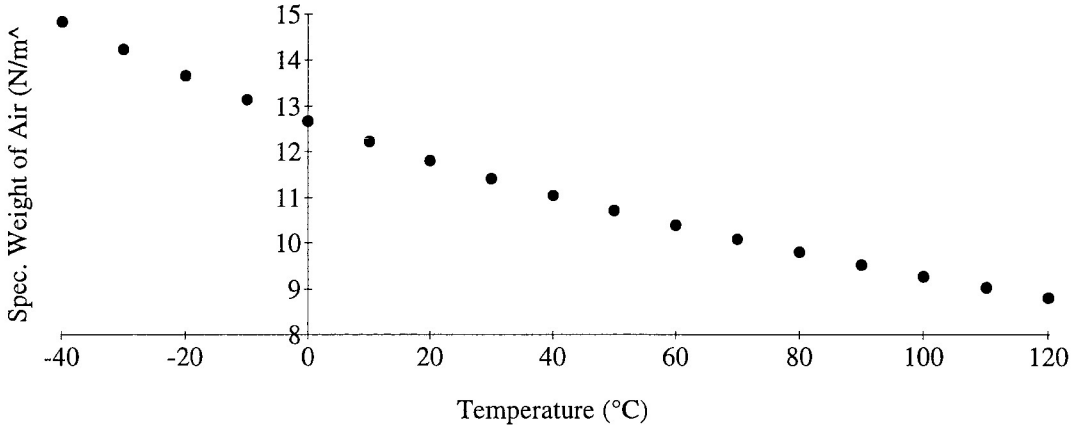

Figure 3.4.1 - Specific Weight of Air at Standard Atmospheric Pressure and Sea Level (Tabular and Graphic Form)

Based upon the previous assumptions and (3.4.1), the relationship between air temperature at the floor in Booth's Amphitheater and air temperature and velocity in Houchins' Narrows is

$$T_B = a'V_H^2 + b + T_H, \tag{3.4.2}$$

Julian Days and Year	Minimum Temperature (°C)	Maximum Temperature (°C)
91 - 110, 1996	-6.029	10.23
111 130, 1996	2.707	13.39
131 - 150, 1996	2.913	14.5
151 170, 1996	9.01	15.83
195 - 210, 1996	10.43	14.07
221 - 240, 1996	10.36	15.37
245 - 265, 1996	8.01	12.89
270 - 290, 1996	3.586	13.26
321 - 346, 1996	-3.179	8.7
348 - 366, 1996	-10.29	6.119
1 - 20, 1997	-12.89	6.468
21 - 40, 1997	-5.936	7.66
41 - 60, 1997	-3.179	8.51
61 77, 1997	-3.456	7.81

Table 3.4.1 - Minimum and Maximum Air Temperatures in Houchins' Narrows

where a' and b are appropriate constants to be determined using regression techniques in the following section. However, air velocity in Houchins' Narrows is related to air flux in Houchins' Narrows by (1.3.1). Squaring (1.3.1) and substituting into (3.4.2) yields

$$T_B = a\mathbf{F}_H^2 + b + T_H. \tag{3.4.3}$$

The set $\{1,T_H,\mathbf{F}_H\}$ will be the set of basis functions used in the regression of section 3.5. Using (3.4.3) together with the regression coefficients in the following section, a Phase 1 Bernoulli model will be constructed. The model will be called a "Phase 1 Bernoulli model" since it is the first phase in a series of refinements based upon Bernoulli's equation.

3.5 Regression Analysis of Houchins' Narrows and Booth's Amphitheater Data

In order to verify that data measurements match the behavior dictated by (3.4.4), it is necessary to construct a three dimensional scatter plot showing the observed dependence of air temperature at the floor of Booth's Amphitheater upon air temperature and air flux in Houchins' Narrows. So, let $\mathbf{F}_H$ be air flux in Houchins' Narrows, T_H be air temperature in Houchins' Narrows, and T_B be air temperature at the floor of Booth's Amphitheater for each point in time and plot the series of ordered triples ($\mathbf{F}_H$, T_H, T_B) on a set of axes. Doing so for Julian Days 1 20 of 1997 results in the three dimensional scatter plot of Figure 3.5.1.

It is easy to see the data are following a definite relationship; in fact, a reasonable guess at what relationship the data follows is quadratic in air flux in Houchins' Narrows plus a linear air temperature term in Houchins' Narrows, just as predicted. Hence a reasonable guess at the relationship seen in Figure 3.5.1 is given by (3.4.4). The constants a and b are determined using nonlinear regression techniques, the results of which are shown in Regression Sheet 3.5.1. Using the values for a and b in the regression sheet gives the following relationship between air temperature at the floor of Booth's Amphitheater and air temperature and flux in Houchins' Narrows:

$$T_B = .0103\mathbf{F}_H^2 + 4.452 + T_H. \tag{3.5.1}$$

An idea for how effective this model is at predicting air temperature at the floor of Booth's Amphitheater may be obtained through analysis of Regression Sheet 3.5.1.

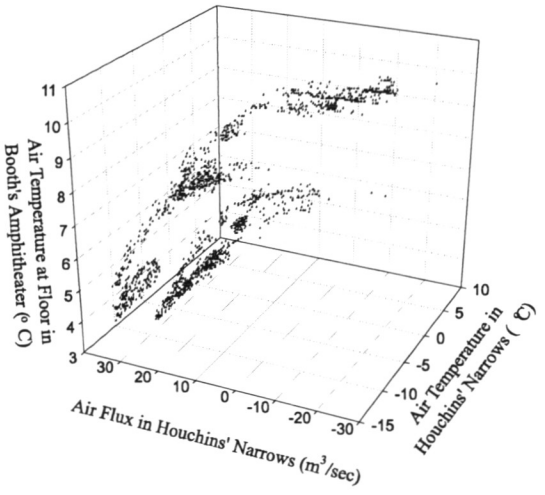

Figure 3.5.1 - Scatter Plot of Air Temperature at Floor of Booth's Amphitheater with Air Temperature and Flux in Houchins' Narrows, Julian Days 1 - 20 of 1997

R = 0.854 Rsqr = 0.730 Adj Rsqr = 0.730

Standard Error of Estimate = 1.958

	Coefficient	Std. Error	t	P	VIF
a	0.0103	0.000127	80.727	<0.001	2.811
b	4.452	0.0749	59.430	<0.001	2.811

Analysis of Variance:

	DF	SS	MS	F	P
Regression	1	19857.040	19857.040	5181.662	<0.001
Residual	1918	7350.114	3.832		
Total	1919	27207.154	14.178		

Normality Test: Failed (P = 0.040)
Constant Variance Test: Failed (P = <0.001)
Power of performed test with alpha = 0.050: 1.000

Regression Sheet 3.5.1 - Regression Results Using (3.4.4) as Basis Function

For example, a value of R-squared equaling .730 indicates the model accounts for 73.0 % of the variance in the data. Failing the normality test indicates the residuals are not normally distributed, so the model does not on average predict the air temperature at the floor of Booth's Amphitheater. Failing the constant variance test indicates there is variance in the residuals which may not be explained by the basis functions considered in this model. The terms a and b both have P-values of <.001, indicating 99 percent confidence in the accuracy of the values of the best fit coefficients.

3.6 Heat Exchange with Audubon Avenue in the Rotunda Room of Mammoth Cave - Phase 2 Bernoulli Model

Assumption 3 in section 3.3 was to disregard energy losses due to mechanical devices outside the system in question. However, air flowing from Houchins' Narrows to Booth's Amphitheater must go through the Rotunda, into which Audubon Avenue runs. Here energy may be lost or gained depending on the direction of the airflow. This idea is illustrated in Figure 3.6.1 below.

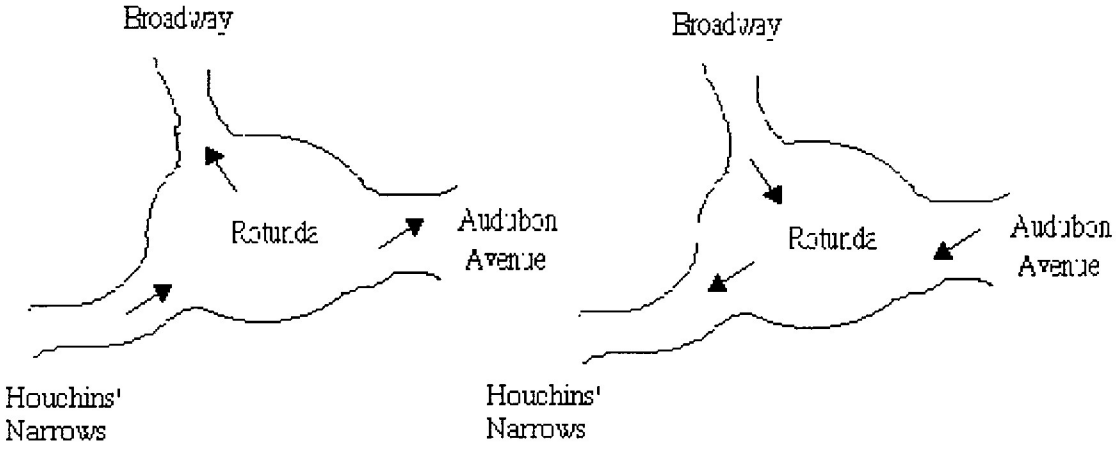

Figure 3.6.1 - Possible Scenarios for Energy Exchange in the Rotunda in Winter and Summer, Respectively

Assuming incompressibility, airflow in a branching cave system is analogous to current flow in an electric circuit. Hence, Kirchhoff's Current Law may be applied to flow at the junction in the Rotunda. Tocci (1983) states Kirchhoff's Current Law as

> "At any junction point or node in an electric circuit the sum of the currents flowing into the junction must equal the sum of the currents flowing away from the junction at any instant of time."

Thus, consider Figure 3.6.2 which shows a portion of an electric circuit with one input and two outputs. Letting I_1 represent the amount of current flow in the input circuit and

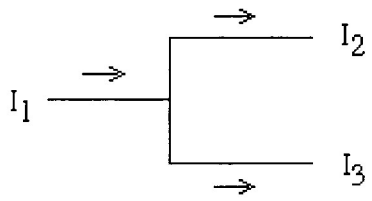

Figure 3.6.2 - Current Flow in a Branching Electric Circuit

I_2 and I_3 represent the amount of current flow from the two outputs, Kirchhoff's Current Law implies that the relationship between these three variables is

$$I_1 = I_2 + I_3 . \tag{3.6.1}$$

If airflow going between Houchins' Narrows and Booth's Amphitheater is analogous to current flow through an electric circuit, then the corresponding equation to (3.6.1) which relates air flux in Houchins' Narrows to air flux in Booth's Amphitheater and air flux in Audubon Avenue is given by

$$\mathbf{F}_H = \mathbf{F}_A + \mathbf{F}_B , \tag{3.6.2}$$

where $\mathbf{F}_H$, $\mathbf{F}_A$, and $\mathbf{F}_B$ are air flux values in Houchins' Narrows, Audubon Avenue, and Broadway as it moves past Booth's Amphitheater, respectively. Simple algebraic manipulation of (3.6.2) gives

$$\mathbf{F}_A = \mathbf{F}_H - \mathbf{F}_B . \tag{3.6.3}$$

But $\mathbf{F}_A$ represents energy loss between Houchins' Narrows and Booth's Amphitheater, thus the introduction of a linear air flux term into (3.4.4) to account for this energy loss is appropriate.

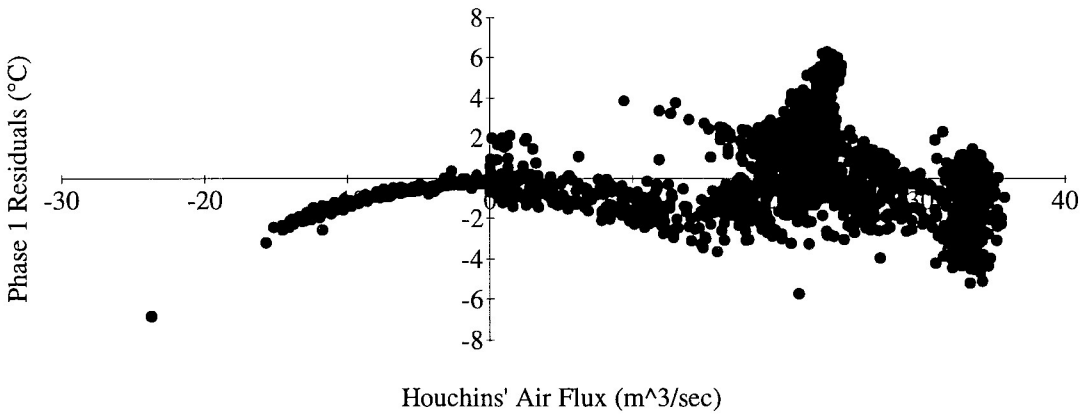

Figure 3.6.3 - Bernoulli Phase 1 Residuals

Figure 3.6.3 shows the residuals from the Phase 1 Bernoulli model in section 3.5 as they relate to air flux in Houchins' Narrows. The scatter plot shows a clear relationship between the residuals and air flux when the flux values are below about 15 cubic meters per second. So, beyond this point some other force is causing fluctuations

in air temperature at the floor of Booth's Amphitheater. Up to the flux value of about 15 cubic meters per second, the residuals are approximately quadratic in Houchins' Narrows air flux, and it is appropriate to introduce a linear flux term into (3.4.3) to use as a basis for regression analysis of Houchins' Narrows and Booth's Amphitheater data. Introducing a linear air flux term will change the best fit coefficient on the square flux term in (3.4.3), and a quadratic function in air flux will be added to the original basis function. Hence, air temperature at the floor of Booth's Amphitheater as a function of air temperature and flux in Houchins' Narrows is given by

$$T_B = a\mathbf{F}_H^2 + b\mathbf{F}_H + c + T_H . \qquad (3.6.4)$$

The results of the regression performed on the CAM data for Julian days 1 - 20 of 1997 are shown in Regression Sheet 3.6.1 below. The value for R-squared here is .725

R = 0.851 Rsqr = 0.725 Adj Rsqr = 0.724

Standard Error of Estimate = 1.831

	Coefficient	Std. Error	t	P	VIF
a	0.00684	0.000238	28.780	<0.001	11.239
b	0.106	0.00640	16.624	<0.001	11.091
c	4.220	0.0714	59.095	<0.001	2.922

Analysis of Variance:

	DF	SS	MS	F	P
Regression	2	16894.815	8447.407	2520.808	<0.001
Residual	1917	6424.003	3.351		
Total	1919	23318.817	12.152		

Normality Test: Passed (P = 0.163)
Constant Variance Test: Failed (P = <0.001)
Power of performed test with alpha = 0.050: 1.000

Regression Sheet 3.6.1 - Regression Results Using (3.6.4) as Basis Function

which is lower than the .730 value of R-squared obtained using the Phase 1 Bernoulli model. However, the Phase 2 Bernoulli model passes the normality test where the Phase 1 Bernoulli model does not. Hence, even though this upgraded model does not improve the value of R-squared, it is still an improvement on the Phase 1 Bernoulli model since the residuals are normally distributed and the model is on average predicting the behavior of air temperature at the floor of Booth's Amphitheater.

3.7 Heat Exchange with the Surroundings in the Historic Section of Mammoth Cave - Phase 3 Bernoulli Model

The air flowing through the Historic Section of Mammoth Cave comes into direct contact with the rock walls and ceilings of these passages. Hence, heat exchange between the air and the rock is expected, and line plots for air temperature and rock temperature in Houchins' Narrows support this claim. The line plots for Julian days 1 - 20 of 1997 are shown in Figure 3.7.1. Rock temperature tends to follow air temperature

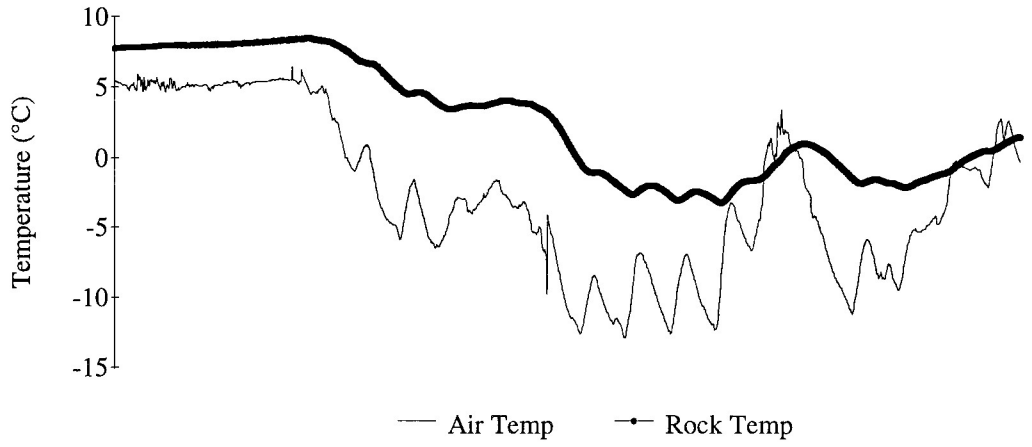

Figure 3.7.1 - Air Temperature and Rock Temperature in Houchins' Narrows, Julian Days 1 - 20 of 1997

by taking on approximately the same values as the air temperature. This relation indicates the exchange of heat between the air and the rock in Houchins' Narrows.

Since there is heat exchange between the air and rock in the Historic Section of Mammoth Cave and therefore in the section of cave between Houchins' Narrows and Booth's Amphitheater, there is energy loss or gain in going from Houchins' Narrows to Booth's Amphitheater. To account for this heat exchange in the model of air temperature at the floor of Booth's Amphitheater, let

$$\Delta T_{H\text{-}R} = T_H \quad T_R \tag{3.7.1}$$

denote the temperature difference between air and rock in Houchins' Narrows. Adding this basis function to (3.6.4) gives

$$T_B = a\mathbf{F}_H^2 + b\mathbf{F}_H + c + T_H + e\Delta T_{H\text{-}R}. \tag{3.7.2}$$

Assuming the temperature in Houchins' Narrows T_H represents potential energy, then it is expected that some of this potential energy may be lost or some may be gained in the Rotunda Room when air flows into or out of Audubon Avenue. This potential may also be lost to or gained from the rock walls and the ceiling of the passages. It is therefore appropriate to introduce a scaling factor onto the T_H term in (3.7.2). Hence, (3.7.2) becomes

$$T_B = a\mathbf{F}_H^2 + b\mathbf{F}_H + c + dT_H + e\Delta T_{H\text{-}R}. \tag{3.7.3}$$

Using (3.7.3) as the basis for regression analysis of Houchins' Narrows and Booth's Amphitheater gives the results in Regression Sheet 3.7.1. The value of R-squared is .99 indicating 99% of the variance in the data is taken into account.

R = 0.995 Rsqr = 0.990 Adj Rsqr = 0.990

Standard Error of Estimate = 0.185

	Coefficient	Std. Error	t	P	VIF
a	0.000346	0.0000296	11.710	<0.001	16.945
b	-0.0201	0.000746	-26.933	<0.001	14.701
c	6.042	0.0111	543.681	<0.001	6.896
d	0.420	0.00164	255.732	<0.001	5.819
e	-0.367	0.00205	-179.414	<0.001	8.944

Analysis of Variance:

	DF	SS	MS	F	P
Regression	4	6619.927	1654.982	48126.677	<0.001
Residual	1915	65.853	0.0344		
Total	1919	6685.780	3.484		

Normality Test: Passed (P = 0.669)
Constant Variance Test: Passed (P = 0.185)
Power of performed test with alpha = 0.050: 1.000

Regression Sheet 3.7.1 - Regression Results Using (3.7.3) as Basis Function

The remaining one percent may be assumed to be noise associated with the instrumentation. Both the normality test and the constant variance test are passed further indicating that this is an effective model. All P-values associated with the coefficients a,b,c,d, and e are less than .001 indicating at least 99 percent confidence in the value of these coefficients.

Using the values for a,b,c,d, and e in Regression Sheet 3.7.1 and substituting into (3.7.3) gives

$$T_B = .000346F_H^2 - .0201F_H + 6.042 + .420T_H - .367\Delta T_{H\text{-}R} \qquad (3.7.4)$$

Figure 3.7.2 shows T_B as predicted by (3.7.4) compared to the actual data measurements. The model determined by (3.7.4) is extremely effective in predicting the real temperature measurements of air temperature at the floor of Booth's Amphitheater.

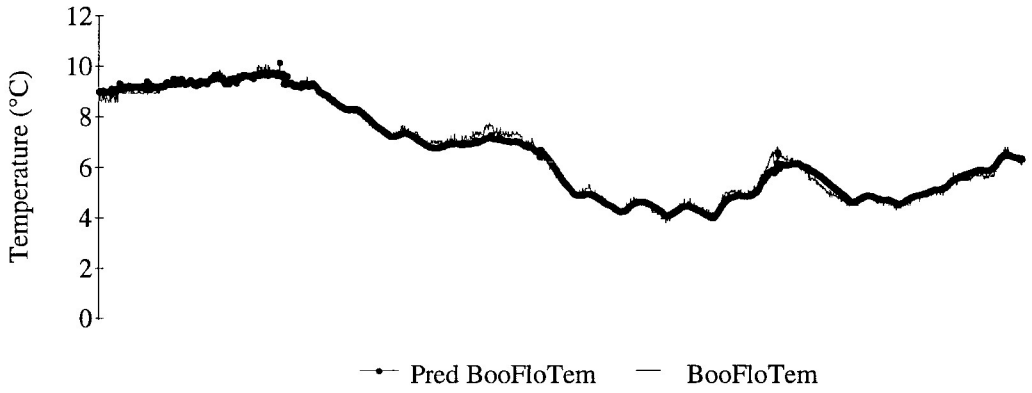

Figure 3.7.2 - Air Temperature at the Floor of Booth's Amphitheater as Predicted by (3.7.4) Compared to the Actual Measurements for Julian Days 1 - 20, 1997

The next objective is to determine how effective the model obtained for Julian days 1 - 20 of 1997 is at modeling other days throughout the year. The topic is discussed in the following section.

3.8 Applicability of the Phase 3 Bernoulli Model to Other Booth's Amphitheater Data Sets

Equation (3.7.4) was extremely effective in determining air temperature at the floor of Booth's Amphitheater for Julian days 1 - 20 of 1997. However, the question arises: just how well does this model predict for other data sets? To answer this question, (3.7.4) will be used to predict air temperature at the floor of Booth's Amphitheater for Julian days 348 - 366 of 1996 and Julian days 21 - 40 of 1997.

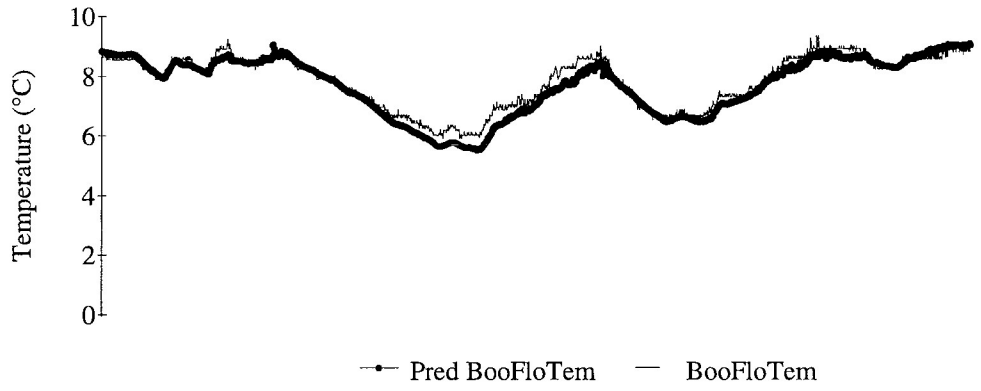

Figure 3.8.1 - Figure Showing How (3.7.4) Predicts Booth's Floor Temperature for Julian Days 348 -366, 1996

Figure 3.8.1 shows the predicted values and the actual values for air temperature at the floor probe in Booth's Amphitheater for Julian days 348 - 366 of 1996. Equation (3.7.4) still does an effective job of predicting values for these Julian days, but it is not so accurate for Julian days 1 - 20 of 1997, the data set for which the regression coefficients were determined. The same is true for Julian days 21 - 40 of 1997, as illustrated in Figure 3.8.2.

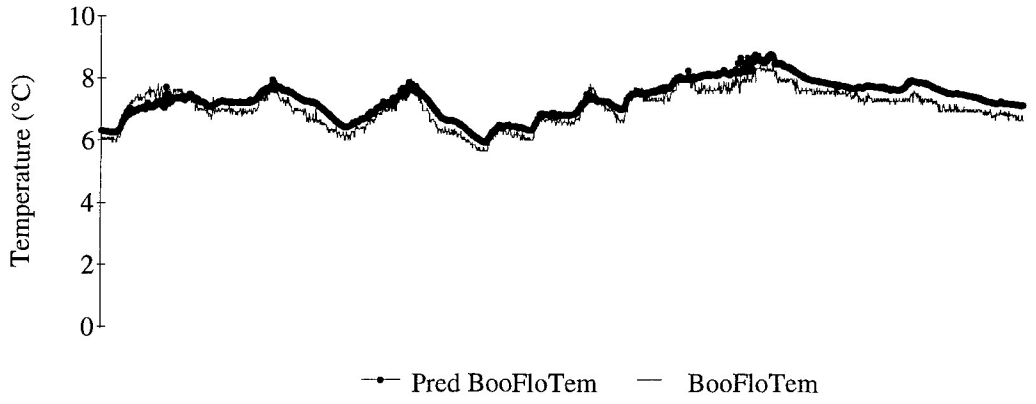

Figure 3.8.2 - Figure Showing How (3.7.4) Predicts Booth's Floor Temperature for Julian Days 21 - 40, 1997

Equation (3.7.4) does not do as well at predicting the values in data sets other than for Julian days 1 20 of 1997. However, it still is effective at predicting the behavior of air temperature at the floor of Booth's Amphitheater. It is therefore reasonable to assume that the basis function given by (3.7.3) will still hold for these data sets and that performing a regression analysis for each data set will yield an effective model. A summary of the regression results using (3.7.3) as a basis function is given in

Month	Data Set	a	b	c	d	e	R-squared
4	hn&ba 91-110, 1996	0.00022	-0.0288	4.943	0.463	-0.423	0.961
4.5	hn&ba 111-130, 1996	0.000179	-0.0249	4.432	0.541	-0.475	0.909
5	hn&ba 131-150, 1996	-0.000321	-0.0251	4.239	0.584	-0.576	0.911
6	hn&ba 151-170, 1996	-0.000383	-0.0255	2.695	0.747	-0.772	0.816
7	hn&ba 195-210, 1996	-0.0000319	-0.0183	7.471	0.278	-0.202	0.486
8	hn&ba 221-240, 1996	-0.00022	-0.0229	-1.402	1.098	-1.082	0.587
9	hn&ba 245-265, 1996	-0.0000364	-0.0128	5.786	0.453	-0.456	0.828
10	hn&ba 270-290, 1996	0.0000141	-0.0128	6.24	0.412	-0.371	0.924
11.5	hn&ba 321-346, 1996	0.0000898	-0.0258	6.935	0.306	-0.252	0.947
12	hn&ba 348-366, 1996	0.000476	-0.0301	6.849	0.317	-0.251	0.98
1	hn&ba 1-20, 1997	0.000346	-0.0201	6.042	0.42	-0.367	0.99
1.5	hn&ba 21-40, 1997	-0.000107	-0.0297	6.335	0.321	-0.261	0.943
2	hn&ba 41-60, 1997	-0.000649	-0.0182	5.985	0.408	-0.37	0.978
2.5	hn&ba 61-77, 1997	-0.0000598	-0.0207	6.832	0.273	-0.212	0.885

Table 3.8.1 Regression Results when Phase 3 Bernoulli Model is Applied to Indicated Data Sets

Table 3.8.1. The names of data files listed under the second column of Table 3.8.1 are formatted as follows:

"hn&ba" indicates Booth's Amphitheater temperature data is modeled as a function of Houchins' Narrows data.

"91 - 110" - for example, indicates Julian days of data used in regression.

"1996" - for example, indicates year from which data sets are taken.

Figure 3.8.3 shows the values of R-squared from Table 3.8.1. The model achieves values of R-squared above .90 for months between October (month 10) and May (month 5) indicating the Phase 3 Bernoulli model is adequate for months when air temperature outside the cave system may fall below the air temperature within the cave system. However, in July (month 7) the value of R-squared decreases to a value of .486.

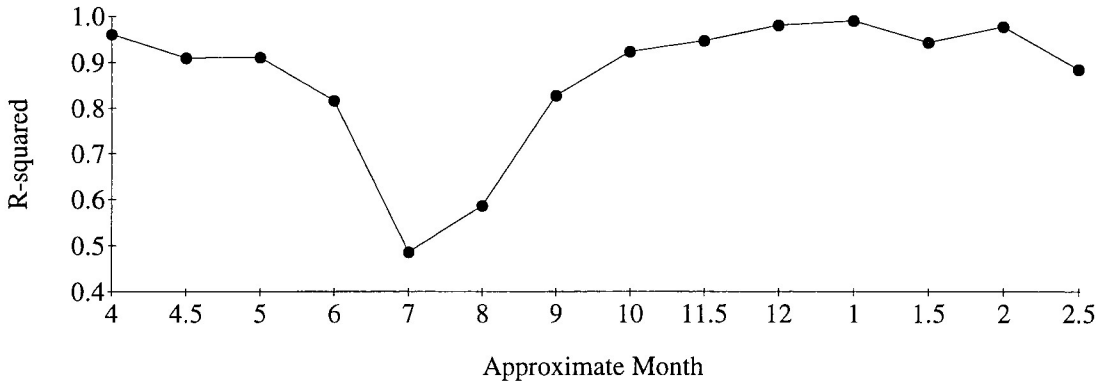

Figure 3.8.3 - Values of R-squared for the Phase 3 Bernoulli Model when Applied to Houchins' Narrows and Booth's Amphitheater Data During the Indicated Months of 1996 and 1997

The low values of R-squared are indicators of the inappropriate application of the Phase 3 Bernoulli model to summer data. This failure may be explained by the nature of airflow during the summer. During the summer, air flows out of Houchins' Narrows. This air flowing out of Houchins' Narrows has passed through much of the upper portions of the cave system and so its temperature has stabilized by the time it has reached the Historic Section of Mammoth Cave. The air temperature at all CAM sites in the Historic Section should then be approximately equal, and so the air temperature at the floor of Booth's Amphitheater should be approximately the same as the air temperature in Houchins' Narrows. This result is shown to be true in Figure 3.8.4 by the temperature differential between the air in Booth's Amphitheater and the air in Houchins' Narrows being about zero. However, the temperature differential driving the air flux in the summer data is that between Houchins' Narrows air and the air in another, upper location in the cave. Only by considering this temperature differential will an accurate model be derived.

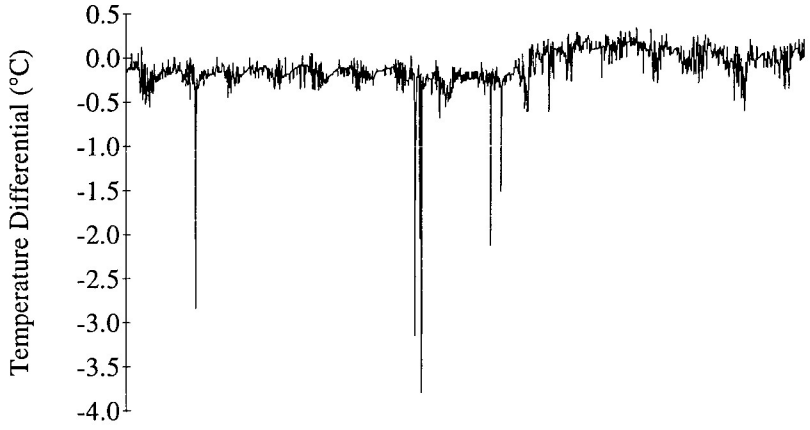

Figure 3.8.4 - Temperature Differential Between Houchins' Narrows Air Temperature and Booth's Amphitheater Floor Air Temperature Data for Julian Days 195 - 210 of 1996

Figure 3.8.5 shows the best fit coefficients a,b,c,d, and e which correspond to the values of R-squared in Figure 3.8.3. Similar to the values of R-squared in Figure 3.8.3, the values of the coefficients do not change significantly from September to May. However, in the summer the values are unstable and vary greatly. This factor is another indicator of the inappropriate application of the Phase 3 Bernoulli model to summer data.

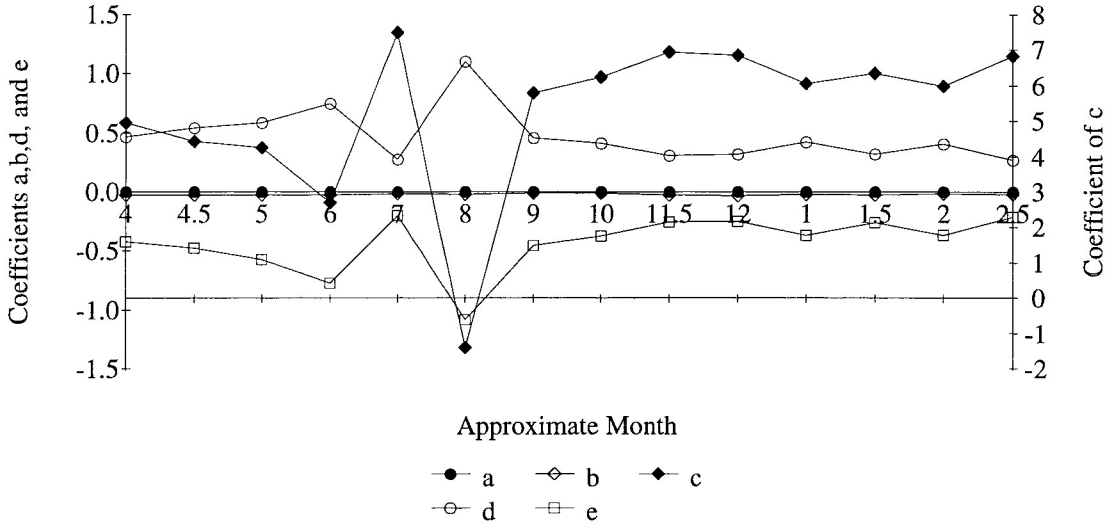

Figure 3.8.5 - Best Fit Coefficients Corresponding to the R-squared Values in Figure 3.8.3

3.9 Application of the Bernoulli Model to Other CAM Sites

Up to this point, all regression fits have been between Houchins' Narrows and Booth's Amphitheater data. It would be equally as interesting to see how the model predicts conditions at CAM sites other than Booth's Amphitheater. Letting α represent the abbreviation for the CAM site in question, the regression will have the form

$$T_\alpha = a\mathbf{F}_H^2 + b\mathbf{F}_H + c + dT_H + e\Delta T_{H\text{-}R}. \qquad (3.9.1)$$

Performing this regression analysis for the CAM sites at Corkscrew, Wright's Rotunda, River Hall, and Rafinesque Hall on data from Julian days 1 - 20 of 1997 results in the coefficients in Table 3.9.1. Abbreviations used for CAM sites are as defined in Table 3.1.1.

Month	Data Set	a	b	c	d	e	R-squared
1	hn&co 1-20, 1997	-0.0000128	0.00264	7.917	0.233	-0.258	0.976
1	hn&ba 1-20, 1997	0.000346	-0.0201	6.042	0.42	-0.367	0.99
1	hn&wr 1-20, 1997	-0.000315	0.109	8.415	0.339	-0.617	0.319
1	hn&ri 1-20, 1997	-0.0000208	0.00727	7.365	0.0769	-0.124	0.844
1	hn&ra 1-20, 1997	-0.0000134	0.00515	5.953	0.175	-0.202	0.963

Table 3.9.1 The Phase 3 Bernoulli Model Applied to the Indicated Data Sets from Julian Days 1 - 20 of 1997

The model is effective at predicting values at locations near Houchins' Narrows since the values for R-squared at Corkscrew, Booth's Amphitheater, River Hall, and Rafinesque Hall are all above .84. However, CAM sites further in the cave have lower values of R-squared. The value of R-squared for Wright's Rotunda data is .319 since the variations in air flux in Houchins' Narrows are not resulting in variations in air temperature in Wright's Rotunda. Atmospheric conditions in Houchins' Narrows have little effect on conditions in Wright's Rotunda, as seen by the data in Figure 3.9.1.

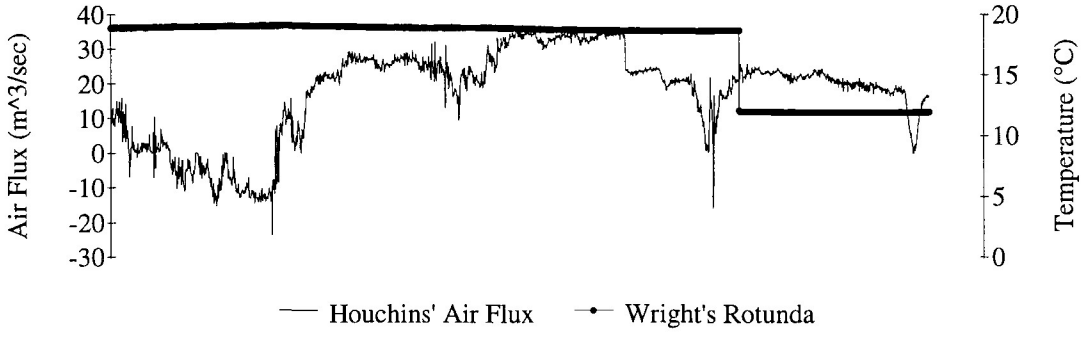

Figure 3.9.1 Air Flux in Houchins' Narrows and Air Temperature in Wright's Rotunda, Julian Days 1 20 of 1997

3.10 Conclusions

Chapter 3 has constructed a mathematical model which predicts air temperature at CAM sites throughout the Historic Section of Mammoth Cave based upon atmospheric conditions in Houchins' Narrows. The task was accomplished using Bernoulli's equation as the primary description of temperature driven airflow within a tube. Then, the effects of a branching cave system and heat flow between the air and its surroundings are added to account for energy the air loses in going from Houchins' Narrows to the CAM site in question. When combined, these factors resulted in an effective mathematical model.

With a model constructed to predict conditions at CAM stations other than those at Houchins' Narrows, the next logical step is to construct a model to predict atmospheric conditions in Houchins' Narrows. One approach to this construction is time series analysis. This task is begun in the following chapter.

CHAPTER 4

FORECASTING HOUCHINS' NARROWS DATA WITH TIMES SERIES ANALYSIS

4.1 Introduction

Science and Resource Management personnel in Mammoth Cave National Park have been gathering atmospheric data from Houchins' Narrows since January of 1996. With such a large set of data available, it is possible to completely understand and model the processes determining atmospheric parameters within Houchins' Narrows. The use of time series analysis is one approach to modeling this data.

Time series analysis uses the idea of a *recursion relation*. That is, the measured quantity at time t is assumed to be a function of the t - 1 previous measurements, or

$$X_t = g(X_{t-1}, X_{t-2}, \ldots, X_1). \tag{4.1.1}$$

It is the goal of time series analysis to determine the function g which effectively predicts the data in question.

The ultimate goal of Science and Resource Management at Mammoth Cave National Park is to configure air panels on the gate in the Historic Entrance of Mammoth Cave to regulate air and restore natural conditions. Different configurations will result in a different set of atmospheric conditions throughout the cave.

Time series analysis may first be used to predict air flux, air temperature, and rock temperature measurements at the Houchins' Narrows CAM site. Then, using the Phase 3 Bernoulli model developed in Chapter 3, temperatures may be predicted at the remaining CAM stations. This analysis will determine if the current retrofitting is having the desired effect. If not, a new configuration will be established. This process will be repeated several times. If the proper configuration is achieved, then no further study will be necessary. If the desired atmospheric conditions are not achieved, the time series of Houchins' Narrows data necessary to produce the desired results will be determined through experimentation with the Phase 3 Bernoulli model. The necessary air panel configuration to generate the determined time series may be interpolated from the time series data already gathered under different retrofits.

The process of arriving at a model that will predict values in a time series is a long one and is more complex than anything done thus far in this thesis. For these reasons, Chapter 4 of this thesis will not represent an attempt to arrive at a model for predicting the sequences of atmospheric data in Houchins' Narrows but will be an attempt to prepare the data for modeling. This chapter will provide the foundation for further research.

4.2 Houchins' Narrows Air Flux Data as a Time Series

By definition, a *time series* is a sequence of observations taken as time progresses. Hence, the sequence of air flux values $\{\mathbf{F}_t\}$ in Houchins' Narrows obtained by Science and Resource Management personnel is a time series and may be modeled using the tools of time series analysis. Moreover, there are a finite number of observations taken at

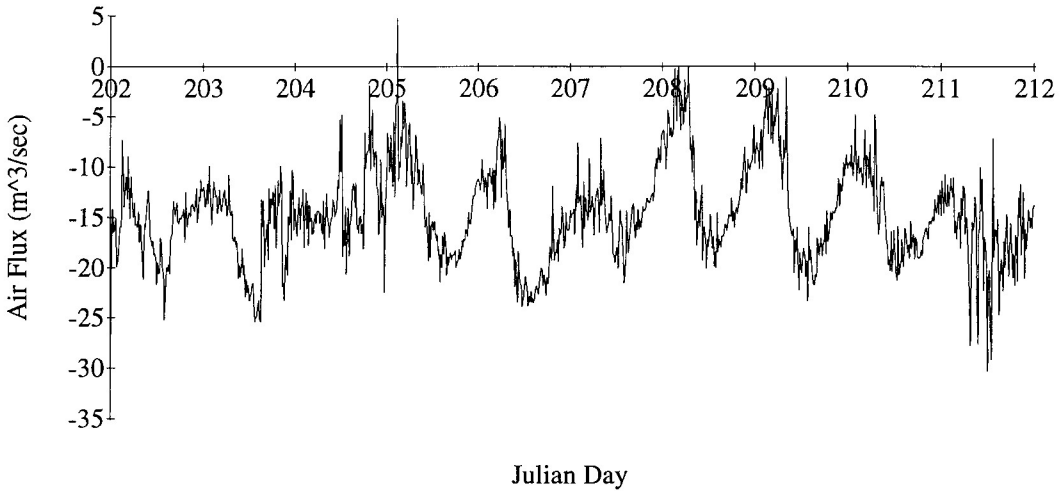

Figure 4.2.1 - The Sequence of Air Flux Values for Julian Days 202 - 211 of 1996

discrete time steps, so the sequence $\{\mathbf{F}_t\}$ is a *discrete time series*. Figure 4.2.1 shows the sequence of air flux values in Houchins' Narrows for Julian days 202 - 211 of 1996.

To model the air flux data in Figure 4.2.1, it is first important to develop some of the basic definitions and theorems involved in time series analysis; this development will be accomplished in the following section.

4.3 A Brief Introduction to Stationary Processes

In time series analysis, each observation X_t from the sequence of observations $\{X_t\}$ is considered to be a random variable with its own probability distribution function. Analysis of the time series will use some of the basic properties of random variables as indicators of the characteristics of the time series. The following definitions are useful for this purpose and were taken from Brockwell and Davis (1996).

Definition 4.3.1 - Let { X_t } be a time series with $E(X_t^2) < \infty$ for all t. The mean μ as a function of time t is given by

$$\mu_X(t) = E(X_t). \tag{4.3.1}$$

The covariance of { X_t } is given by

$$\gamma_X(r,s) = \mathrm{Cov}(X_r, X_s) = E[(X_r - \mu_X(r))(X_s - \mu_X(s))], \tag{4.3.2}$$

where r, s, and t are integers.

Definition 4.3.2 The process { X_t } is stationary if

(i) $\mu_X(t)$ is independent of t,

and

(ii) $\gamma_X(t+h, t)$ is independent of t for each h and so only depends upon h.

There are two forms of stationarity: *weak stationarity* and *strict stationarity*. Definition 4.3.2 is the definition of weak stationarity. Much of the theory of time series analysis is devoted to stationary processes; in order to use this theory it is necessary to either transform nonstationary data until the residuals are stationary or study nonstationary processes. Hence, it is necessary to develop a way of determining if the sequence in question is a stationary process. The next few definitions will be used to accomplish that procedure.

Definition 4.3.3 - Let { X_t } be a stationary time series. The autocovariance function (ACVF) of { X_t } is

$$\gamma_X(h) = \mathrm{Cov}(X_{t+h}, X_t) . \tag{4.3.3}$$

The autocorrelation function (ACF) of { X_t } is

$$\rho_X(h) = \frac{\gamma_X(h)}{\gamma_X(0)} = \mathrm{Cor}(X_{t+h}, X_t) . \tag{4.3.4}$$

Definitions 4.3.1 through 4.3.3 are in terms of the random variable X_t. However, it is not practical to consider random variables since the time series which are generally considered are small samples from a sequence of realized values of the random variables. The sample analogue of the combination of the previous definitions is therefore given in Definition 4.3.4.

Definition 4.3.4 - Let $x_1, \ldots, x_n$ be observations of a time series. The sample mean of $x_1, \ldots, x_n$ is

$$\bar{x} = \frac{1}{n} \sum_{t=1}^{n} x_t . \tag{4.3.5}$$

The sample autocovariance function is

$$\hat{\gamma}(h) = \frac{1}{n} \sum_{t=1}^{n-|h|} (x_{t+|h|} - \bar{x})(x_t - \bar{x}), \qquad -n < h < n. \tag{4.3.6}$$

The sample autocorrelation function is

$$\hat{\rho}\,(h) \;=\; \frac{\hat{\gamma}(h)}{\hat{\gamma}(0)}, \quad -n < h < n. \tag{4.3.7}$$

These definitions provide enough basic information for creating a method to determine if a given time series is a stationary process. Based upon information in Brockwell and Davis (1996), the method involves the ACF and is given in the following proposition.

Proposition 4.3.1 - Let γ be the autocovariance function and ρ be the autocorrelation function of some process $\{ X_t \}$. Then ρ is the autocorrelation function of a stationary process if and only if $\rho(0) = 1$.

Proposition 4.3.1 therefore provides a convenient method for verifying if a given time series is stationary or is not stationary.

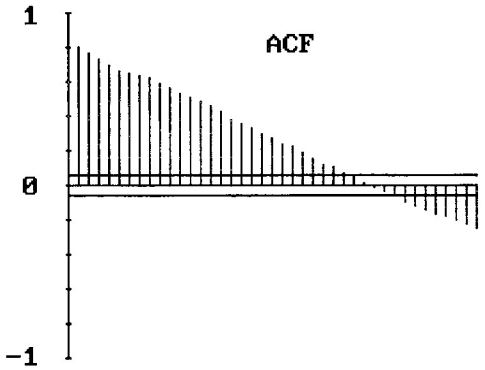

Figure 4.3.1 Sample Autocorrelation Function (ACF) of Houchins' Narrows Air Flux Data, Julian Days 202 - 211 of 1996

Figure 4.3.1 shows that air flux data in Figure 4.2.1 is not a stationary process since the ACF at lag 0 is not equal to one. Assuming the realizations in Figure 4.2.1 represent the mean of the process which defines air flux in Houchins' Narrows during this time span, the mean varies as time progresses. It is therefore necessary to perform some preliminary modeling of the data until the residuals are a stationary process and then model the residuals using the tools of time series analysis.

4.4 Detrending Houchins' Narrows Air Flux Data Using the Classical Decomposition Model

One possible approach taken to transform the air flux data in Figure 4.2.1 into a stationary time series is to break the original sequence $\{F_t\}$ into three components: a trend component, a seasonal component, and a noise component. The process is called the *classical decomposition.* Letting m_t denote the trend component, s_t denote the seasonal component, and Y_t denote a zero mean noise sequence, the classical decomposition model of the general sequence $\{X_t\}$ is given in Definition 4.4.1.

Definition 4.4.1 The classical decomposition model for the time series $\{X_t\}$ is given by

$$X_t = m_t + s_t + Y_t, \qquad t = 1, \ldots, n, \tag{4.4.1}$$

where $E(Y_t) = 0$, $s_{t+d} = s_t$, *and* $\sum_{j=1}^{d} s_j = 0$.

By (4.4.1), subtracting the trend and seasonal components from the original time series will give the noise sequence $\{Y_t\}$ -- that is,

$$Y_t = X_t - m_t - s_t, \qquad t = 1, \ldots, n. \tag{4.4.2}$$

Figure 4.4.1 shows the original air flux sequence $\{\mathbf{F}_t\}$ along with the estimated trend and seasonal components. The air flux data in Figure 4.2.1 has a trend which is modeled well by the quadratic function of time i given by

$$\mathbf{F}(i) = -17.6462 + .01590\, i - .0000153\, i^2 . \tag{4.4.3}$$

Since summer air flux data exhibits diurnal flow patterns as discussed in section 2.5, the seasonal component of the data has an approximate period of d = 96 time steps (there are 96 data measurements taken each day).

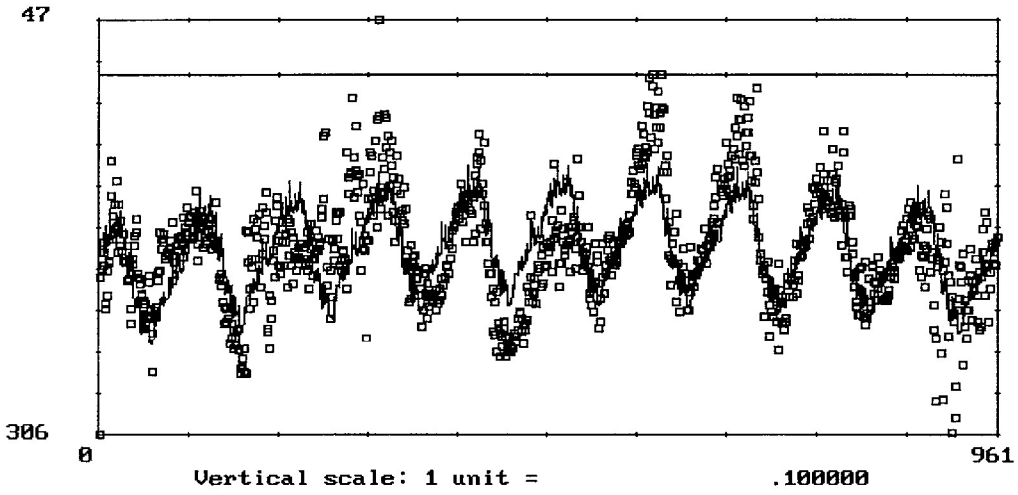

Figure 4.4.1 - The Original Air Flux Time Series for Julian Days 202 - 211 of 1996 Shown with the Best Fit Trend and Seasonal Components

Figure 4.4.2 shows the residuals from the models fit in Figure 4.4.1, with the mean of the process removed. Figure 4.4.2 shows a process which has a mean of about

zero; this claim may be verified by considering the frequency distribution for the residuals given in Figure 4.4.3. The distribution is approximately normal with mean zero. Hence, the residuals $\{Y_t\}$ are indeed a zero mean process.

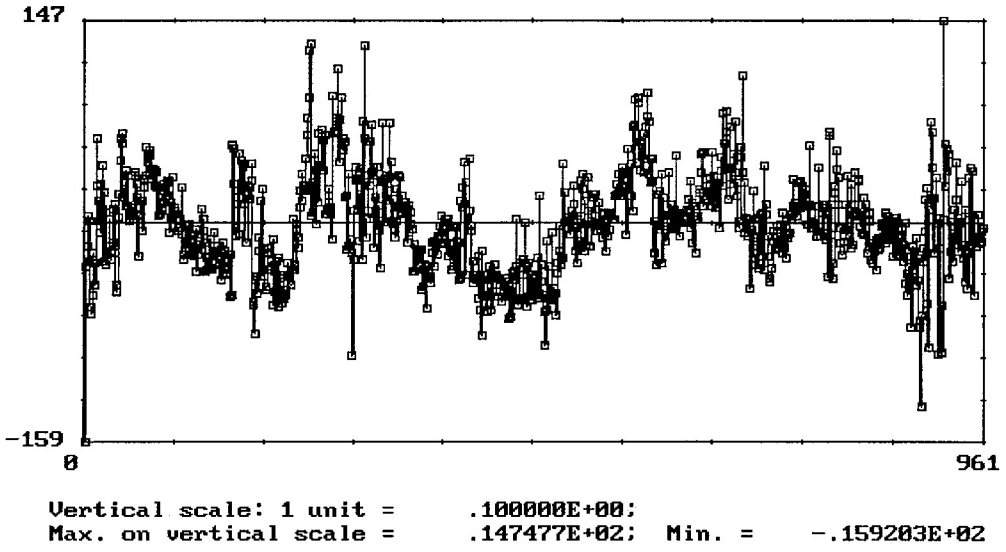

Figure 4.4.2 - Classical Decomposition Residuals when Seasonal Component with Period d = 96 Data Points and Quadratic Trend Component are Removed

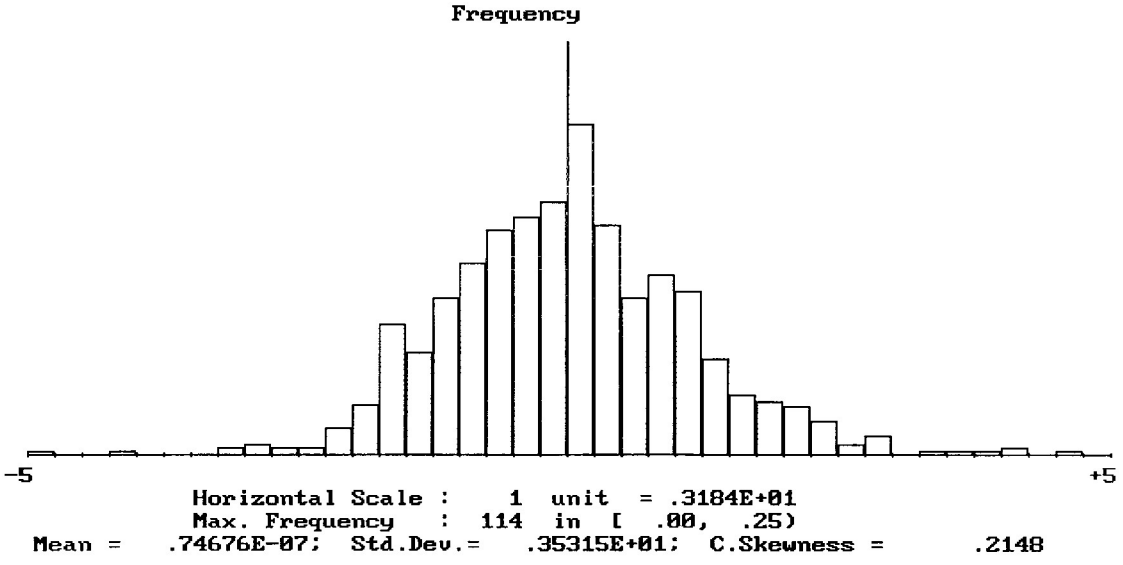

Figure 4.4.3 - Frequency Distribution for Residuals in Figure 4.3.2

However, this outcome does not indicate whether the residuals in Figure 4.4.2 are a stationary time series. To arrive at an answer to this question, the ACF for the data is plotted in Figure 4.4.4. Since the value of the sample ACF at lag zero is not equal to one, the sequence of residuals obtained by removing seasonal and quadratic trend

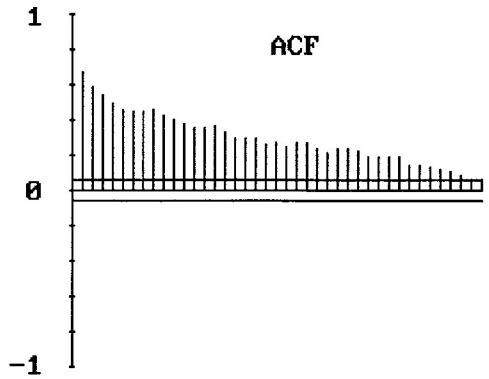

Figure 4.4.4 - The Sample Autocorrelation Function (ACF) for Residuals in Figure 4.4.2

components from air flux data for Julian days 202 - 211 is not a stationary time series. This example illustrates that there is no way to guarantee a given series of models will result in a set of residuals which are a stationary process, and it is often necessary to experiment with a range of models before a stationary time series is acquired.

4.5 Smoothing Air Flux Data with a Finite Moving Average Filter

Since the classical decomposition model did not arrive at a sequence of residuals which were a stationary process, it is necessary to manipulate the data to find a model which will result in a stationary sequence of residuals. One such way to manipulate the data is through a finite moving average filter, essentially a smoothing process which

averages a specified number of data points. It is defined as follows based on a discussion in Brockwell and Davis (1996).

Definition 4.5.1 - Let q be a nonnegative integer and { X_t } be a time series. The (2q + 1) - term moving average filter is then given by

$$\hat{m}_t = \frac{1}{(2q+1)} \sum_{j=-q}^{q} X_{t-j}, \qquad q+1 \le t \le n-q, \tag{4.5.1}$$

where X_t is given by

$$X_t = \begin{cases} X_1 & \text{if } t < 1 \\ X_n & \text{if } t > n \end{cases}. \tag{4.5.2}$$

Figure 4.5.1 shows the 5 - term moving average and the original sequence for air flux in Houchins' Narrows during Julian days 202 - 211 of 1996. This may produce a better fit than was obtained by using only the classical decomposition model in the previous section. The sequence arrived at through the 5 - term moving average filter is shown alone in Figure 4.5.2.

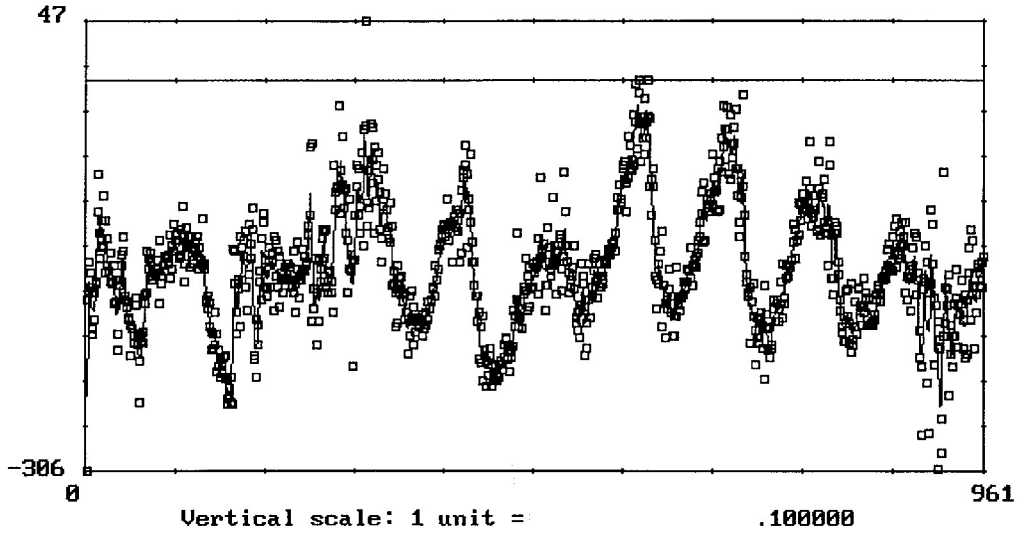

Figure 4.5.1 - The Original Sequence of Air Flux Values from Figure 4.2.1 Along with its 5 - term Moving Average

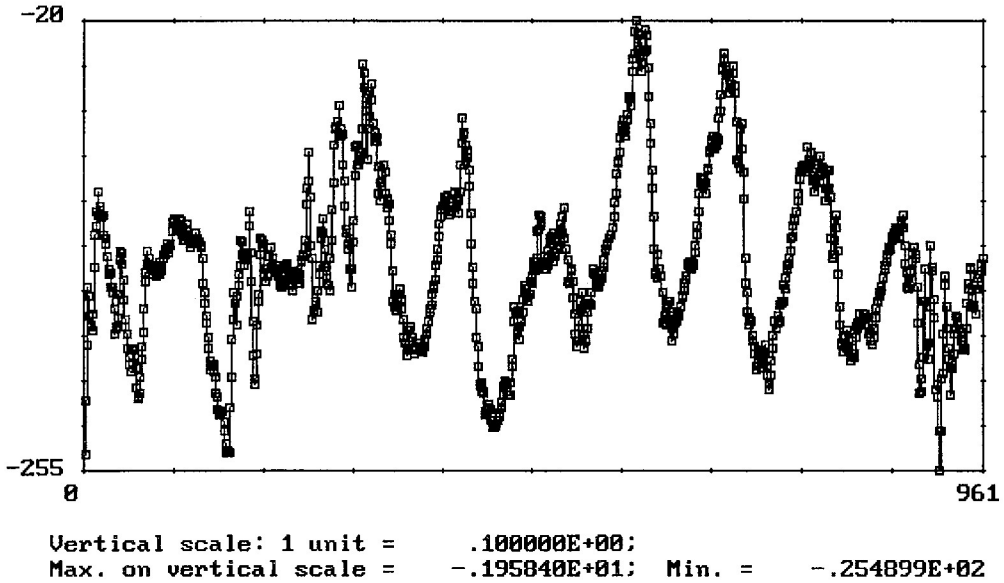

Figure 4.5.2 - The 5 - term Moving Average for Air Flux Data, Julian Days 202 - 211 of 1996

Figure 4.5.3 shows the sample ACF for the 5 - term moving average sequence of data derived from the original air flux sequence $\{\mathbf{F}_t\}$. The value of the ACF at lag zero is very nearly one, so this sequence is approximately stationary. However, the data has not been detrended or deseasonalized. The maximum lag available with the ITSM96 software (software which is supplied with Brockwell and Davis (1996)) is 40, so it is likely that much of the seasonality and trend which might be seen in the behavior of the ACF is not visible in Figure 4.5.3 due to the relatively small number of lags available.

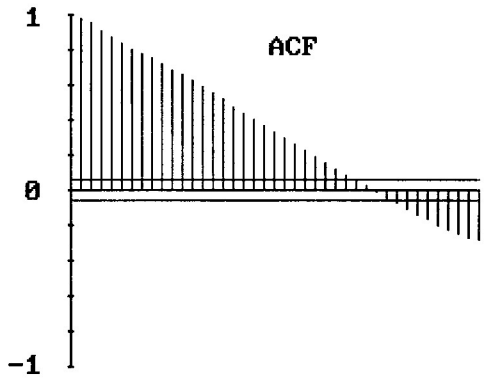

Figure 4.5.3 - The Sample ACF of the Smoothed Data in Figure 4.5.2

Figure 4.5.4 shows the smoothed air flux data along with its estimated seasonal and trend components. Again, the period of the data's "Seasonal" component is estimated at d = 96 data points and the quadratic trend component is given by

$$\mathbf{F}(i) = -17.6668 + .01599\, i - .0000154\, i^2 . \qquad (4.5.3)$$

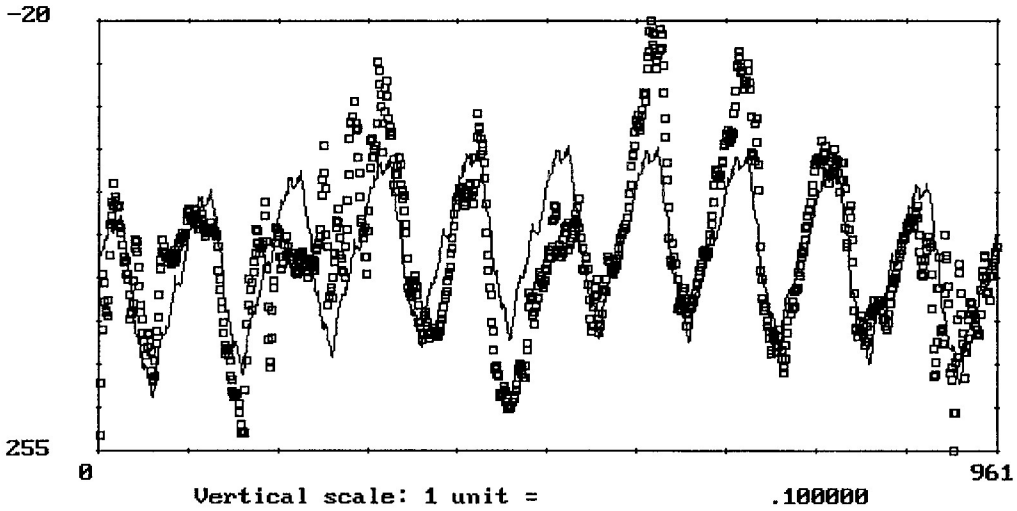

Figure 4.5.4 - Smoothed Air Flux Data with Its Estimated Seasonal and Trend Components, Julian Days 202 - 211 of 1996

The residuals derived from the seasonal and trend fit in Figure 4.5.4 are shown in Figure 4.5.5. The residuals show behavior similar to that of the smoothed data.

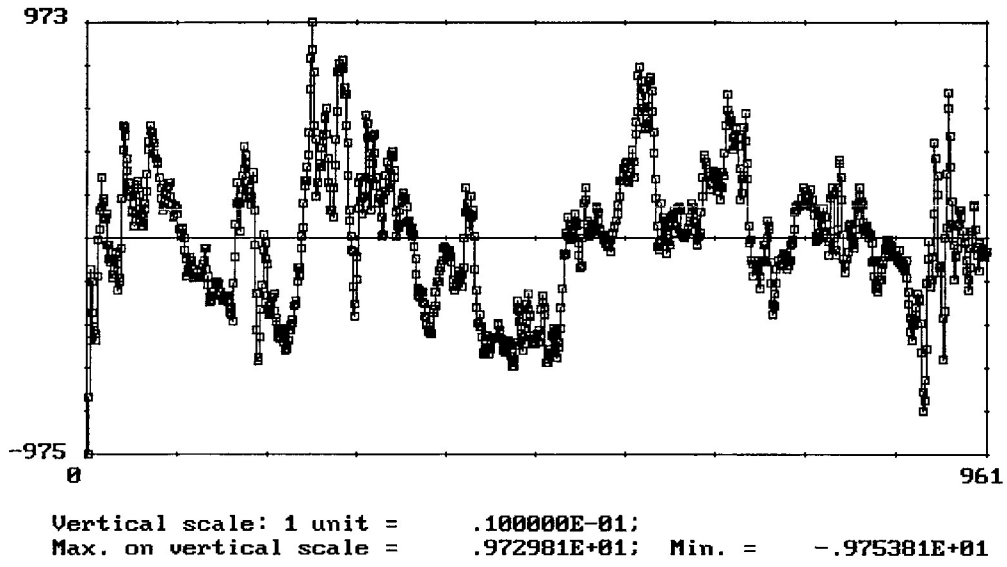

Figure 4.5.5 Residuals of the Deseasonalized and Detrended Smoothed Air Flux Data, Julian Days 202 - 211 of 1996

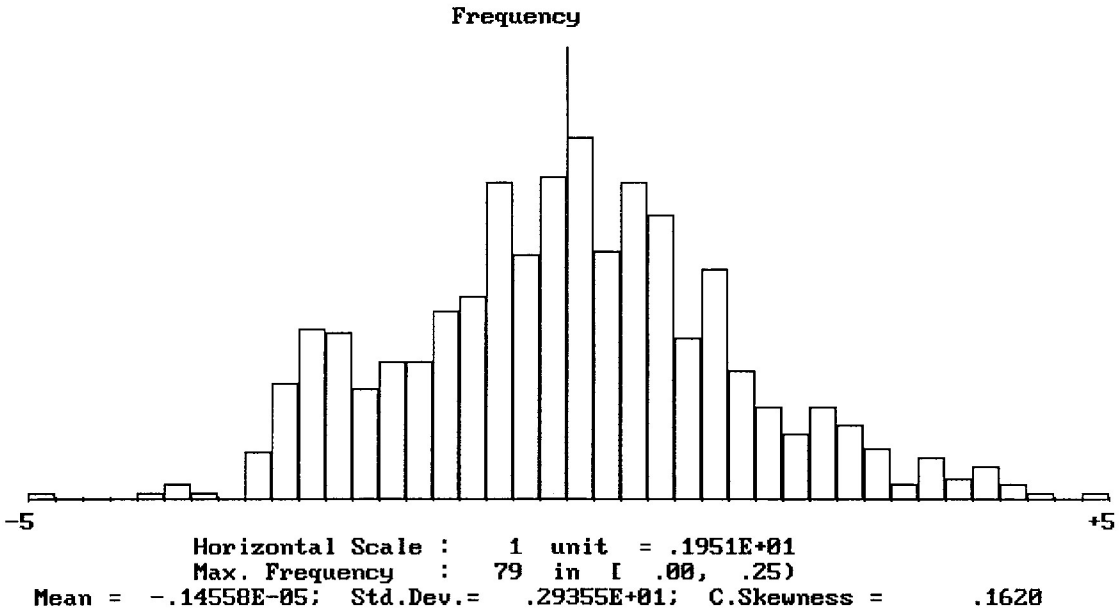

Figure 4.5.6 - Frequency Distribution of the Residuals in Figure 4.5.5

The frequency distribution of the residuals in Figure 4.5.6 shows that the residuals are a zero mean process. Further, the ACF in Figure 4.5.7 shows that the sequence of residuals in Figure 4.5.5 is approximately a stationary time series (the sample ACF at lag zero is close to one).

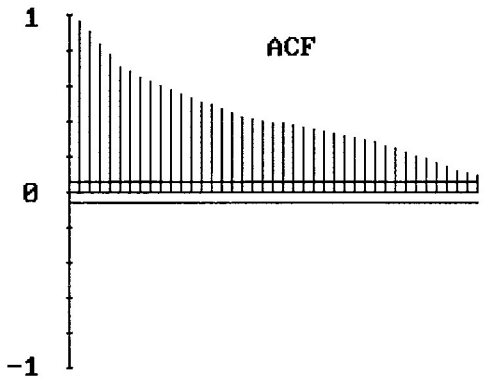

Figure 4.5.7 - Sample ACF of the Residuals in Figure 4.5.5

It has now been established that the sequence of residuals is stationary. Next, the sequence of residuals must be analyzed to determine if it is a sequence of independent, identically distributed (iid) random variables. If this is the case, no further modeling is necessary since the values may be randomly generated. On the other hand, if the sequence is not iid, then it will be necessary to utilize more of the tools of time series analysis.

The sample ACF in Figure 4.5.7 shows the autocorrelations up to lag 40. At each of these lags, the sample ACF falls outside the bounds $\pm 1.96/\sqrt{n}$ (these are the horizontal bounds shown around the lag axis) where n is the number of data points. An iid sequence with finite variance and large n may be approximated by a normal random variable with mean zero and variance 1/n, denoted N(0,1/n). Hence, it is expected that 95% of the sample ACF values should fall within the bounds $\pm 1.96/\sqrt{n}$ for an iid sequence of random variables. The sample ACF in Figure 4.5.7 does not have 95% of its values falling within the bounds $\pm 1.96/\sqrt{n}$, so the sequence of residuals shown in
Figure 4.5.5 is not a realization from a sequence of iid random variables.

4.6 Conclusions and Further Directions with Time Series Analysis

In Chapter 4, the author began to analyze air flux data from Houchins' Narrows through the use of time series analysis. The original sequence of air flux values for Julian days 202 - 211 of 1996 were not realizations from a stationary process and so had to be detrended and deseasonalized. The residuals in section 4.5 obtained by removing the trend and seasonal components from the original air flux time series are realizations from a stationary process since the autocorrelation function at lag zero is approximately equal to one.

Since the residuals obtained in the previous section were not realizations from an iid sequence of random variables, it is necessary to use more tools from time series analysis to arrive at an accurate model for the data. One model commonly used for stationary processes is the *autoregressive moving average* model. This model predicts values using a linear combination of previous values along with a linear combination of white noise components. Its definition follows.

Definition 4.6.1 - The process $\{ X_t \}$ is an ARMA(p,q) process if $\{ X_t \}$ is stationary and if for every t

$$X_t - \phi_1 X_{t-1} \cdots - \phi_p X_{t-p} = Z_t + \theta_1 Z_{t-1} + \cdots + \theta_q Z_{t-q}, \tag{4.6.1}$$

where $\{ Z_t \} \sim WN(0, \sigma^2)$. ($\{ X_t \}$ is an ARMA(p,q) process with mean μ if $\{X_t - \mu\}$ is an ARMA(p,q) process.)

The process $\{Z_t\}$ in (4.6.1) is a sequence of random variables known as white noise, a sequence of uncorrelated random variables with given means and variances. The next stage in the modeling procedure begun in this chapter will construct an ARMA model for airflow data in Houchins' Narrows during the summer.

In this chapter, the author has considered air flux data in the summer, when the time series data were well-behaved and obtaining a stationary process was relatively easy. However, atmospheric data sets are most complex during the winter, and winter is the time during the year when atmospheric conditions deviate most from those which are desired by Science and Resource Management personnel. It is therefore both more

difficult and more important to understand these processes during seasons other than the summer.

It is highly likely that atmospheric data from Houchins' Narrows during time periods other than summer may not be detrended and deseasonalized to arrive at a stationary time series (as was the case with the summer air flux data analyzed in this chapter). Processes such as this are known as *nonstationary* processes, and, just as is the case with stationary processes, there are methods available to predict time series which are nonstationary. Hence, an extremely important goal to achieve in the future is to analyze and predict non-summer data using techniques for nonstationary time series.

CHAPTER 5

CLOSING REMARKS

5.1 Thesis Summary

Atmospheric conditions within Mammoth Cave have been altered by modified entrances and passageways. Because of these changes, bats no longer inhabit the cave in the large numbers that have historically been present, valuable artifacts are in danger of being destroyed, and rockfalls are occurring at an increased rate. In order to restore the natural entrance ecotone, the increase in airflow must be understood and models of airflow must be created. Use of atmospheric data obtained by Science and Resource Management personnel at Mammoth Cave National Park allows both the evaluation of a proposed mechanism driving airflow in Mammoth Cave and the creation of mathematical models describing this airflow.

Convective heat transfer, also known as the chimney effect, is the primary driving force behind airflow in Mammoth Cave. An effective model of the temperature at various sites within the Historic Section of Mammoth Cave was established using a modified, temperature dependent version of Bernoulli's equation. The final model was labeled a Phase 3 Bernoulli model since it was the third phase in a series of refinements based upon the incompressible fluid flow equation known as Bernoulli's equation. When regression analysis was performed on atmospheric data from the Historic Section of Mammoth Cave using the set of basis functions implied by the Phase 3 Bernoulli model,

values of R-squared as high as .99 were obtained, resulting in a model which was extremely effective in predicting air temperatures in Mammoth Cave.

When coupled with this Phase 3 Bernoulli model, using time series analysis to predict conditions in Houchins' Narrows will allow the prediction of air temperature at other CAM sites. This knowledge should allow Science and Resource Management personnel to bring into place an effective air panel configuration on the gate of the Historic Entrance in Mammoth Cave. Each air panel configuration will produce a unique time series in each set of data within the Historic Section of Mammoth Cave (especially at the Houchins' Narrows CAM site). Hence, when enough air panel configurations have been utilized, time series values under other configurations may be interpolated using the data gathered.

With atmospheric conditions restored, bats should return to the Historic Section of Mammoth Cave, destruction of cave artifacts should cease, and the rate of rockfalls should decrease to previous, normal levels.

5.2 Restoration of the Natural Entrance Ecotone in Mammoth Cave

The primary goal of the study conducted by Science and Resource Management personnel is to restore natural conditions within the Historic Section of Mammoth Cave. However, before atmospheric conditions may be restored, the original set of conditions must be known. One of the best indicators of past conditions in Mammoth Cave is the nature of past bat populations in Mammoth Cave, and knowledge of the species of bat present at a given location will indicate the correct set of atmospheric conditions for that location (Olson 1996). Bats are effective indicators of past environmental conditions

since they are extremely sensitive to even slight changes in environmental parameters (National Speleological Society 1984).

Using the desired set of environmental parameters at a CAM site together with the models derived in this thesis, the proper air panel configuration may be determined. This goal may be attained by using the following procedure:

1. Determine the desired set of atmospheric conditions at the CAM site in question.
2. Using the Phase 3 Bernoulli model, experiment with different data from Houchins' Narrows until the desired parameter values are obtained at the CAM site.
3. Interpolate what the air panel configuration should be to arrive at the correct sets of Houchins' Narrows data.

Using this procedure should allow the determination of the proper air panel configuration to restore the Natural Entrance Ecotone in Mammoth Cave.

APPENDIX 1

FREQUENCY DISTRIBUTIONS FOR AIR FLUX IN HOUCHINS' NARROWS

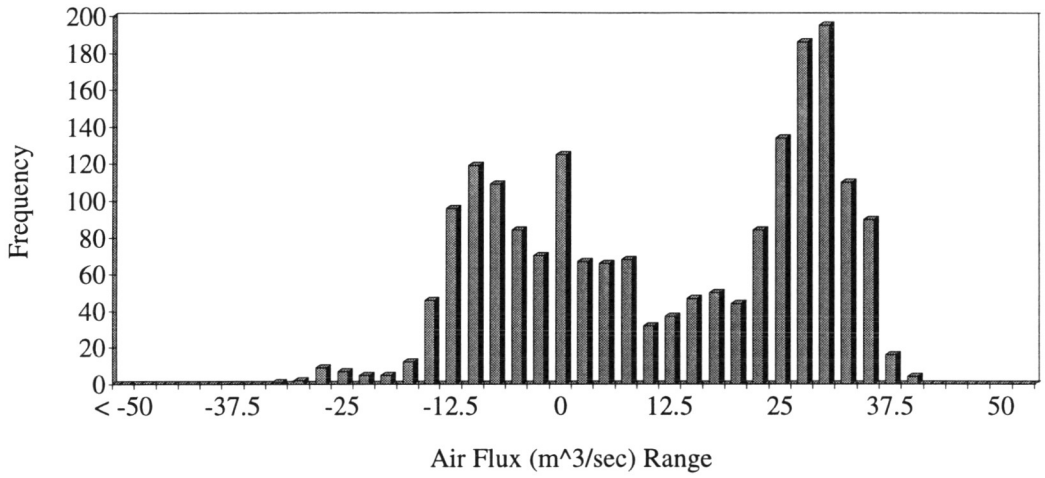

Julian Days 91 -110, 1996

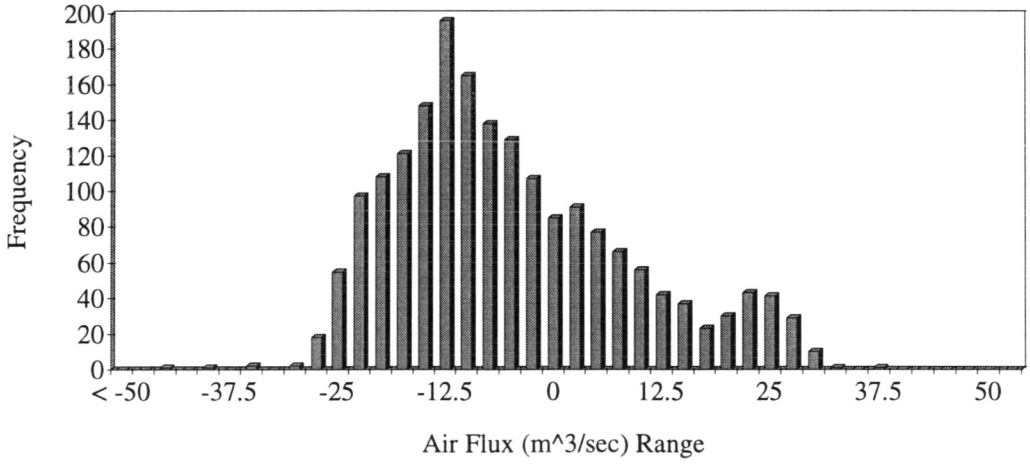

Julian Days 111 - 130, 1996

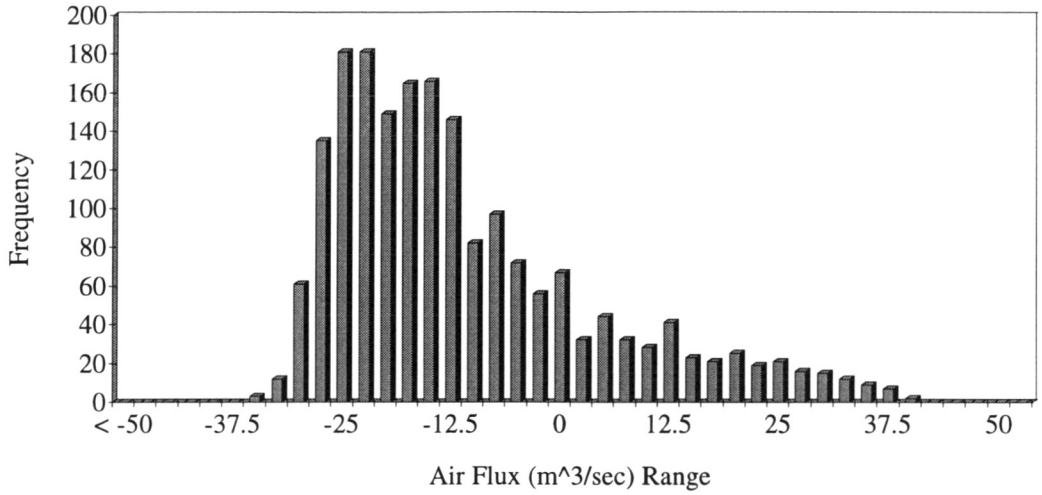

Julian Days 131 - 150, 1996

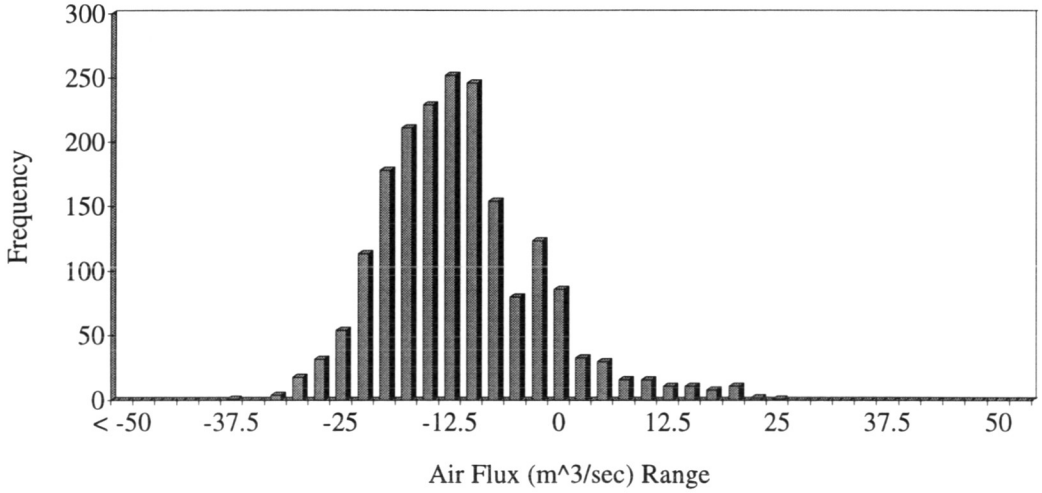

Julian Days 151 - 170, 1996

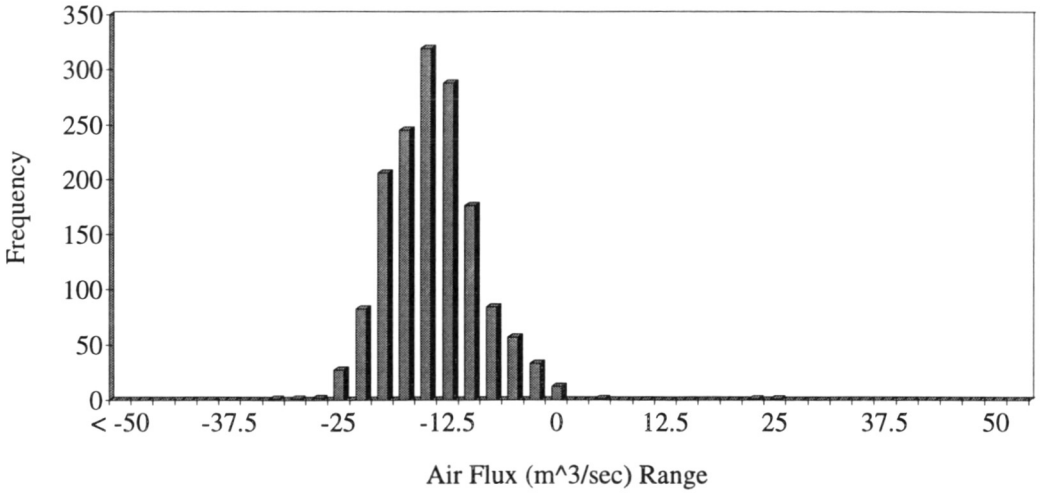

Julian Days 195 - 210, 1996

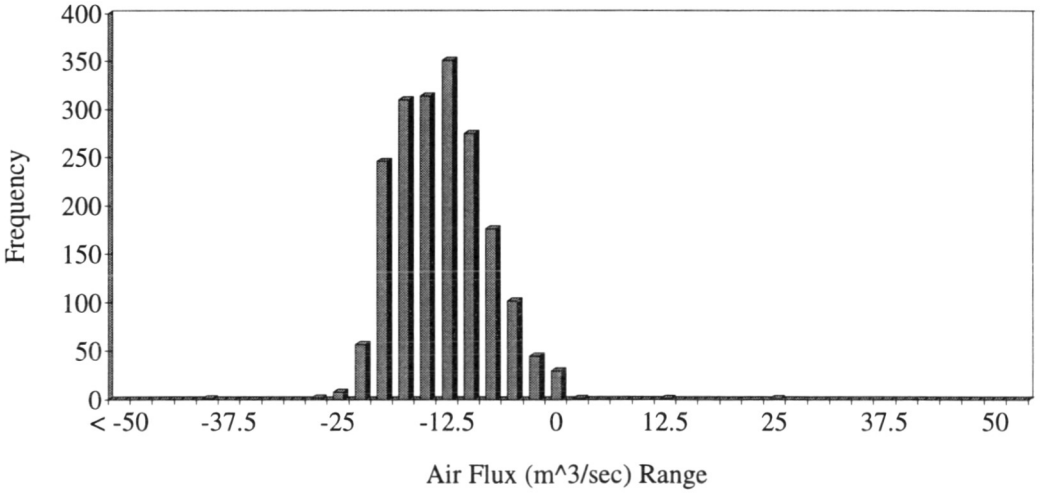

Julian Days 221 - 240, 1996

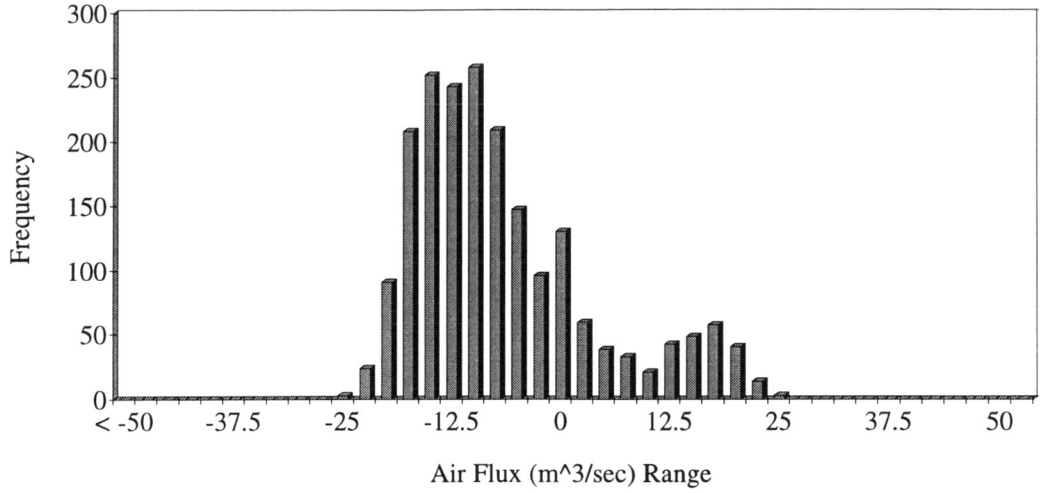

Julian Days 245 - 265, 1996

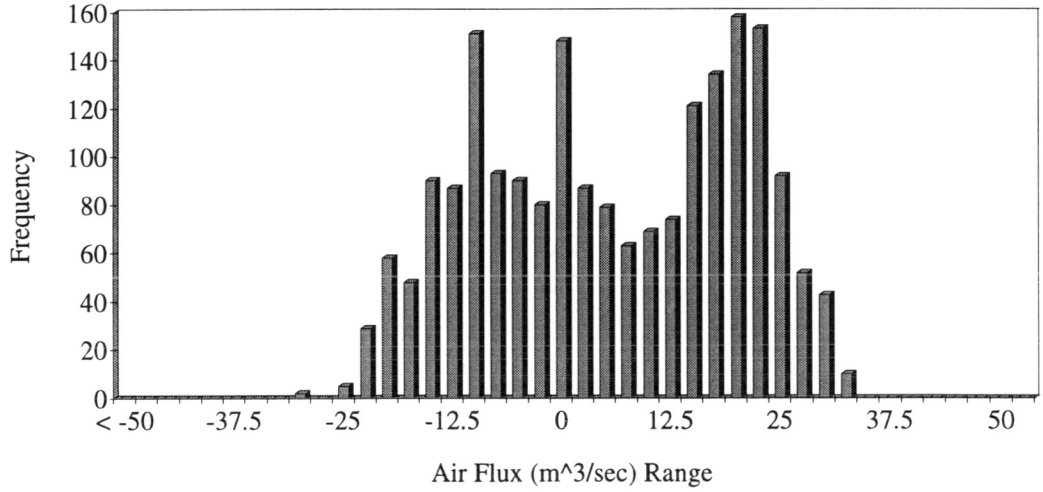

Julian Days 270 - 290, 1996

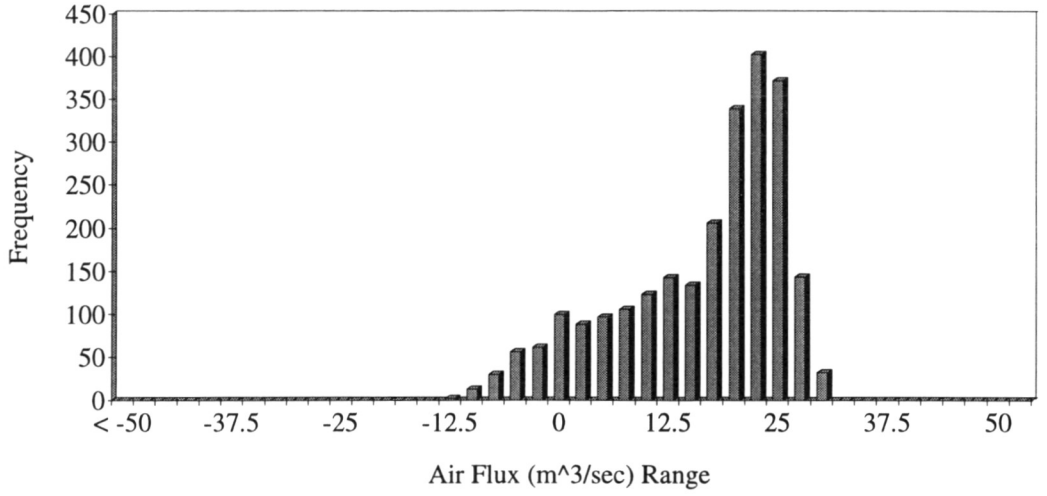

Julian Days 321 - 346, 1996

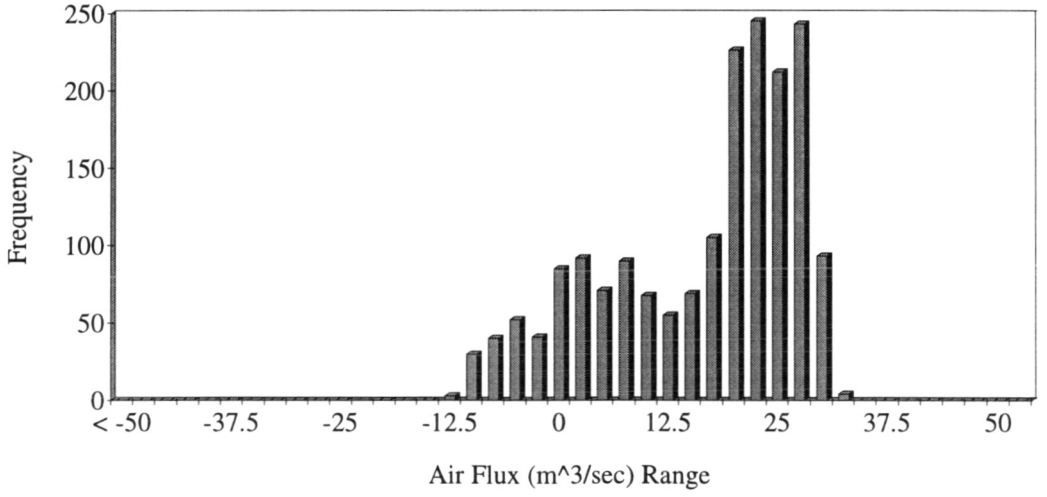

Julian Days 348 - 366, 1996

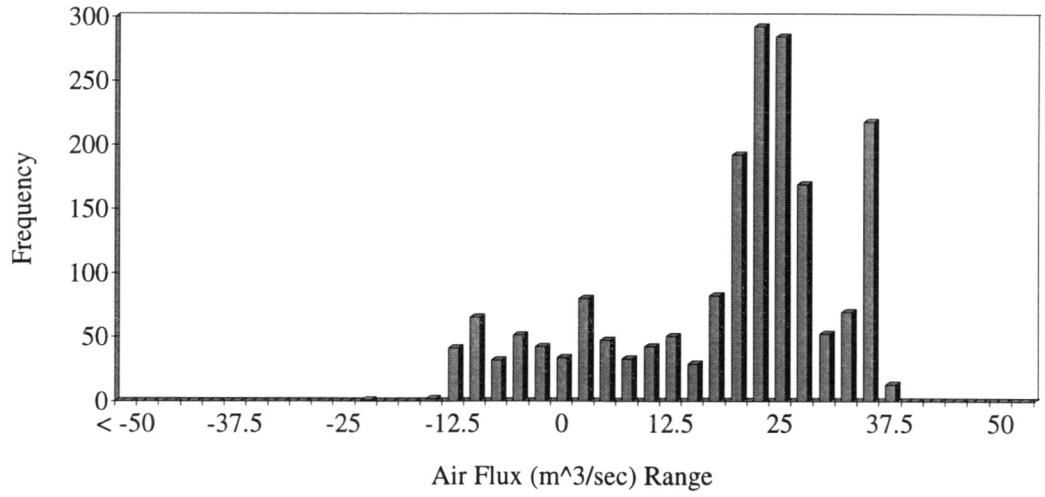

Julian Days 1 - 20, 1997

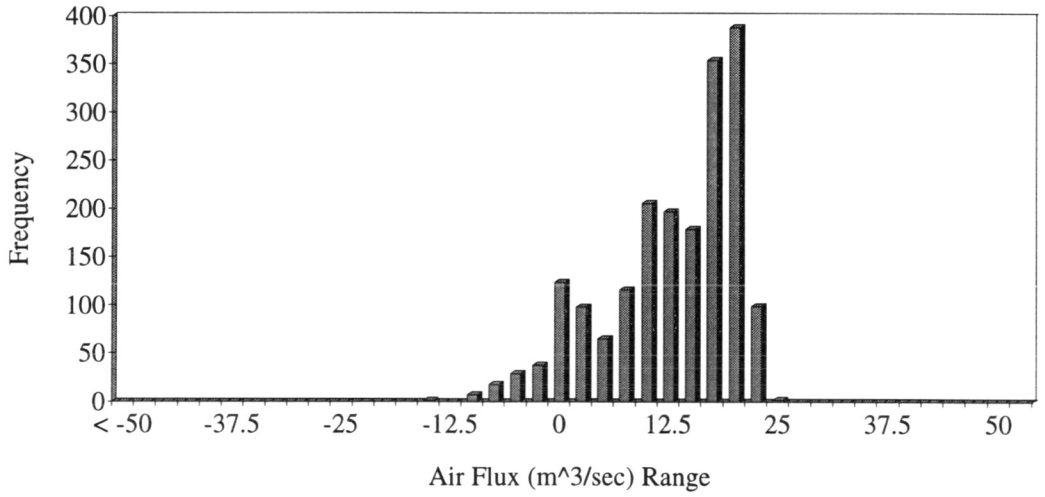

Julian Days 21 - 40, 1997

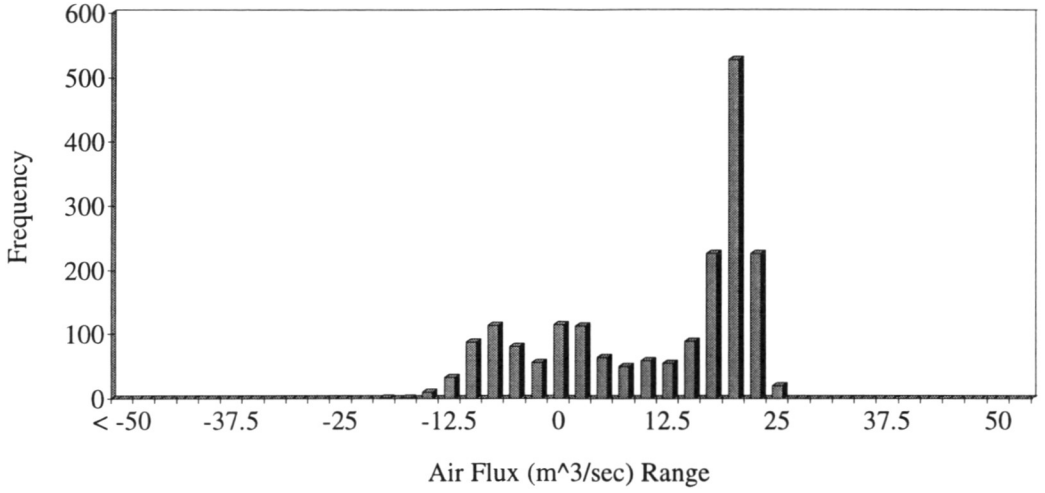

Julian Days 41 - 60, 1997

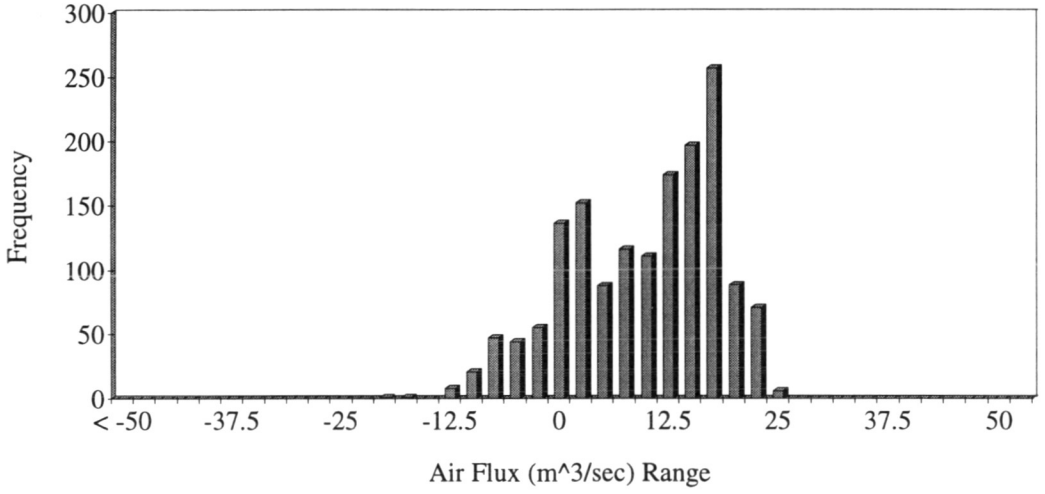

Julian Days 61 - 77, 1997

APPENDIX 2

AIR FLUX IN HOUCHINS' NARROWS AS A FUNCTION OF TEMPERATURE DIFFERENTIAL BETWEEN HOUCHINS' NARROWS AND BOOTH'S AMPHITHEATER DATA

Temperature Differential (°C)

Julian Days 91 - 110, 1996

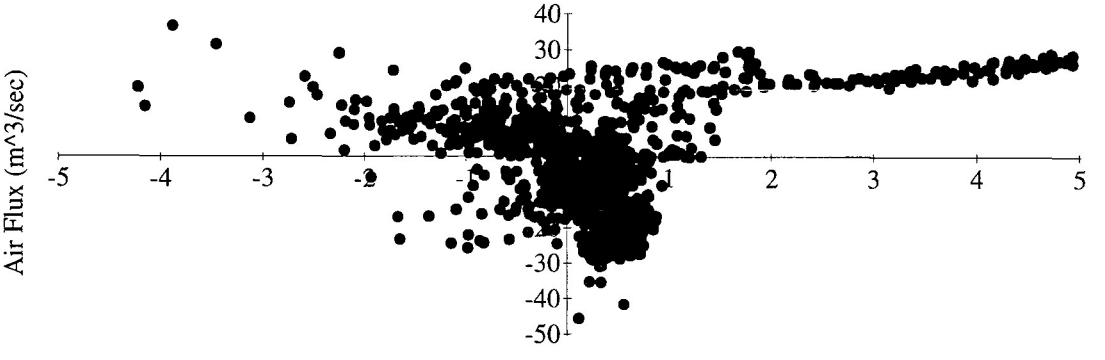

Temperature Differential (°C)

Julian Days 111 - 130, 1996

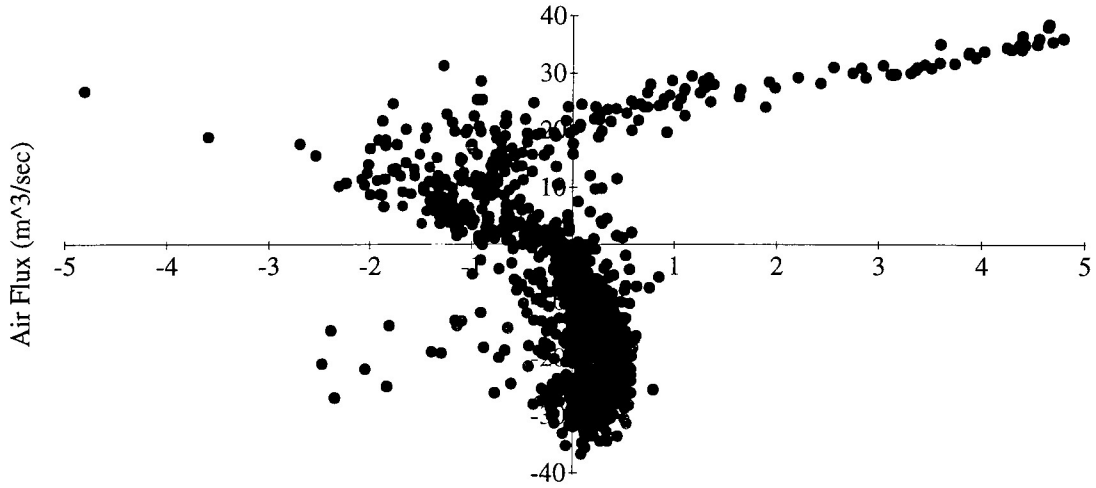

Julian Days 131 - 150, 1996

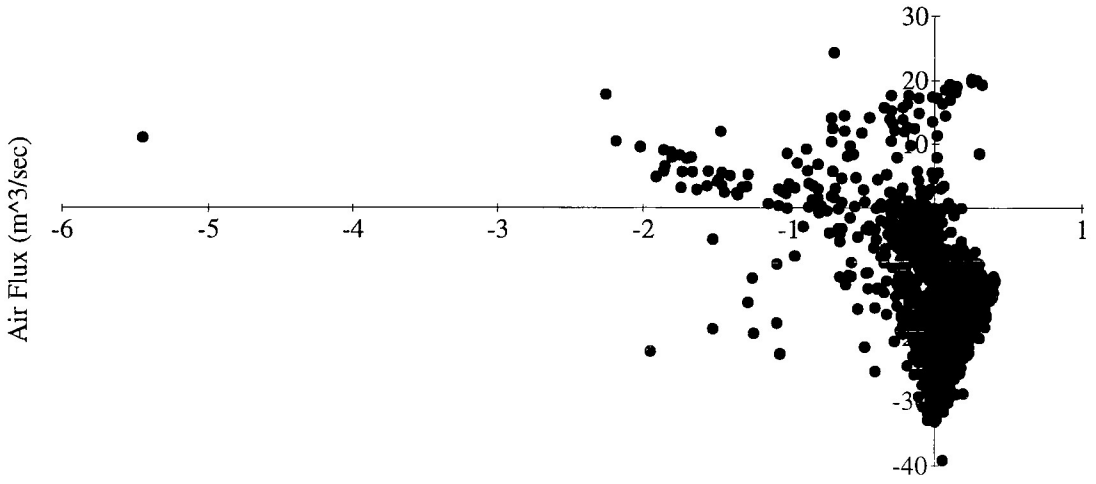

Julian Days 151 - 170, 1996

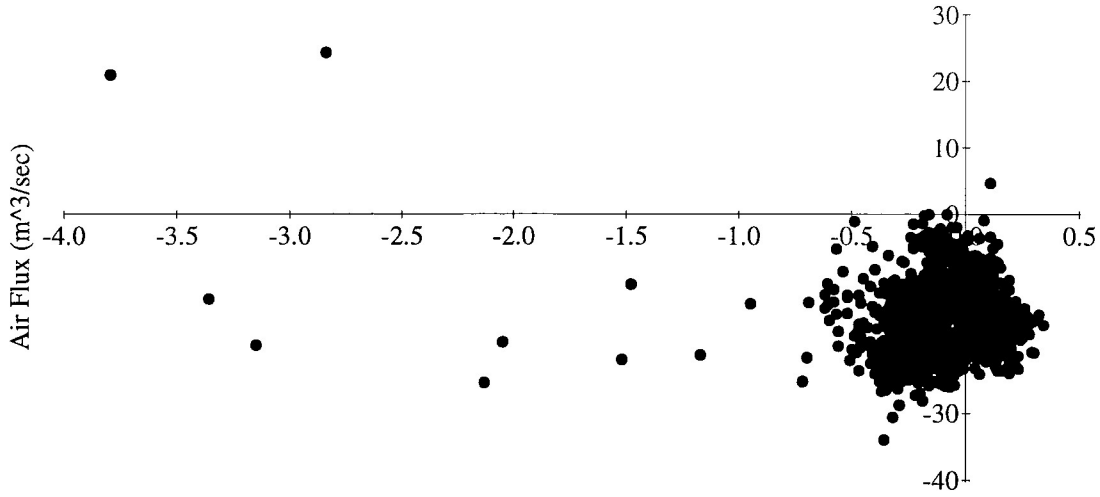

Julian Days 195 - 210, 1996

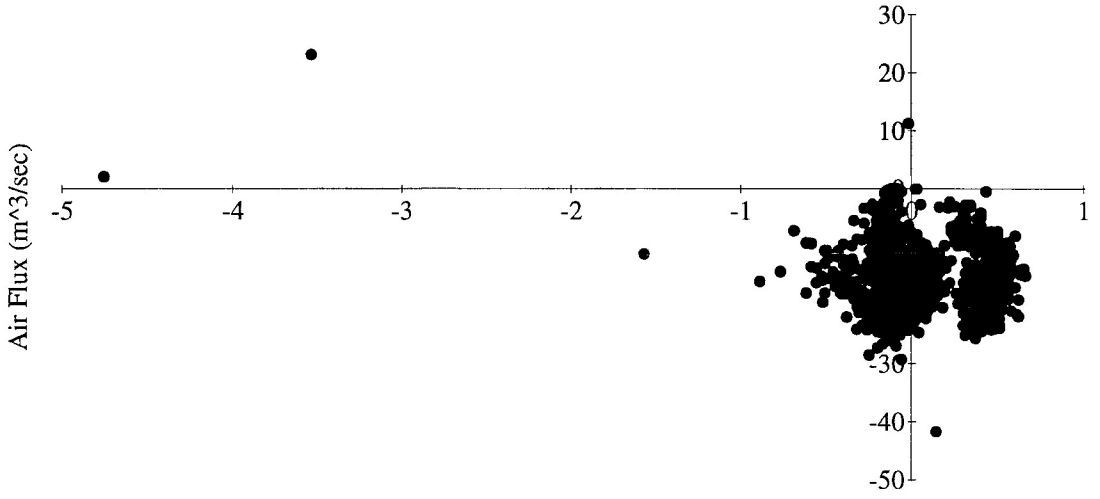

Julian Days 221 - 240, 1997

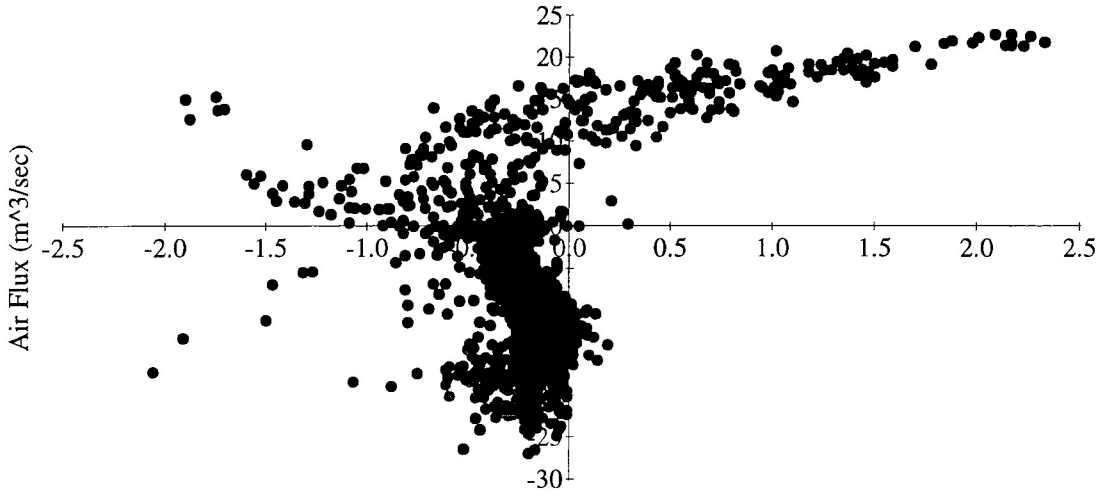

Julian Days 245 - 265, 1996

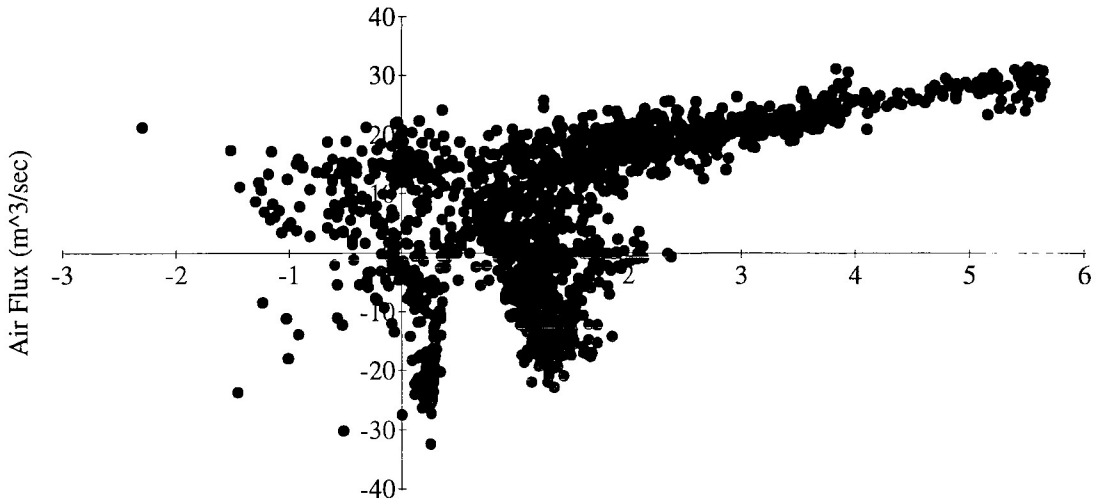

Julian Days 270 -290, 1996

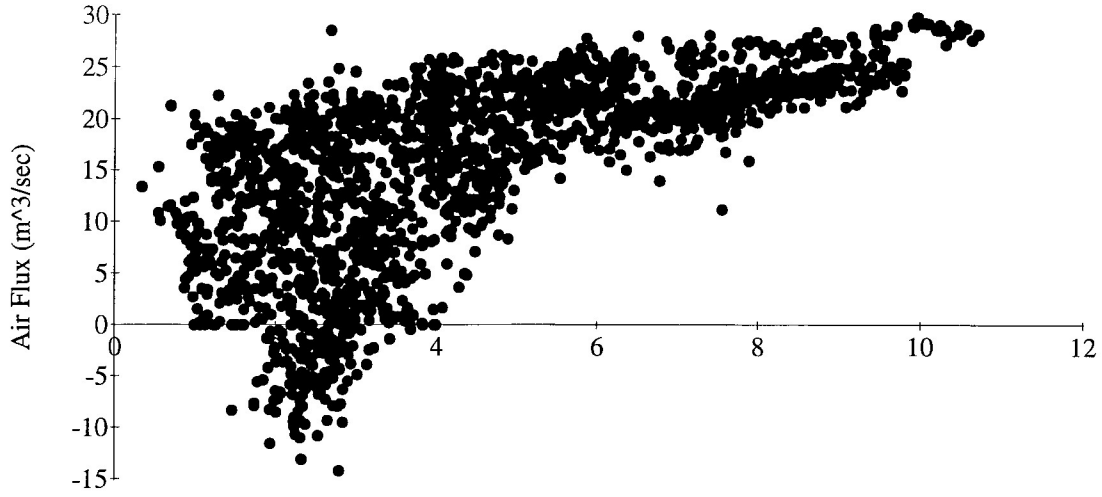

Julian Days 321 - 346, 1996

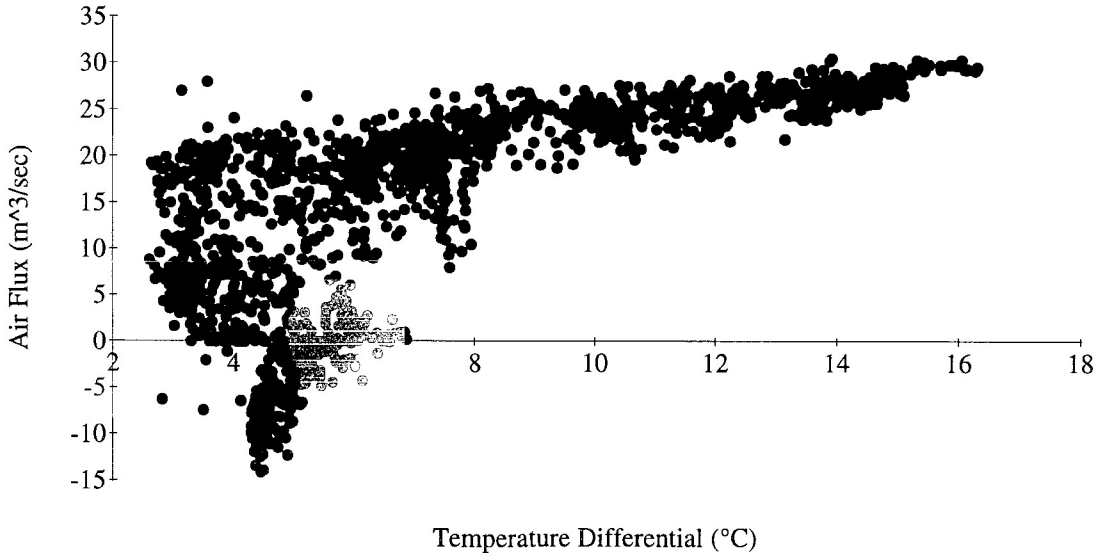

Julian Days 348 - 366, 1996

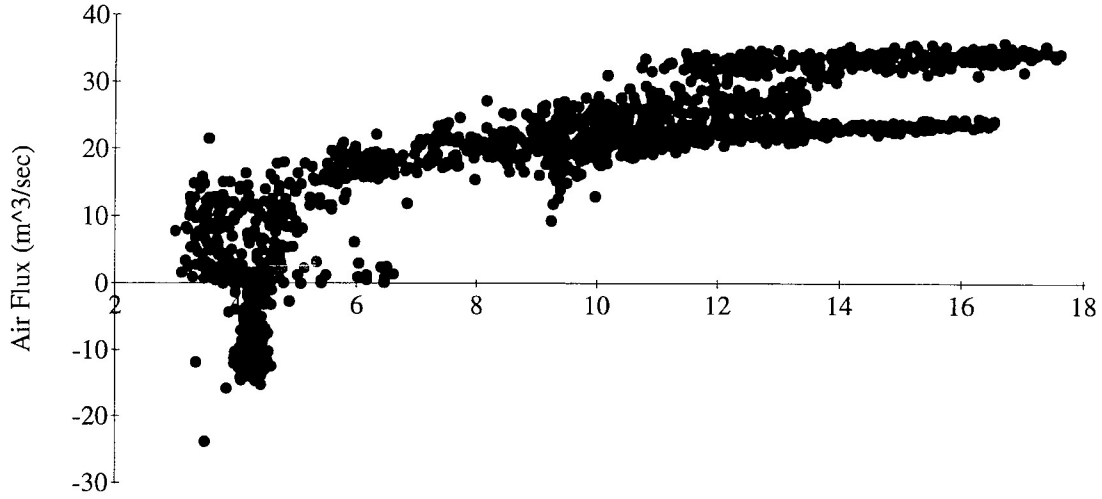

Julian Days 1 20, 1997

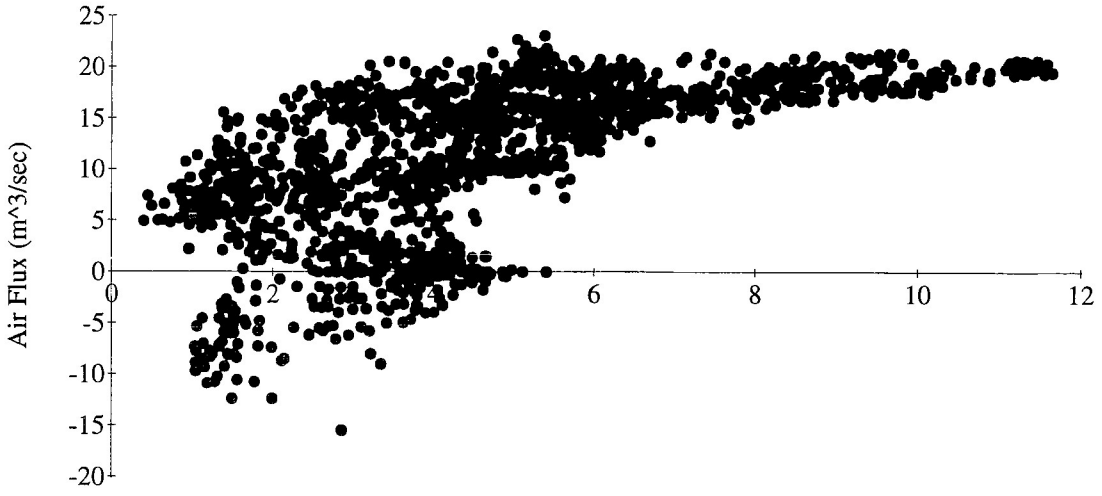

Julian Days 21 - 40, 1997

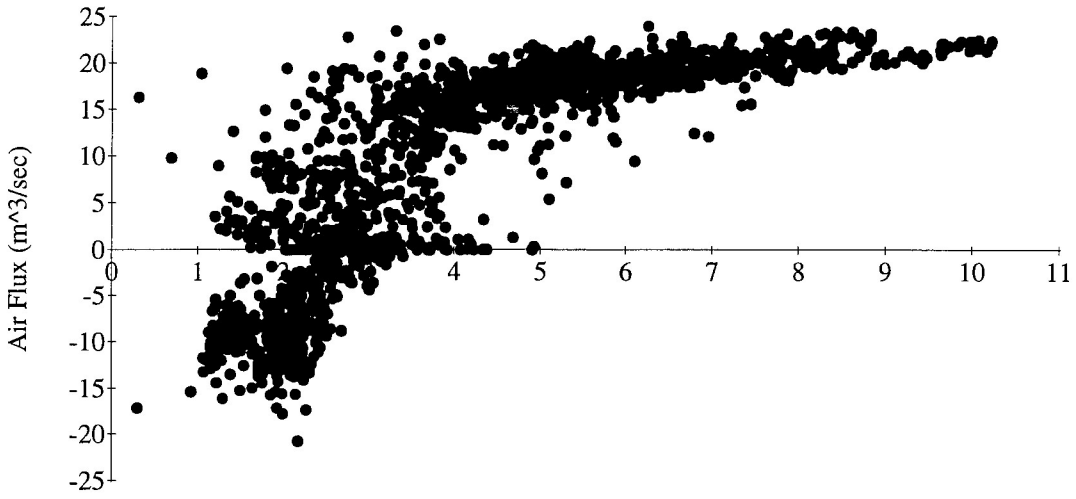

Julian Days 41 - 60, 1997

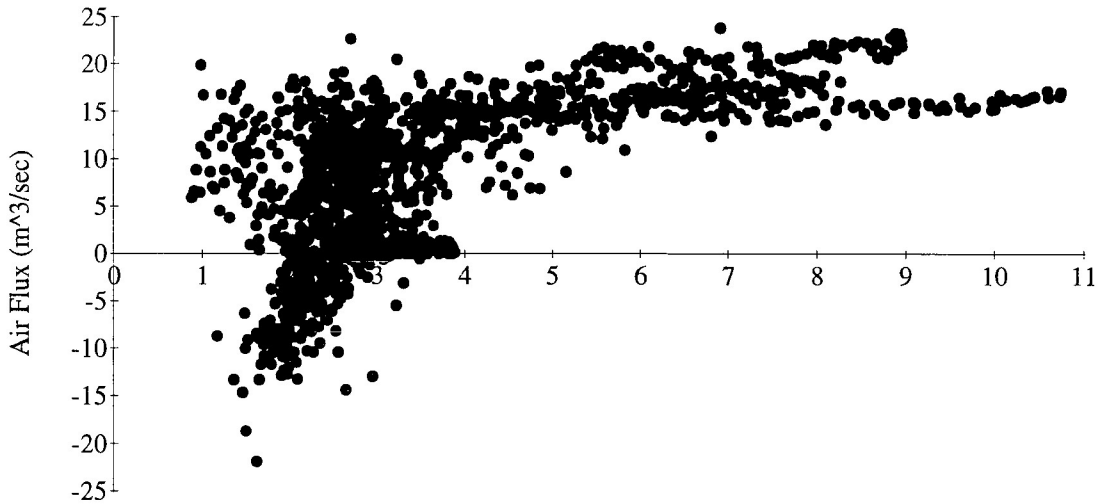

Julian Days 61 - 77, 1997

APPENDIX 3

BOOTH'S AMPHITHEATER AIR TEMPERATURE DATA

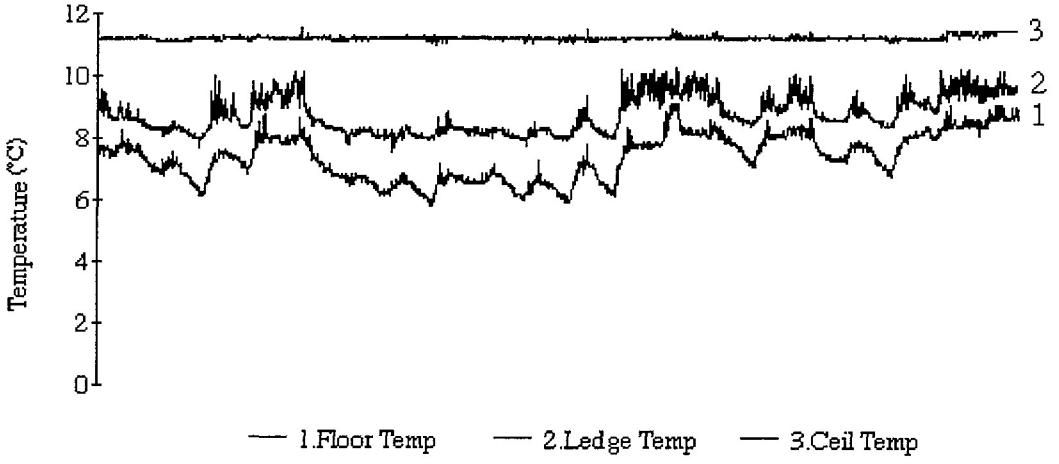

Julian Days 91 -110, 1996

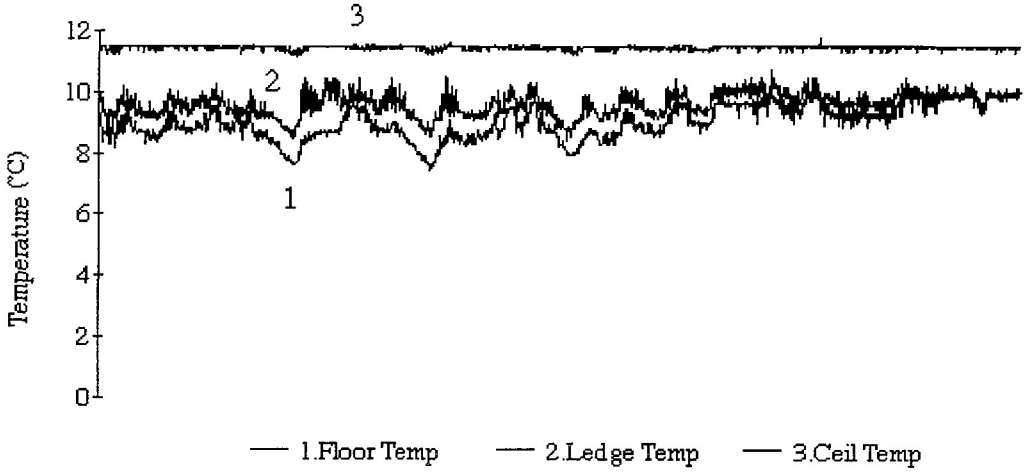

Julian Days 111 - 130, 1996

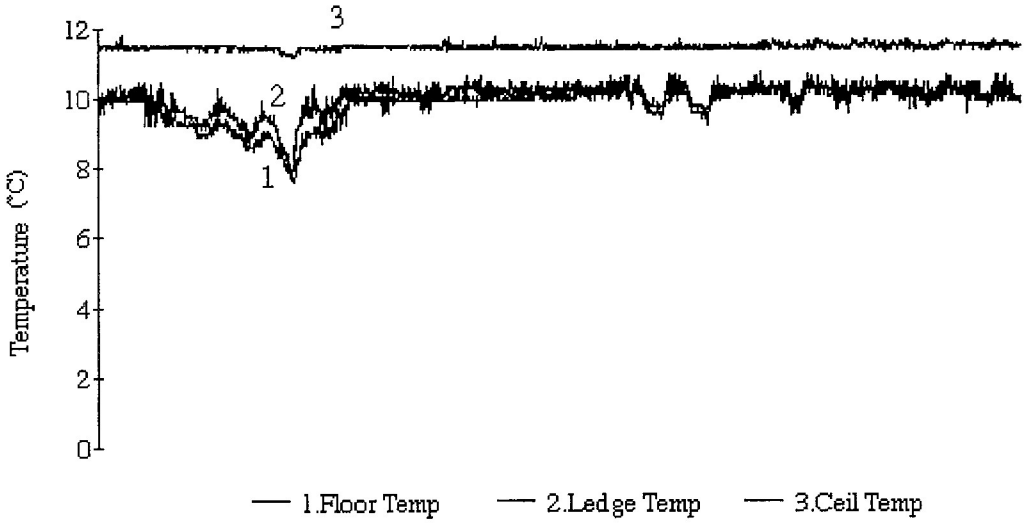

Julian Days 131 - 150, 1996

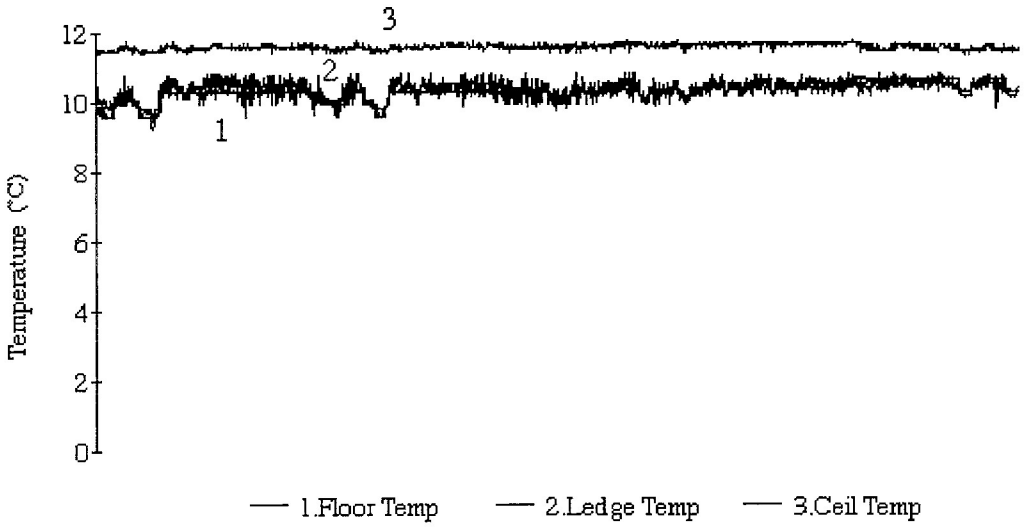

Julian Days 151 - 170, 1996

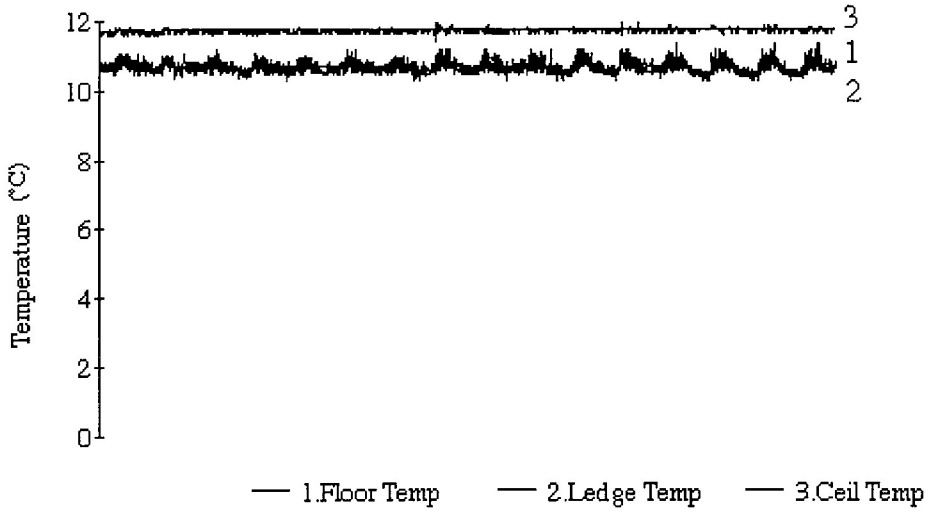

Julian Days 195 - 210, 1996

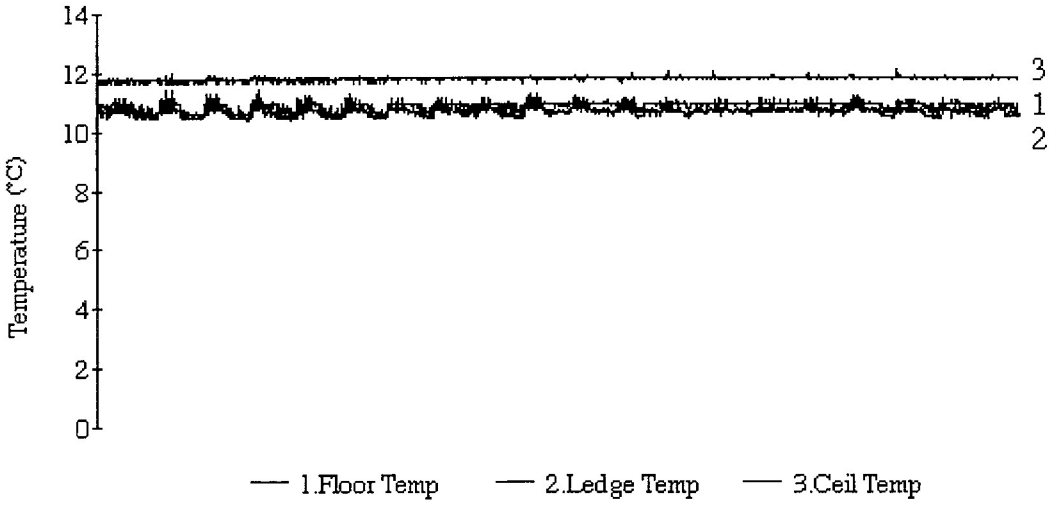

Julian Days 221 - 240, 1996

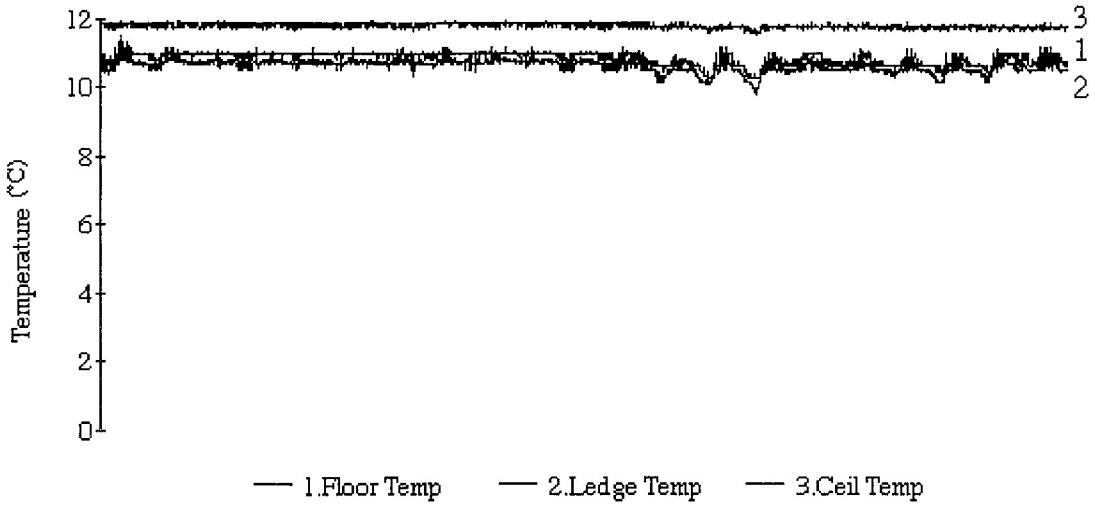

Julian Days 245 - 265, 1996

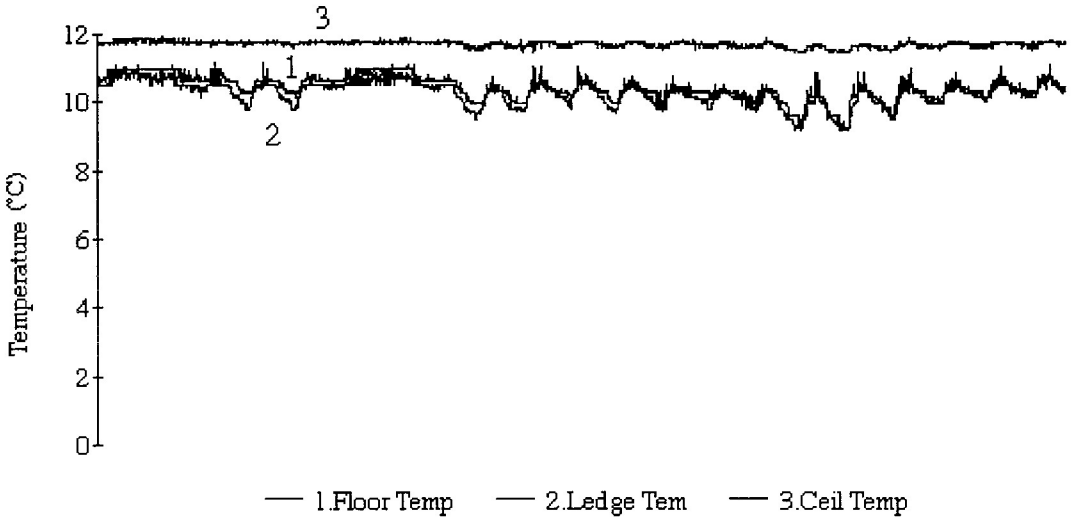

Julian Days 270 - 290, 1996

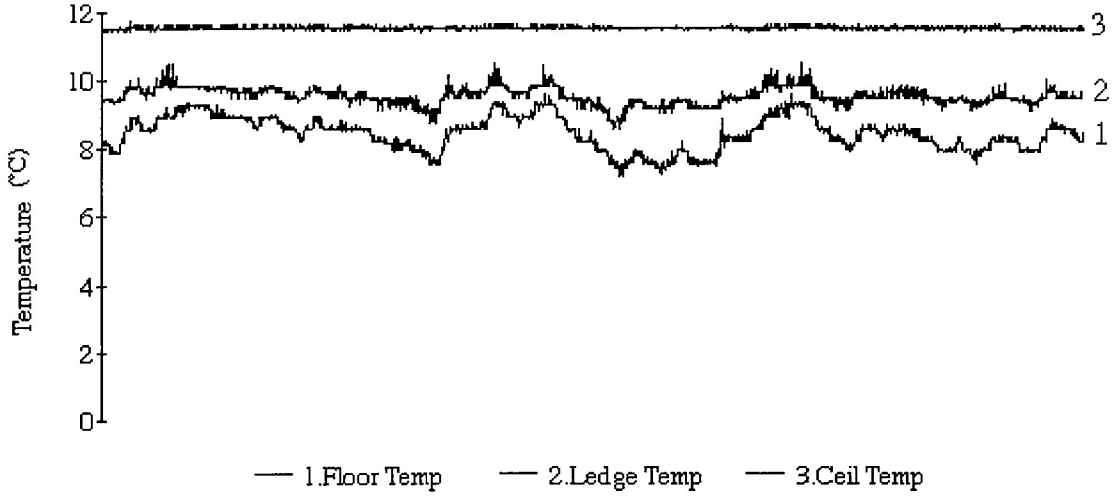

Julian Days 321 - 346, 1996

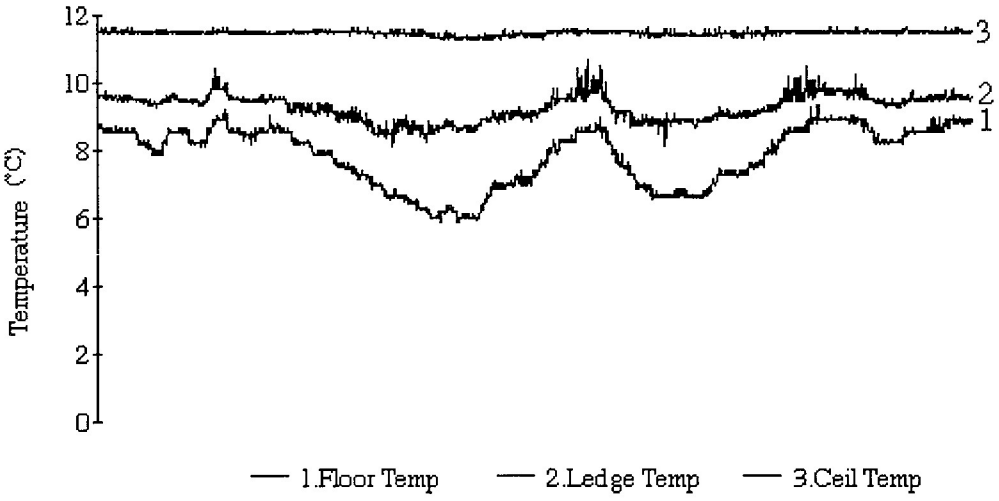

Julian Days 348 - 366, 1996

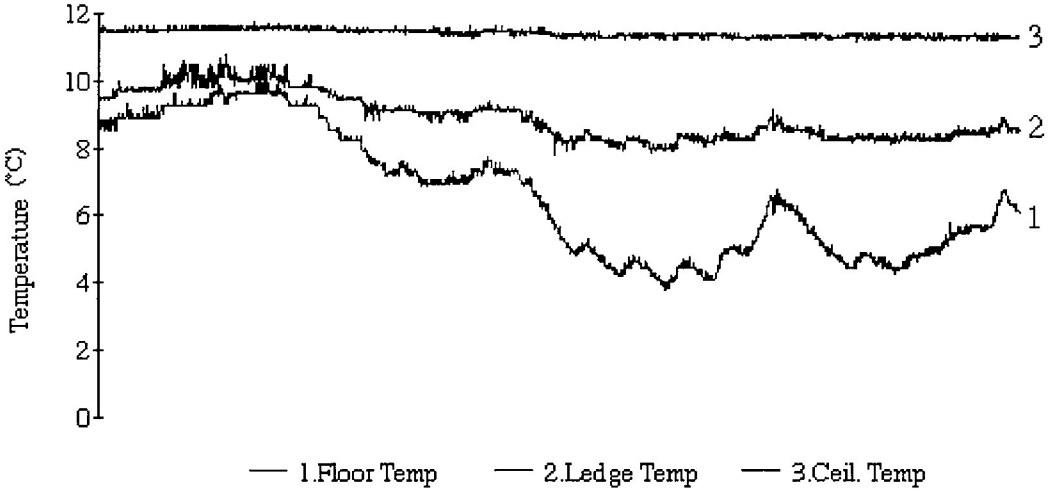

Julian Days 1 - 20, 1997

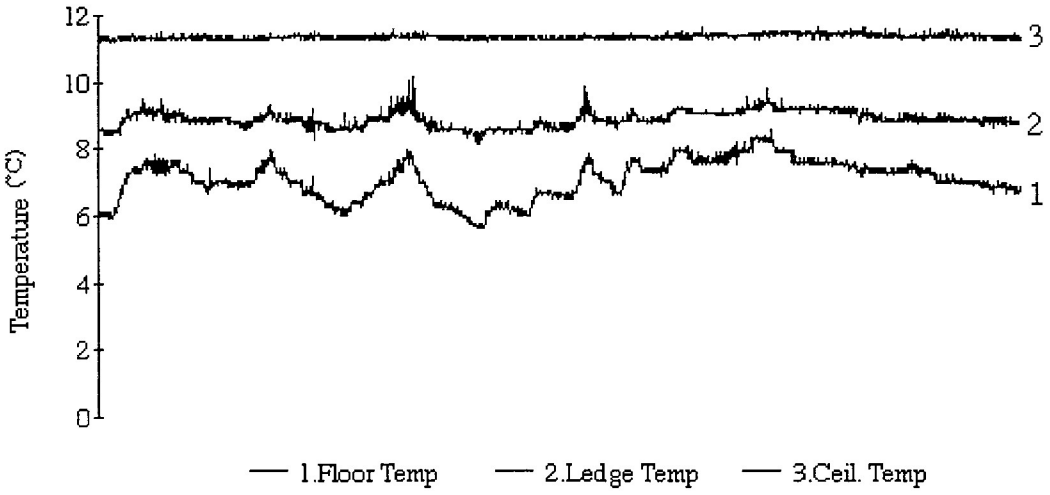

Julian Days 21 - 40, 1997

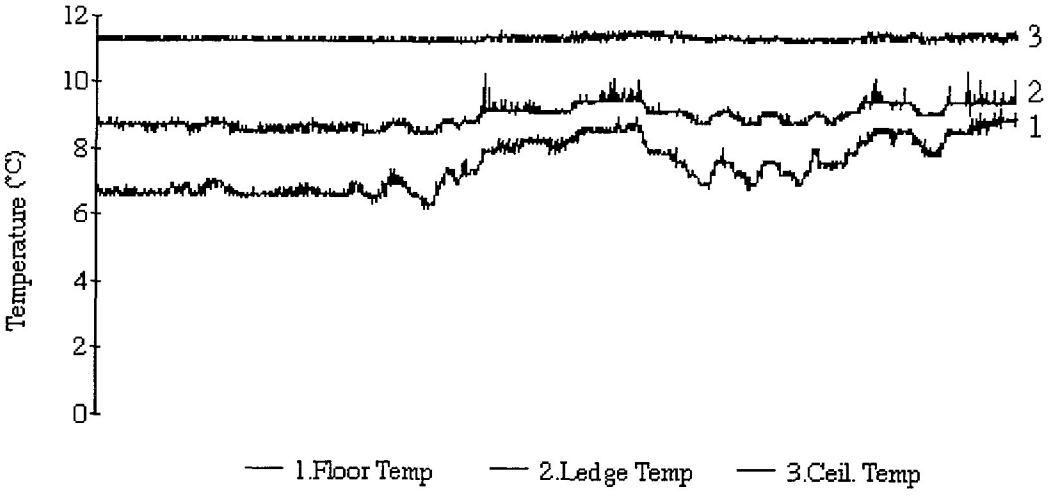

Julian Days 41 - 60, 1997

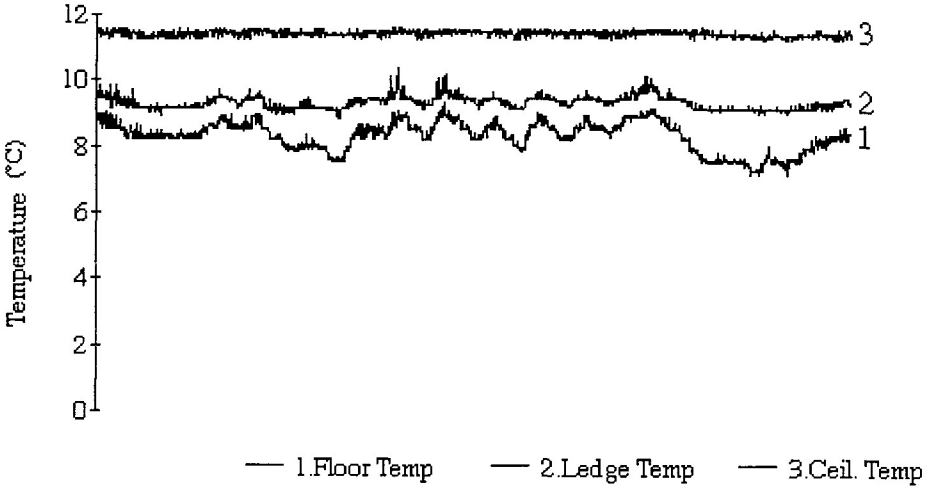

Julian Days 61 - 77, 1997

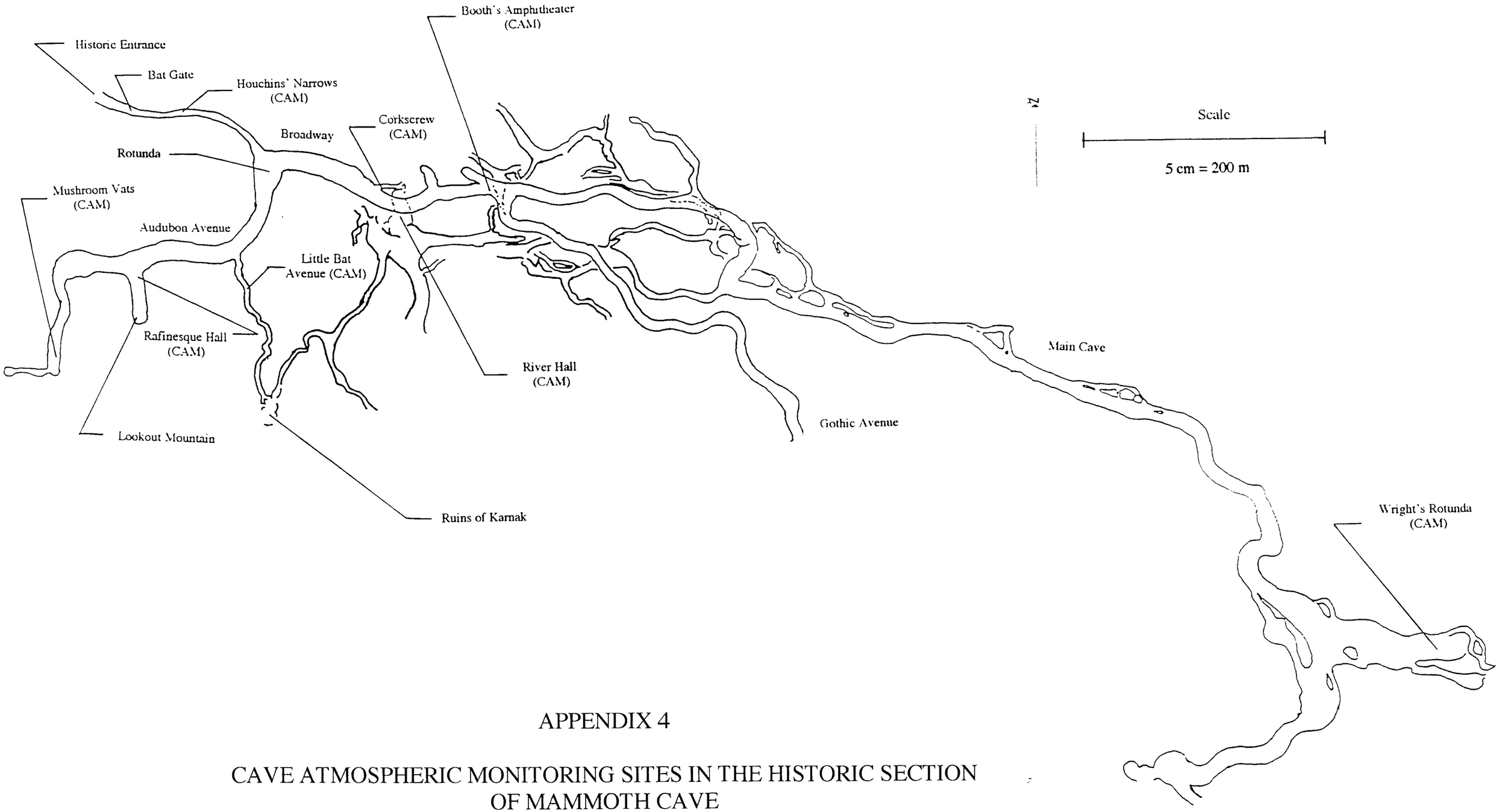

APPENDIX 4

CAVE ATMOSPHERIC MONITORING SITES IN THE HISTORIC SECTION OF MAMMOTH CAVE

Based on a Map by Max Kaemper (Kaemper 1908)

BIBLIOGRAPHY

Anonymous. *Cave Animals: Historical References.* National Park Service document, (unpublished).

Anonymous. "The Subterranean Voyage, or the Mammoth, Partially Explored." *The Enquirer* Vol. 6, No. 109 (20 April 1810).

Anonymous. "The Mammoth Cave." *The National Magazine*, 1856.

Bird, Robert Montgomery. *Peter Pilgrim.* 1838.

Blane, William H. "Mammoth Cave, Winter of 1822 - 1823." In: *An Excursion Through the United States and Canada.* London: Baldwin, Craddock, and Joy, 1824.

Brockwell, Peter J. and Richard A. Davis. *Introduction to Time Series and Forecasting.* New York: Springer - Verlag New York, Inc., 1996.

Bullitt, Alexander Clark. *Rambles in the Mammoth Cave.* 1844.

Joseph, Alexander, Pomeranz, Kalman, Prince, Jack, and David Sacher. *Physics for Engineering Technology*, 2nd ed. New York: John Wiley & Sons, 1978.

Kaemper, Max. *Map of the Mammoth Cave Kentucky.* Map. Redrafted in 1981 by Diana O. Daunt for the Cave Research Foundation with Cooperation of Mammoth Cave National Park. 1908.

Lyons, Joy Medley. *Mammoth Cave: The Story Behind the Scenery.* Las Vegas, Nevada: KC Publications, Inc., 1991.

Meriam, Ebenezer. "Mammoth Cave." *New York Municipal Gazette,* V.1. 1844.

Mooney, Douglas D. and Randall J. Swift. *A Course in Mathematical Modeling.* Classroom Resources Materials Series, Mathematical Association of America, Washington D.C., (in press).

Mott, Robert L. *Applied Fluid Mechanics*, 2nd ed. Columbus, Ohio: Charles E. Merrill Publishing Company, 1979.

National Speleological Society. *Bats Need Friends.* Huntsville, Alabama: The National Speleological Society, 1984.

Nelson, John M. "Mammoth Cave." *The Glasgow Times* 7 June 1934.

Olson, Rick. *Ecological Restoration in the Natural Entrance Ecotone of Mammoth Cave With Emphasis on Endangered Species Habitat and Mitigation of Visitor Impact.* Project Proposal (unpublished), 1995.

Olson, Rick. "This Old Cave: The Ecological Restoration of the Historic Entrance Ecotone of Mammoth Cave, and Mitigation of Visitor Impact." *Proceedings of the Fifth Annual Mammoth Cave National Park Science Conference*. 1996.

Palmer, Arthur N. *A Geological Guide to Mammoth Cave National Park.* Teaneck, New Jersey: Zephyrus Press, 1981.

Silliman, Benjamin. "On the Mammoth Cave of Kentucky." *The American Journal of Science and Arts*, V. 11. 1851.

Thompson, Ralph Seymour. *The Sucker's Visit to the Mammoth Cave*. 1870.

Tocci, Ronald J. *Introduction to Electric Circuit Analysis,* 2nd ed. Columbus: Charles E. Merrill Publishing Company, 1983.

Toomey III, R.S. *Known Quaternary Paleontological Resources of the Mammoth Cave System*, draft. February 16, 1995.

Vigne, Godfrey T. *Six Months in America.* 1831.

Wefer, Fred L. "The Meteorology of Harrison's Cave, Barbados, West Indies." Chapter 4 in *A Study of Environmental Factors in Harrison's Cave, Barbados, West Indies*. Huntsville, Alabama: National Speleological Society, 1994.